STATE OF ALASKA

DEPARTMENT OF NATURAL RESOURCES

DIVISION OF GEOLOGICAL AND GEOPHYSICAL SURVEYS

John W. Katz — *Commissioner*

Geoffrey Haynes — *Deputy Commissioner*

Ross G. Schaff — *State Geologist*

December 1981

By
R.J. Motyka, M.A. Moorman, S.A. Liss

STATE OF ALASKA
Department of Natural Resources
DIVISION OF GEOLOGICAL & GEOPHYSICAL SURVEYS

According to Alaska Statute 41, the Alaska Division of Geological and Geophysical Surveys is charged with conducting 'geological and geophysical surveys to determine the potential of Alaska lands for production of metals, minerals, fuels, and geothermal resources; the locations and supplies of ground waters and construction materials; the potential geologic hazards to buildings, roads, bridges, and other installations and structures; and shall conduct other surveys and investigations as will advance knowledge of the geology of Alaska.'

In addition, the Division shall collect, evaluate, and publish data on the underground, surface, and coastal waters of the state. It shall also process and file data from water-well-drilling logs.

DGGS performs numerous functions, all under the direction of the State Geologist---resource investigations (including mineral, petroleum, and water resources), geologic-hazard and geochemical investigations, and information services.

Administrative functions are performed under the direction of the State Geologist, who maintains his office in Anchorage (3001 Porcupine Dr., 99501, ph 274-9681).

Table 18 gives the chemical composition of fumarolic gas samples obtained
from sites A and C. The proportions of constituent gases are similar in the two
fumarolic areas. The dominant gas in both fields is carbon dioxide. The nitrogen
and argon are probably of atmospheric origin, and are probably dissolved in in-
filtrating surface waters (Mazor and Wasserberg, 1965). The low concentration of
oxygen in both cases is probably due to oxidation of H_2S and H_2.

Reservoir Properties

The occurrence of the thermal springs at the base of fumarole fields in
Makushin Valley suggests that at least part of the spring waters may originate
as condensation of steam in surface waters, which then percolate into the
porous colluvium and country rock to eventually emerge as springs. The high
silica content of the thermal waters, however, indicates that a large portion
of the waters must have originated from a subsurface reservoir where tempera-
tures exceed 150°C, assuming the silica is in equilibrium with quartz. Surface
waters infiltrating this reservoir may become heated on descent, causing dis-
solution of cations in the wall rock, a process aided in part by the slight
acidity of the waters. The levels of calcium, and particularly magnesium,
relative to sodium and potassium indicate the residence time of waters in the
reservoir is too short for these constituents to equilibrate to the estimated
reservoir temperature. Silica can equilibrate rather rapidly, within several
days to a few weeks. This suggests the reservoir supplying the thermal-spring
waters lies at fairly shallow depths. The low chloride content and the
slightly acid-sulfate chemistry of the thermal waters, together with their
association with fumarolic activity, are evidence for a perched reservoir
supplied by meteoric waters that are heated by steam and volcanic gases rising
through a vapor-dominated zone from a much deeper reservoir.

Table 18. Chemical composition of fumarolic gases from Makushin Valley
           thermal field (analysis in volume percent).

	Site A	Site C
H_2	0.49	0.252
Ar	0.083	0.0715
O_2	<0.0001	<0.0001
N_2	7.93	5.608
CH_4	0.0018	0.0308
CO_2[b]	89.14	91.29
H_2S[b]	2.38	2.75

[a]J. Weldon and R. Poreda, analysts, Scripps
   Institution of Oceanography, La Jolla, Calif.
[b]M. Moorman, analyst, DGGS.

The hydrogen sulfide probably has a magmatic origin, as does as least part
of the carbon dioxide (Craig, 1963; White, 1968). An analysis of

the ratio of ^{3}He:^{4}He in the fumarolic gases obtained in cooperation with R. Poreda at the Scripps Institute of Oceanography is given below:

	MV-A	MV-C
$\dfrac{(^3\text{He}/^4\text{He}}{(^3\text{He}/^4\text{He})\text{AIR}}$	4.9	6.6

An enrichment in ^{3}He in fumarolic gases has been correlated with magmatic activity on a worldwide basis, the source of ^{3}He thought to be derived from primordial mantle material (Lupton and Craig, 1975; Craig and others, 1978; R. Poreda, pers. commun.). The values for the Makushin fumaroles are within the range of other volcanic island-arc geothermal systems.

The hydrogen content of the gases is probably produced by high-temperature reaction of water with ferous oxides and silicates contained in the deep reservoir rocks (Seward, 1974).

Table 19 gives the results of applying the D'Amore and Panichi (1980) gas geothermometer to the Makushin fumarole samples. From the proportions of gases present, B is chosen as 0 and the respective reservoir temperature estimates are 278°C and 232°C for sites A and C. These estimates must be used with caution. The accuracy of this geothermometer has not yet been generally accepted. Furthermore, the gases have probably undergone reaction with a shallow reservoir which may have affected their H_2S and H_2 contents.

Despite the uncertainties in the gas geothermometers, the large flux of steam and the probable magmatic origin of some of the fumarolic gases indicate the existence of a high-temperature, deep geothermal reservoir.

Table 19. Gas geothermometry, Makushin Valley fumaroles
(temperatures °C).

B*	Site A	Site C
-7	380	316
0	278	232
7	204	169

*for explanation of B, see table 3b.

Comments

The Makushin Valley hydrothermal system is similar in most respects to the Glacier Valley system. Both are characterized by extensive fields of mild fumarolic activity and thermal springs low in chloride and rich in sulfate and bicarbonate. The proximity of these fields to each other and to the active summit caldera indicate a common source of heat underlies the volcano. Comparison with similar volcanic systems elsewhere in the world suggests the origin of the hydrothermal system is a high-temperature sodium-chloride brine overlying a cooling body of magma. Gases and steam escaping from this deep reservoir give rise to reservoirs rich in secondary bicarbonate-sulfate at shallower levels and to the fumarolic fields on the flanks and summit of the volcano.

The difference in chloride and silica contents of springs A3 and D2, the similarity in their B:Cl ratios, and the large combined flow of the springs indicate that the deep thermal waters may be diluting in a shallow subsurface aquifer. If so, all three geothermometers would tend to underestimate the deep-reservoir temperature estimates. Following the method of Truesdell and Fournier (1977), application of the quartz mixing model suggests deep-reservoir temperatures as high as 235°C.

Comments

No geophysical exploration or exploratory drilling has yet been done near the Akutan hot springs. Thickness of the alluvial fill in the valley is unknown but is probably on the order of 100 m. Bedrock underlying the valley may be an extension of the volcanic breccia sequence exposed along the valley walls. If capped by hydrothermal cementation, such a porous and permeable host rock could house a substantial hot-water reservoir at fairly shallow depths, one that might be easily tapped.

The linear distribution of the thermal springs suggests they are related to a subsurface fracture system, perhaps a seismically induced break in the cap of the hypothetical shallow reservoir. The massive dikes that appear to traverse the mouth of the valley may be acting as barriers to the intrusion of seawater into the hypothermal system.

The estimated deep-reservoir temperature of 180°C is sufficient for a variety of applications, including the generation of a modest amount of electrical power, e.g., a 1-MW well-head-driven Rankine binary system. The nearness of this hot-water system to a well-protected deep-water harbor with a population center and potential industrial users (e.g., fishing processors) make the Akutan hot spring site a particularly attractive one for future development. The ridge that lies between the site and Akutan volcano should help provide a protective barrier from eruptions from the active volcano.

CONTENTS

FIGURES

TABLES

METRIC CONVERSION FACTORS

To convert kilometers to miles, divide kilometers by 1.61.
To convert meters to feet, divide meters by 0.3048.

ASSESSMENT OF THERMAL SPRINGS SITES ALEUTIAN ARC, ATKA ISLAND TO BECHEROF LAKE -- PRELIMINARY RESULTS AND EVALUATION

By R.J. Motyka, M.A. Moorman, S.A. Liss

ABSTRACT

Twenty of more than 30 thermal spring areas reported to exist in the Aleutian arc extending from Atka Island to Becherof Lake were investigated during July and August, 1980. Thermal activity of three of these sites had diminished substantially or no longer existed (Ukinrek, Bogoslof, and Peulik). At least seven more sites where thermal-spring activity is probable or certain were not visited because of their remoteness or because of time constraints. The existence of several other reported thermal spring sites could not be verified; these sites are considered questionable.

On the basis of geothermometry, subsurface reservoir temperatures in excess of 150°C are estimated for 10 of the thermal spring sites investigated. These sites all occur in or near regions of Recent volcanism. Five of the sites are characterized by fumaroles and steaming ground, indicating the presence of at least a shallow vapor-dominated zone. Two, the Makushin Valley and Glacier Valley thermal areas, occur on the flanks of active Makushin Volcano located on Unalaska Island, and may be connected to a common source of heat. Gas geothermometry suggests that the reservoir feeding the Kliuchef thermal field, located on the flanks of Kliuchef volcano of northeast Atka Island, may be as high as 239°C.

The Geyser Bight thermal-springs area constitutes the hottest and most extensive hot-water hydrothermal-convective system known in Alaska. Most of the thermal springs there, dispersed over a 4-km^2 area on central Umnak Island, are at or near boiling. Deep reservoir temperatures are conservatively estimated at 210°C and may be as high as 264°C. A geothermal reservoir temperature of 180°C is estimated for Akutan hot springs, a 1-km-long zone of 60°-80°C thermal springs with an estimated total flow rate of 600 lmp, located 10 km northeast of the active Akutan Volcano. The Emmons Lake hot-springs site, located in a remote region of the southwest Alaska Peninsula, has an estimated reservoir temperature of 178°C; discharge from the 60°C thermal springs was measured at 600 lpm. The Mother Goose hot springs (50°-60°C), located at the base of Mt. Chiginagak, an active volcano on the Alaska Peninsula, are distinguished by their enormous rate of discharge ($\sim$4,000 lpm) and by the mixed character of their thermal-water chemistry. Deep reservoir temperatures at Mother Goose are tentatively estimated at 150°C.

Five thermal-springs sites were identified to have reservoir temperatures in the range of 90°-150°C: Partov hot springs, Cold Bay hot springs, False Pass hot springs, Port Moller hot springs, and Akun Strait hot springs.

Three sites are identified as having reservoir temperatures $<90^\circ C$: Egg Island, Kenmore, and Summer Bay. Mixing models for the Summer Bay site, however, suggest the parent thermal water for this system may originate from a $160^\circ C$ reservoir.

The thermal-springs sites in the study region fall into three general terrain associations: 1) those which occur on the flanks or at the base of Recent volcanoes; 2) those systems which occur near Recent volcanoes and/or near lineations that suggest fracture or fault control for the thermal-spring occurrence; and 3) those systems remote from any Recent volcano, typically at or near the coast, and which appear to be related to local fractures or dikes. These associations are reflected in the wide variation in water chemistry of the Aleutian-arc thermal springs. Springs directly associated with fumarole and steam fields on or near Recent volcanoes are characterized by extremely low chloride concentrations (<50 ppm) and often low pH. Some of the near-neutral low-chloride springs are comparatively rich in bicarbonate and sulphate and have high levels of magnesium and calcium relative to sodium and potassium. Such waters appear to originate from the heating of surface waters circulating in shallow reservoirs by condensing steam and volcanic gases rich in H_2S and CO_2.

Thermal waters from high-temperature systems associated with inferred deep-fracture systems such as Geyser Bight and Akutan hot springs are typified by mild to moderate concentrations of alkali-chlorides, low Na/K ratios, and high levels of silica. Geyser Bight and Hot Springs Cove are also characterized by high levels of boron compared to other Aleutian-arc hot springs. The constituents of these thermal waters are probably derived in large part from the interaction of hot-water with wall rocks during long-term residence in deep-seated geothermal reservoirs. Part of the constituents may also be of magmatic origin. Depths to such reservoirs are largely unknown; but based on occurrences elsewhere in the world, they are probably 1 to 3 km deep.

Generally, thermal springs that are associated with relatively low subsurface temperatures and which occur at or near the coast are moderately concentrated sodium-chloride waters, usually with measurable quantities of bromide. The constituents in these waters probably originated in part from the circulation of sea water in deep fracture systems, with magnesium and sulphate being selectively removed in high-temperature water-rock reactions.

Carbon dioxide is the dominant gas present in all but one of the nine gas samples obtained from hot springs and fumaroles in the study area. Methane gas predominates at Port Moller hot springs. Notably high proportions of hydrogen (5.9 percent) and hydrogen sulfide (1.6 percent) were detected in samples obtained from the Kliuchef thermal field. Enrichments of ^3He in gases obtained from Makushin Valley fumaroles are typical of island-arc settings. The excess ^3He is thought to be of mantle origin.

Many of the hydrothermal systems in the study region appear to be intimately associated with the magmatic activity. Deep reservoirs probably reside in magmatically heated older rock formations that are capped by late Quaternary volcanics. Thermal springs remote from centers of Recent volcanism probably derive their heat solely from the regional geothermal gradient by circulation along deep fracture systems.

Three locations have been identified in this study where the potential for developing and using geothermal energy is highly promising to outstanding: Akutan Island, northern Unalaska Island, and northeast Atka Island. All three areas have high-temperature ($>150^\circ$C) geothermal resources that are located near existing population centers with excellent well-protected, deep-water harbors. Two of these centers, Akutan and Unalaska villages, presently serve as the major supply and processing ports for most of the American-based Aleutian-Bering Sea fishing fleets. The third, Atka Village, is a subsistence community and is actively seeking an energy base for developing a local fish-processing industry. The geothermal reservoir temperatures estimated in all three localities are probably high enough to produce at least moderate amounts of electrical power (1-5 MW) by using Rankine-type binary systems or by flash-steam production. Cascaded uses are possible for direct space heating and industrial processing.

Although the Geyser Bight geothermal resource is the hottest and most extensive thus far identified in Alaska, the lack of protected deep-water harbors and potential users on Umnak Island make the development of this resource impractical at this time.

INTRODUCTION

More than 20 sites reported to have thermal springs in the region extending from Atka Island on the west to Becherof Lake on the east were investigated by DGGS during July and August of 1980 (fig. 1). In addition, information regarding the existence of several other reported thermal spring sites was obtained through personal communication with either long-time residents of the area in question or with persons who had actively searched for these springs. This report presents the preliminary results of the investigations and an evaluation of the geothermal energy potential of the individual sites. Several additional thermal-spring sites are known to exist in this region but were not investigated because of their remoteness, their occurrence in one of the federal conservation units, or the lack of time.

The Aleutian arc consists of the entire chain of the Aleutian Islands and its structural extensions, the Alaska Peninsula, and the Aleutian Range (Coats, 1950). At least 76 major volcanoes occur along this arcuate belt, extending over 2,400 km from Mt. Spurr on the east to Buldir Island on the west. Of these, at least 36 have been reported active since 1760. The Aleutian chain of active volcanoes lies immediately north of the Aleutian Trench, a convergent boundary between the North American and the Pacific lithospheric plates. This convergence produces one of the most seismically active belts in the world. Much of the seismicity originates from the Benioff Zone, the subcrustal region where the Pacific plate is being actively subducted under the margin of the North American plate along the Aleutian Trench. With the exception of Amak and Bogoslof Islands, the Aleutian volcanoes all lie about 100 km above the Benioff Zone. The eruption of Aleutian magmas appears to be intimately related to the subduction process.

The Aleutian arc is sparsely populated (<10,000 inhabitants) and the few villages that exist are widely dispersed (fig. 1). Atka is the westernmost Aleut village in the Aleutian chain; regions further west constitute a restricted federal military reserve area. Despite the low population of the Aleutian arc, the continued exploitation of the rich fisheries of the Bering Sea and North Pacific Oceans has made the region increasingly economically important. At least two of the prime centers for this industry, Unalaska and Akutan, have particularly promising geothermal resources nearby. The village of Atka, which has the potential of becoming a third fishing center, also has a promising geothermal resource nearby.

Assessment work on thermal-spring sites in Alaska is part of a joint State of Alaska - U.S. Department of Energy program to determine the hydrothermal resource potential of Alaska. More than 100 hot-spring sites are reported to exist in the state, with significant concentrations and belts of thermal springs along the Aleutian Range, in southeastern Alaska, and across central Alaska. The first comprehensive inventory of the thermal

Figure 1. Reported thermal spring sites, Aleutian Arc, Atka Island to Becherof Lake.

EXPLANATION

Thermal-spring sites

1. Atka West
2. Atka North
3. Korovin
4. Kliuchef
5. Seguam
6. Chuginadak
7. Kagamil
8. Geysers Bight
9. Hot Springs Cove
10. Partov
11. Okmok
12. Bogoslof
13. Glacier Valley
14. Makushin Valley
15. Summer Bay
16. Akutan
17. Akun

18. Unimak
19. False Pass
20. Kenmore
21. Egg Island
22. Frosty Peak
23. Cold Bay
24. Emmons Lake
25. Pavlof
26. Balboa Bay
27. Port Moller
28. Stepovak Bay
29. Port Heiden
30. Surprise Lake
31. Mother Goose
32. Mt. Peulik
33. Ukinrek
34. Gas Rocks

•   Sampled, 1980
o   Not visited, 1980
*   Not found, 1980
□   Activity diminished
*   Village

springs of Alaska was published in 1917 by Waring. Since then brief summaries of Alaskan thermal springs have appeared in Waring (1965), Miller (1973), White and Williams (1975), and Muffler (1979). The most recent comprehensive summaries of Alaska thermal spring investigations have been compiled by Markle (1979) and by Turner and others (1980).

The scope of the initial assessment of geothermal resources as undertaken by DGGS includes: 1) investigating all thermal-spring sites previously reported but not visited or studied by a scientific team, 2) providing up-to-date data and more detailed studies of previously investigated sites, and 3) locating and investigating any additional thermal-spring sites not previously reported. The assessment work includes reconnaissance of site geology and hydrology, investigation of thermal-spring characteristics including temperatures and flow rates, and geochemical sampling and analysis of the rocks and thermal waters at the site. This information is used to describe the site, to estimate reservoir temperature, to determine the extent of mixing of thermal waters with colder waters whenever possible, and to evaluate the geothermal energy potential of the site. As the initial investigation and assessment of thermal-spring sites in various regions of Alaska are completed, the information compiled is released in DGGS open-file reports. The first in this series is the preliminary evaluation of thermal-spring sites in southern Southeastern Alaska (Motyka and others, 1980). The data for all the thermal-spring sites of Alaska will eventually be compiled into a geothermal atlas. The information is also being used to help select specific sites with the most potential for geothermal energy use and to formulate recommendations for follow-up studies at these sites.

USE OF THE REPORT

The purpose of this open-file report is to provide a ready reference of detailed, current data bearing on the potential uses of hydrothermal systems of the central and eastern Aleutian arc. The report is organized into several sections so that the reader, depending on his familiarity with geothermal resources and their methods of investigation, can use any part of the report separately. The first section is a brief discussion of hydrothermal convective systems. The next part deals with data acquisition and sampling procedures, methods and precision of laboratory analyses, and geothermometric models. Detailed discussions of each site investigated follow next and include the location, general description, geology, spring characteristics, reservoir properties, and comments. The final section provides a general summary of identified central and eastern Aleutian-arc hydrothermal systems. For convenience, a list of abbreviations and unit symbols used in this report is provided in Appendix A. Precision of water analyses is given in Appendix B. A summary of Aleutian Arc hot spring water chemistry is given in Appendix C.

HYDROTHERMAL CONVECTION SYSTEMS

Hydrothermal convection systems consist of a heat source, a fluid, and a rock medium having adequate vertical permeability to allow hot, low-density fluids to rise and more dense, cooler fluids to descend

elsewhere in the system. In hydrothermal convection systems, most of the heat is transported by convective circulation of fluids rather than by thermal conduction through solid rocks.

Hydrothermal systems are classified into two main types---vapor dominated and hot water---according to the phase controlling heat and mass transfer in the deep thermal reservoir (White and others, 1971). Vapor-dominated systems have deep reservoirs controlled predominantly by steam, usually at temperatures $\sim 240^{o}C$. Their surface activity is characterized by fumaroles, acid-sulfate springs, and acid-leached ground with hot-spring chloride levels usually below 50 ppm. Such systems are attractive for electric power generation because they are generally clean and normally require little more than drilling into the steam reservoir for the development of power. However, vapor-dominated systems are relatively rare and occur only under unusual geological conditions. One example is the Geysers in northern California, which has been used for electrical power generation for several decades. No deep vapor-dominated systems have yet been conclusively identified in Alaska, although several sites in the Aleutians appear to have at least shallow vapor-dominated zones (this report).

Hot-water systems are dominated by circulating liquid that transfers most of the heat and largely controls subsurface pressures, although moderate amounts of steam may also be present; surface activity is characterized by the presence of springs discharging thermal water with chloride levels above 50 ppm and with neutral to alkaline pH. Some hot-water systems boil at depth, and the escaping steam forms a shallow vapor-dominated zone and causes fumaroles and acid-sulfate springs, similar to the surficial features of deep vapor-dominated systems. Hot-water convection systems are divided into three temperature ranges (White and Williams, 1975):

1) High-temperature systems: reservoir temperatures are above $150^{o}C$. Such systems can be used for a variety of applications, including the generation of electricity, space heating, and processing. At least five high-temperature systems have thus far been identified in the Aleutian arc (this report).

2) Intermediate-temperature systems: reservoir temperatures are between $90^{o}C$ and $150^{o}C$. These systems can be used for space heating, some industrial processing purposes, and perhaps aquaculture. Future technological advances may eventually make electrical generation from intermediate systems practical. At least 28 intermediate-temperature systems have been identified in Alaska.

3) Low-temperature systems: reservoir temperatures lie below $90^{o}C$. Such systems can be used for space heating and perhaps agriculture (e.g., greenhouses), but most likely only in locally favorable circulstances. Over 80 low-temperature systems have so far been identified in Alaska (Turner and others, 1980). Some of these may prove to have higher temperature reservoirs on closer examination.

-7-

FIELD TECHNIQUES AND SAMPLING PROCEDURES

A standard procedure of sample and data acquisition was followed at each thermal area visited. At sites having multiple springs, water samples were normally obtained from the thermal spring with the highest temperature and greatest discharge. At some sites more than one thermal spring was sampled. When cold ground-water springs were found in the immediate area, samples were normally taken for silica analysis for subsequent silica mixing models.

Water samples were collected, filtered, and treated following procedures described in Presser and Barnes (1974). The samples were always obtained at the spring source or as close to the source as possible. Filtration was usually through a 0.45-micron filter. Some samples, however, were filtered through 0.05- or 0.1-micron filter for aluminum and iron determinations. Thermal-water samples obtained for silica analysis were normally diluted in a 1:10 ratio with de-ionized distilled water to prevent precipitation and polymerization of silica as the sample cooled. Hydrochloric acid was used for those samples requiring acidification.

Bicarbonate and pH were determined in the field using methods described by Barnes (1964). Field pH values were determined to the nearest 0.05 pH unit. The pH meter was normally calibrated against standard buffer solutions before and after each measurement. Readings were normally reproducible to $\pm$ 0.05 pH units. Waters were titrated with 0.01639N sulfuric acid for bicarbonate determinations.

Water conductance is reported in micromhos per centimeter at 25°C with a measurement accuracy of $\pm$ 3 percent. The manufacturer's calibration of conductivity cells was verified against standard solutions prior to departure for the field.

Water temperatures and shallow soil temperatures were measured with digital thermistor thermometers. All measurements are reported in degrees Celsius. The resolution and accuracy of the digital thermometer are 0.05°C and 0.1°C, respectively. Spring temperature measurements were usually made at or as close to the spring orifice as possible.

Wherever possible, spring discharge was measured by using a pygmy flow meter and reported in liters per minute (lpm). Accuracies of these measurements were commonly impaired by shallow channels, low water velocities, and friction in the vane bearings. At some springs the discharge was determined by the time to fill a 4-liter bucket. When it is not possible to measure discharge by either of these two methods, a visual estimate was made.

A reconnaissance of site geology was normally made at each thermal area. This entailed examination and sampling of local bedrock, determination of local faults and fracture systems, and examination and sampling of hot-spring deposits, if any.

LABORATORY ANALYSES: METHODS USED AND PRECISION

Whenever possible, laboratory methods of determination used by DGGS were taken from the list of methods of choice for each chemical species as prescribed by Presser and Barnes (1974). Table 1 summarizes the methods used and presents the expected precision of laboratory analyses for 17 constituents commonly found in water as determined by U.S. Geological Survey laboratories. Atomic-absorption analyses were run on a Perkin-Elmer model-603 spectrophotometer with air-acetylene and nitrous-oxide-acetylene flames under conditions listed in the manufacturer's procedure manual. Colorimetric determinations were made on a Hitachi 100-60 VIS-UV double-beam spectrophotometer with a matched set of four 10-mm cells. An Orion model-701 digital pH meter and Orion specific ion and reference electrodes were used in the measurement F^-. DGGS water-analysis procedures conform to USGS established methods and quality assurance.

Most of the precisions given in table 1 for the various methods of analysis are based on data obtained through multilaboratory analysis of test samples prepared by USGS laboratories (Skougstad and others, 1979). Where possible, precision is expressed in terms of a regression equation over a stated range. The precision, expressed in terms of the relative deviation (the ratio of the standard deviation to the mean times 100 percent) for various laboratory determinations, is given in Appendix B.

GEOTHERMOMETRY

Chemical geothermometry has become an important tool for estimating reservoir temperatures of hydrothermal systems and has proved very useful in determining the geothermal resource potential of a specific region. Therefore, much of the DGGS assessment work is aimed at providing accurate geothermometry for the individual geothermal sites investigated. Summaries of the various geothermometers that have been applied to geothermal systems can be found in Fournier (1977) and Ellis and Mahon (1978). The geothermometers are based on temperature-dependent, water-rock reactions that control the chemical and isotopic compositions of the thermal waters. The most reliable and most frequently used quantitative geothermometers are related to the silica content and to the sodium, potassium, and calcium content of thermal waters. Recent application of sulfate-water, oxygen-isotope geothermometry to geothermal systems indicates this method may become a third important geothermometer, particularly for higher temperature systems (McKenzie and Truesdell, 1977).

-9-

Table 1. Methods and expected precision: DGGS water-chemistry analyses

Chemical	Reference	Description of method	Precision[a]
SiO_2	A, p. 495	Colorimetric; formation and reduction of silicomolybdate	$S_T = 0.031 \, x + 0.60$ (mg/1) Range: 2.0 to 40 mg/1
Al	B, p. 6 A, p. 39 F	AA[b]; chelation with 8-hydroxyquinoline and extraction with MIBK	$S_T = 0.073 \, x + 14.97$ (ug/1) Range: 75 to 800 ug/1
Fe	A, p. 153	AA; direct aspiration	$S_T = 0.056 \, x + 23.90$ (ug/1) Range: 80 to 1,000 ug/1
Ca	A, p. 107	AA; $LaCl_3$ added	$S_T = 0.057 \, x + 0.343$ (mg/1) Range: 0.1 to 60 mg/1
Mg	A, p. 177	AA; $LaCl_3$ added	$S_T = 0.043 \, x + 0.134$ (mg/1) Range: 0.5 to 36 mg/1
Na	A, p. 255	AA; direct aspiration, 2,000 ppm K added	$S_T = 0.039 \, x + 0.448$ (mg/1) Range: 3 to 80 mg/1
K	A, p. 229	AA; direct aspiration, 2,000 ppm Na added	App. B
Li	A, p. 171	AA; direct aspiration	$S_T = 0.048 \, x + 4.84$ (ug/1) Range: 30 to 500 ug/1
HCO_3	A, p. 517, B, C	Potentiometric titration in the field for alkalinity by using 0.01639N H_2SO_4 and calculation from alkalinity and pH data	$\pm$ 2.0 ppm (C)
SO_4	A, p. 615	Conversion to H_2SO_4 then titration with with $BaCl_2$ in presence of thorin indicator	$S_T = 0.046 \, x + 0.575$ Range: 0.5 to 20 mg/1

Chemical	Reference	Description of method	Precision[a]
Cl	A, p. 589	Mohr titration with $AgNO_3$	$S_T = 0.034\,x + 0.33$ (mg/l) Range: 1.0 to 210 mg/l
F	A, p. 523, E	Direct reading using specific ion electrode, Orion TISABII added. (CDTA adjustor and buffer)	App. B
Br	A, p. 581	Dissolved, titimetric, hypochlorite oxidation	$S_O = 0.0044\,x$
I	A, p. 595	Bromine oxidation, then titration with 0.01 N Na thiosulfate	$S_O = 0.009\,x$ Range: 1.0 to 50 mg/l
B	A, p. 311	Colorimetric; complexing with carmine	$S_T = 0.463\,x + 20.2$ (ug/l) Range: 30 to 550 ug/l
H_2S	B, p. 7	Preservation with Zn acetate, then titration with Na thiosulfate in presence of iodine	0.5 ppm detection limit
Sr	A, p. 263	AA; direct aspiration, 1,000 ppm K added, N_2O - acetylene flame	$S_T = 0.104\,x + 15.4$ Range: 0.01 + 5 mg/l
pH	C	- -	$\pm$ 0.05 pH units

[a]X = Concentration in mg or ug/l. Quoted precisions are from Skougstad and others (1979) unless otherwise noted.
[b]AA = Atomic-absorption spectrometer

References:

A. Skougstad and others, 1979.
B. Presser and Barnes, 1974.
C. Barnes, 1964.
D. Rand and others, 1975.

E. Instruction manuals for Orion Ionalyzer Specific Ion Electrodes, 1977, by Orion Research Inc.
F. Barnes, 1975.

Assumptions inherent in using compositions of thermal waters to estimate subsurface temperatures have been summarized by Fournier (1977):

1. Temperature-dependent reactions involving rock and water fix the amount or amounts of dissolved "indicator" constituents in the water.

2. There is an adequate supply of all the reactants.

3. There is equilibrium in the reservoir or aquifer with respect to the specific indicator reaction.

4. No reequilibration of the "indicator" constituents occurs after the water leaves the reservoir.

5. Either no mixing of different waters occurs during movement to the surface or evaluation of the results of such mixing is possible.

The attainment of equilibrium in the reservoir depends on factors such as the kinetics of the particular reaction, the temperature of the reservoir, the reactivity of the wallrock, the concentrations of the indicator elements in the water, and the residence time of the water in the reservoir at the particular temperature. Thus, in some situations, equilibrium in the reservoir may be attained for some reactions and not for others.

Whether a water reequilibrates after leaving a reservoir during flow to the surface depends on similar factors: the rate of flow, the path of ascent, the type and reactivity of wallrock traversed, the initial temperature of the reservoir and the kinetics of the various reactions that may occur. Different reactions may occur in an ascending water at different rates. Therefore, the apparent last temperature of equilibration may be different for different chemical geothermometers.

In this report the silica and cation geothermometers have normally been used for estimating subsurface temperatures. In a few cases sulfate-water oxygen isotope thermometers, obtained through the cooperation of N. Nehring, USGS (Menlo Park, CA), are also available.

The silica geothermometer is based on the experimentally derived relationship between silica solubility, temperature, and pressure (Fournier and Rowe, 1966; Fournier, 1973). Dissolved silica found in thermal waters may be supplied by temperature-dependent reactions between the thermal water and quartz, chalcedony, amorphous silica, or cristobalite. Curve a of figure 2 shows the solubility of quartz as a function of temperature in equilibrium with saturated steam. Curve b shows the amount of silica that would be left in the residual liquid after maximum loss of steam on adiabatic cooling to 100°C and 1 bar pressure. Similar curves can be constructed for the other mineralogic phases of silica.
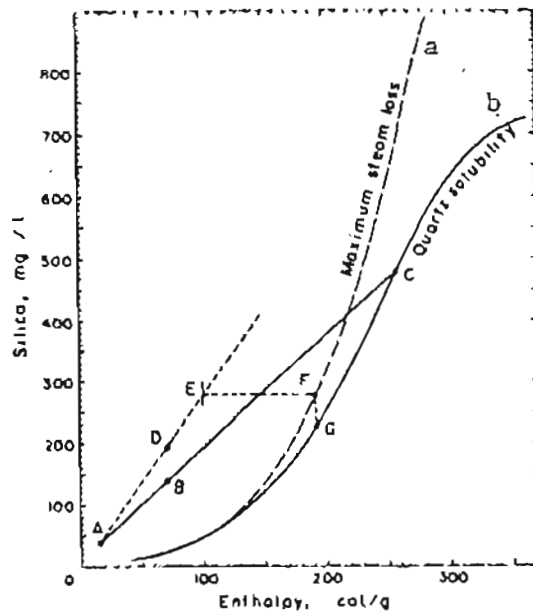
Figure 2. Silica mixing model examples. The graph, which gives the dissolved silica vs enthalpy, is used for determining the temperature of warm spring water derived by mixing a hot-water component with cold water (from Turesdell and Fournier, 1977). Solubility of quartz as a function of temperature is also shown. Curve a shows the solubility in liquid water in equilibrium with saturated steam. Curve b shows the amount of silica that would be left in the residual liquid after maximum loss of steam on adiabatic cooling to 100°C and 1 bar pressure (from Fournier and Rowe, 1966).

Fournier (1973) found that above 150°C, quartz controls the silica equilibrium and that the quartz geothermometer generally works best in the range 150°-225°C. When initial temperatures are above 225°C, silica is likely to precipitate on ascent to the surface because of relatively fast rates of reaction at higher temperatures and the attainment of supersaturation with respect to amorphous silica as the solution cools.

-13-

For reservoirs below 150°C Fournier (1973) found that chalcedony and sometimes cristobalite or amorphous silica rather than quartz may control the dissolved silica content. However, in granitic rocks Fournier reported that quartz may be the controlling mineral down to temperatures as low as 90°C (Brook and others, 1979). Thus, ambiguities can arise from the application of silica geothermometry in the temperature range 90°-150°C.

Figure 2 and similar curves for the other phases of silica can be used to estimate reservoir temperatures. If the water sample is likely to have cooled mainly adiabatically, curve B, which corrects for the maximum possible steam loss, is used. If the sample cooled mainly by conduction, curve A is used.

The following empirical relationships can alternatively be used to estimate reservoir temperature in the range 0°-250°C (where C is the concentration of SiO_2 in mg per kg water).

Amorphous silica $\qquad T, \degree C = \dfrac{731}{4.52 - \log C} - 273.15$

Beta-cristobalite $\qquad T, \degree C = \dfrac{781}{4.51 - \log C} - 273.15$

Alpha-cristobalite $\qquad T, \degree C = \dfrac{1000}{4.78 - \log C} - 273.15$

Chalcedony $\qquad T, \degree C = \dfrac{1032}{4.69 - \log C} - 273.15$

Quartz conductive $\qquad T, \degree C = \dfrac{1039}{5.19 - \log C} - 273.15$

Quartz adiabatic (after steam loss) $\qquad T, \degree C = \dfrac{1522}{5.75 - \log C} - 273.15$

Brook and others (1979) have reviewed the problems associated with interpreting high SiO_2 levels in highly alkaline spring waters (pH>8). In alkaline waters, hydroxide reacts with silicic acid to reduce the proportion of silicic acid to total dissolved silica:

Silicic acid		Hydroxide		Dissociated silicic acid		Water
H_4SiO_4	+	OH^-	=	$H_3SiO_4^-$	+	H_2O
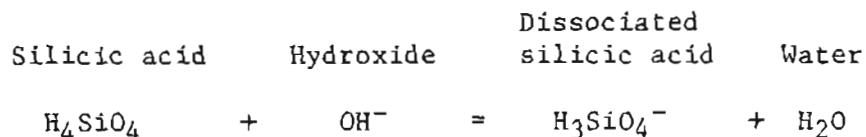
The total dissolved silica increases with increasing hydroxide concentration. The total concentration of dissolved silica measured in the laboratory, however, is H_4SiO_4 plus $H_3SiO_4^-$ and must therefore be reduced by the concentration of $H_3SiO_4^-$ to obtain an accurate estimate of the

subsurface reservoir temperature. There is considerable disagreement about the value of the first dissociation constant of silicic acid at temperatures above 30°C (Seward, 1974). The values used in this report were taken from Ryzhenko (1967).

Most geothermal reservoirs are likely to be below pH 7.5 because of buffering of hydrogen ions by silicate hydrolysis reactions (Fournier, pers. comm.). pH values higher than 7.5 in natural hot spring waters generally result from the loss of CO_2 after the water leaves the high-temperature reservoir. In this report, if there is other supporting evidence that a thermal water comes from a higher-temperature environment at depth, a pH correction has not been applied to the observed silica concentration.

Silica Mixing Models

One of the assumptions inherent in using geothermometry is that thermal spring waters are undiluted. However, the waters issuing from many, if not most, thermal springs probably consist of mixtures of deep hot water and shallow cold water. Fournier and Truesdell (1974) described two mixing models that may be applied to springs with large rates of flow and temperatures below boiling. These models are based on the relationship between the enthalpy and silica content of the ascending thermal water, the cold ground water, and the resultant mixed thermal spring water. In the first model the enthalpy of the hot water plus steam that mixes with and heats the cold water is the same as the initial enthalpy of the deep hot water. In this model the deep hot water may boil below mixing, but all the steam condenses in the cold water. In the second model the enthalpy of the hot water in the zone of mixing is less than the enthalpy of the hot water at depth because of the escape of steam during ascent.

Barrett and Pearl (1978) have summarized the additional assumptions, given below, which are implicit in the use of these mixing models:

1. Initial silica content is controlled by the temperature-dependent reactions between the deep thermal water and the various silica phases.

2. Additional silica is neither dissolved nor deposited after mixing.

3. The temperature and silica content of cold springs are similar to the temperature and silica content of the ground water that mixes with the ascending hot water.

Truesdell and Fournier (1977) have devised a simple procedure for applying these models; by using a plot of dissolved silica vs enthalpy (fig. 2). For the situation in which no steam is lost before mixing, the silica and heat contents (enthalpies) of the cold and warm spring waters are plotted as two points, A and B. A straight line is drawn through

these points to intersect the quartz solubility curve (note that below 100°C the temperature in degrees Celsius is numerically equivalent to cal/g). Point C then gives the original silica content and enthalpy of the deep hot water. The original temperature of the hot-water component is then obtained from steam tables (Keenan and others, 1969). The fraction of hot water in the warm spring is obtained by dividing the distance AB by AC.

For the situation in which the maximum amount of steam is lost from the hot water before mixing, the silica and heat contents of the cold and warm spring waters are plotted as two points, A and D, in figure 2. A straight line is drawn through these points and extended to the enthalpy of the residual liquid water at the assumed temperature of separation and escape of steam, taken here to be 100°C. In this case the residual liquid water before mixing will have an enthalpy of 100 cal/g, point E of figure 2. The original enthalpy of the hot-water component is obtained by moving horizontally across the diagram from point E to the maximum steam loss curve, point F. The original silica content of the hot-water component is given by point G. The fraction of hot water (after steam loss) in the warm spring is obtained by dividing the distance AD by AE. If steam is assumed to escape from water at a temperature above 100°C, the original enthalpy of the hot water will lie at a value along a horizontal line between the maximum steam-loss curve and the quartz solubility curve (no steam loss).

Brook and others (1979) have pointed out that the problem with any unexplored hydrothermal system is in proving that the water issuing at the surface is indeed mixed. One proof would be a linear trend between measured spring temperatures and chloride concentration (Fournier, 1979). Normal groundwater usually has low chloride concentrations, whereas thermal waters from high-temperature systems usually contain about several hundred milligrams per liter of chloride. A linear trend between the isotopic composition of the water (deuterium or oxygen-18) and dissolved chloride is another proof of the mixing (Mariner and Willey, 1976). Unfortunately, very few areas have sufficient springs of different chemical and isotopic composition to prove mixing by such rigorous criteria.

Cation Geothermometers

Na-K

The Na-K geothermometer used in this report is based on the empirically derived relationship:

$$T, °C = \frac{1217}{\log (Na/K) + 1.483} - 273.15$$

where Na and K are concentrations of dissolved sodium and potassium in mg/kg. Fournier (1980) has summarized the basis for this thermometer and made recommendations for its use. In general the Na-K method fails

to give reliable results for waters from environments with temperatures
below 100°C. In particular, low-temperature waters rich in calcium
give anomalous results by the Na-K method. Accuracy of the thermometer
increases over the range 125°C to 200°C.

Where waters are known to come from high-temperature environments
(180°C to 200°C), the Na-K method generally gives excellent results. The
main advantage of the Na-K geothermometer is that it is less affected by
dilution and steam separation than other commonly used geothermometers,
provided there is little Na^+ and K^+ in the diluting water compared to the
reservoir water.

Na-K-Ca

The Na-K-Ca geothermometer is based on an empirical relationship
between the concentrations of sodium, potassium, and calcium ions and
water temperature. Fournier and Truesdell (1973) have presented a
detailed account of the geochemical theory involved in the Na-K-Ca
geothermometer which was specifically developed to deal with calcium-
rich waters that gave anomalously high calculated temperatures by the
Na-K method. Temperature is related to water composition by the
following empirically derived equation:

$$T, °C = \frac{1647}{\log (Na/k) + B [\log (Ca/Na) + 2.06] + 2.47} - 273.15$$

where:

Na, K, Ca = ionic concentration in mg/kg of the sodium, potassium,
            and calcium ions in the hot water.

T, °C = estimated subsurface temperature in degrees Celsius.

B = 1/3 for $T > 100°C$.

B = 4/3 for $T < 100°C$.

The equation is first tested to see if setting B equal to 4/3
yields a temperature below 100°C; if it does not, a value of 1/3 is
used for B to estimate the equilibrium temperature.

Barret and Pearl (1978) have summarized the assumptions for the
use of the Na-K-Ca geothermometer:

1) No mixing occurs between the ascending thermal water and
    shallow ground water.

    Mixing between the hot thermal water and shallow, diluted,
    ground water will have little effect on the sodium-potassium
    ratio but may affect the calculated calcium-sodium ratio because
    of the square-root-of calcium term. If the original calcium content

-17-

of the undiluted thermal water is low, mixing will have little effect
on the geothermometer results. But if that content is high (<50 to
100 mg/l), mixing with dilute ground water will cause the subsurface
temperature estimate to be too low.

2) Sodium, potassium, and calcium concentrations in the thermal
   water are controlled by temperature-dependent equilibria with
   sodic plagioclase, potassium feldspar, and calcium-bearing
   carbonate minerals.

The sodium, potassium, and calcium ratios are strongly affected
by the bedrock mineral suite. Depending on which mineral suite
controls the water composition, a wide range in temperature estimates
is possible. At similar water temperatures, the sodium-potassium-
calcium ratios are widely variable in solutions equilibrated with
potassium feldspar and albite, muscovite and albite, alkali-bearing
carbonates, or other mineral suites.

For example, waters equilibrated with mineral suites con-
taining potassium feldspar but no albite (sodium-deficient mineral
suites) will provide excessive subsurface temperature estimates.
On the other hand, waters equilibrated with mineral suites contain-
ing albite but no potassium feldspar (potassium-deficient mineral
suites) yield temperature estimates that are too low. Waters in
equilibrium with alkali-bearing carbonates (evaporite sequences)
generally yield excessive temperature estimates. However, equili-
bration with zeolites may yield minimum temperature estimates.

3) Little or no reequilibration occurs during ascent.

Changes in the sodium-potassium-calcium ratios in thermal
waters may be great or negligible, depending on the rate of ascent
and the relative reactivity of the rocks and minerals along the
flow path. Low-calcium thermal waters generally yield low sub-
surface temperature estimates because of continued reactions between
water and wallrock during ascent (increased aqueous calcium-ion con-
centration). High calcium-content waters, however, may yield
excessive geothermometer temperature estimates because of calcium-
carbonate deposition (decreased aqueous calcium ion concentration)
during ascent.

Fournier and Potter (1978) reported that the high concentration
of magnesium or the large magnesium-to-calcium ratios in some waters
was interfering with the Na-K-Ca geothermometers. A modification
to the Na-K-Ca geothermometer used in this assessment was recently
devised by Fournier and Potter to correct for these adverse effects
of magnesium. Graphs or empirical formulas are used to determine
temperature corrections when waters have Na-K-Ca calculated tempera-
tures above $70^{\circ}C$ and values of R less than 50, where $R = Mb/(Mg + Ca + K)$

x 100 in molar equivalents. Waters with values of R greater than 50 are thought to come from relatively cool aquifers about equal to the measured spring temperature, regardless of much higher calculated Na-K-Ca temperatures.

Sulfate-water Oxygen Isotope Geothermometer

The sulfate geothermometer has recently found wide acceptance as a reliable indicator of deep geothermal reservoir temperatures (Muffler, 1979; Nehring and others, 1980). A summary of previous work leading to the development of this thermometer and detailed explanation of its application can be found in McKenzie and Truesdell (1977).

The sulfate geothermometer is based on the assumption that the oxygen isotopes in a water and its dissolved sulfate have equilibrated in the geothermal reservoir. The equation for the equilibrium fractionation between dissolved sulfate and water used by McKenzie and Truesdell (1977) is:

$$100 \ln \alpha = 2.88 \ (10^6/T^2) - 4.1$$

$$\text{where } \alpha = \frac{1000 + \delta^{18}O \ (SO_4)}{1000 + \delta^{18}O \ (H_2O)}$$

and T is in $^{\circ}K$. Oxygen isotope values are relative to standard mean ocean water (SMOW) as defined by Craig (1963).

The method of cooling that the water undergoes as it ascends to the surface can affect the $\delta^{18}O$ in the water. Three end-member cases have been discussed by McKenzie and Truesdell (1977) and summarized in Nehring and others (1980). T1 is calculated assuming conductive cooling with no steam loss and, therefore, no change in the $\delta^{18}O$ of the water. T1 is the best temperature estimate when the spring or well is substantially below boiling and in well samples collected with a downhole sampler. T2 is calculated assuming adiabatic cooling where the steam stays in contact with and in isotopic equilibrium with the water until the mixture reaches the surface, where steam loss occurs. T2 is the best temperature estimate for isolated springs of near-boiling temperature and well samples with two-phase flow. T3 is an extreme case of continuous steam loss by the water from the time it leaves the reservoir until it reaches the surface. This case is most applicable to hot springs associated with fumaroles or steaming ground.

The validity of temperatures determined by sulfate geothermometry is adversely affected by mixing of different waters unless corrections are made for changes in isotopic composition of both the sulfate and

water that result from that mixing. A suite of samples may be necessary to correct for dilution by ground water; such corrections were not made in this report.

The formation of sulfate by oxidation of H_2S at low temperatures can also affect the sulfate-oxygen isotope geothermometer. A small amount of low-temperature sulfate can cause a large error in the geothermometer result. Near-surface sulfate can be minimized by selecting the spring with the lowest $SO_4:Cl$ ratio in a group whenever possible. Furthermore, if the $SO_4:H_2S$ ratio is less than 25, the sample should be preserved either by adding Zn, Cd, or other heavy metal to precipitate the H_2S (Nehring and others, 1980). Near-surface sulfate can form from the oxidation of H_2S to H_2SO_4 by sulfur-oxidizing bacteria. A small amount of formaldehyde to kill the bacteria was added to each water sample collected for sulfate-oxygen isotope analysis by DGGS.

Accuracy of Geothermometry

The accuracy of the geothermometers depends on the accuracy of the laboratory analyses for the various constituents used in the geothermometers. The following example illustrated the possible variations in subsurface temperature estimates resulting from normal laboratory analytical error. The 95 percent confidence limits (two times the standard deviation) can be determined from table 1 and Appendix B. With data from Bell Island Hot Springs (Motyka and others, 1980), the variations in constituents used in the silica and cation geothermometers are:

Constituent		Variation
SiO_2	:	108 ± 8 mg/l
Na	:	176 ± 14 mg/l
K	:	7.2 ± 1.6 mg/l
Ca	:	8.3 ± 1.6 mg/l

Applying these ranges of values to the silica and the Na-K-Ca geothermometers gives the following results:

Silica geothermometer	Temperature (^{o}C)		
	Low	Reported	High
Concentration (mg/l)	100	108	116
Adiabatic	133	136	140
Conductive	137	142	146
Chalcedony	110	115	120
Cristobalite	87	91	95
Opal	17	21	25

Cation geothermometer	Temperature (°C)		
	Low	Reported	High
Na-K-Ca (1/3)	129	144	158
Na-K-Ca (4/3)	103	117	130

The low and high temperature ranges given above for the cation geo-
thermometers are based on using the respective minimum and maximum values
in the 95-percent range for Na and Ca, and the maximum and minimum
values, respectively, in the 95-percent confidence range for K. These
choices give the widest possible spread in temperature estimates.

FORMAT FOR DESCRIPTION OF INDIVIDUAL-THERMAL SPRING SITES

The locations of thermal spring areas visited by DGGS in the Aleutian
arc in 1980 are shown in figure 1 and on the generalized geologic maps of
the region in figures 3 and 4. A summary of thermal-spring water geo-
chemistry is given in Appendix C. Lack of time and other factors prevented
investigation of several of the more remote thermal-spring sites. The
existence of several other thermal spring-sites that had previously been
reported could not be substantiated. Other sites reported active in the
past were found to be inactive.

In this report, a general description of the larger Aleutian Islands
is given, followed by a discussion of the individual thermal areas occur-
ring on the particular island, a slight departure in format from a pre-
vious open-file report (Motyka and others, 1980). The individual thermal
areas are described in geographical order eastward from Atka Island to
Becherof Lake. The following form is used in discussing each thermal
spring site investigated:

1. Location: (includes latitude and longitude to the nearest tenth
   of a minute; the topographic quadrangle map and township, range,
   section, and one-quarter section in which the site is located)

2. General description: (includes distance and directions to the
   area from the nearest town or other prominent geographic feature;
   type of surface activity; location and number of springs; area
   of surface activity; location and number of springs; area of
   surface expression; local drainage; topography and terrain; vege-
   tation; type of development if any; and land status)

3. Geology: (includes discussion of thermal-spring host rock; local
   rock types and contacts; and local and regional faults, fractures,
   and photo interpretation of lineaments. A geologic map of the
   area is normally provided; these maps are usually adapted from
   previously published geologic maps of the area, modified by any
   findings obtained during DGGS reconnaissance of the area).
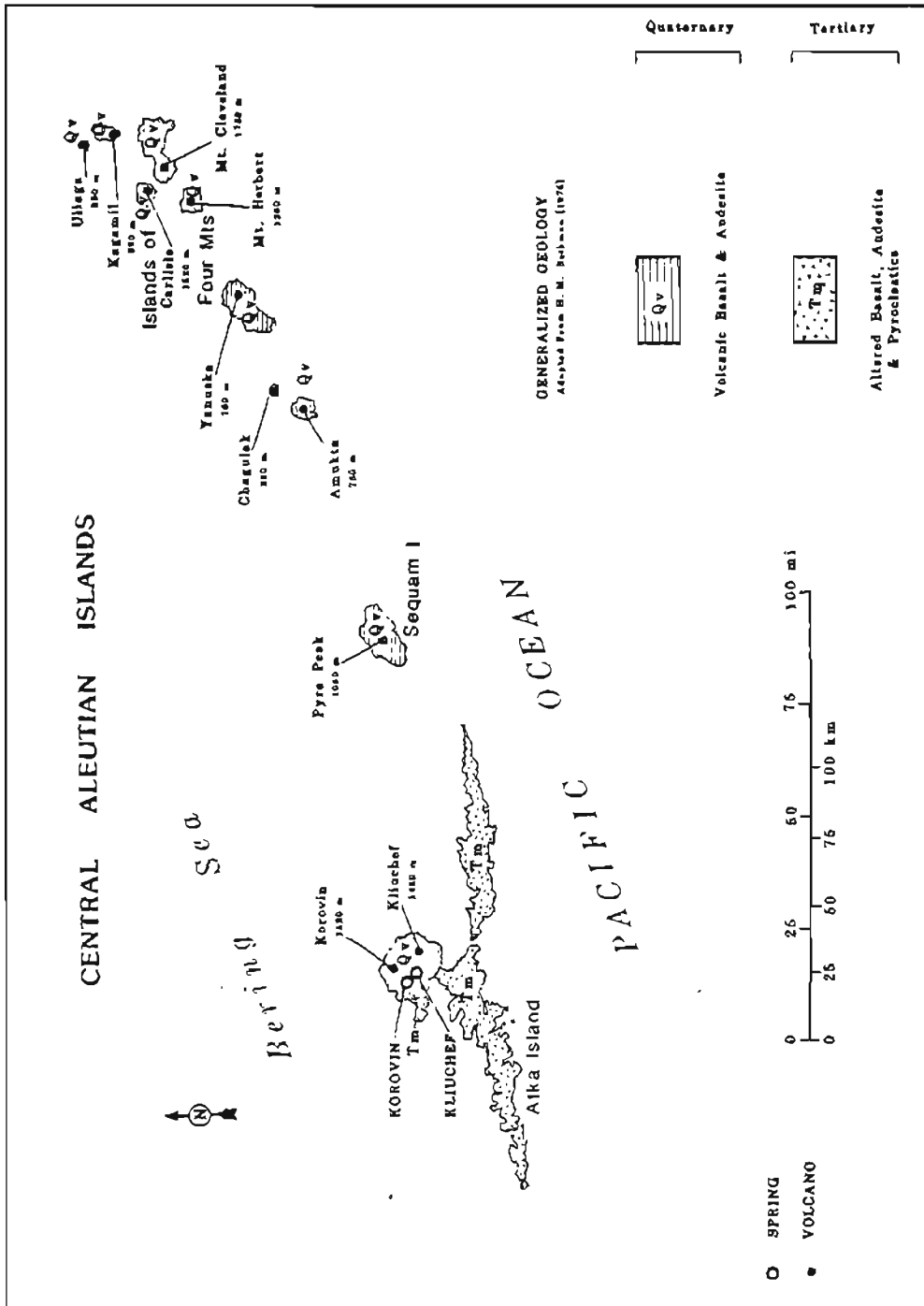
Figure 3. Generalized geology of the central Aleutian Islands.

Figure 4. Generalized geology of the eastern Aleutian Islands.

-23-

4. Spring or thermal-vent characteristics: (includes temperature measurements; associated deposits; gases; unusual characteristics; water chemistry; water type; other physical properties; and comparisons with earlier studies).

5. Reservoir properties: (includes discussion of geothermometry; mixing models where applicable; and estimates of reservoir temperature, volume, and thermal energy content).

The techniques described by the USGS for estimating reservoir properties have been adopted in this report (Brook and others, 1979; Mariner and others, 1978; Nathenson, 1978). A judgment is made as to the minimum, maximum, and most likely subsurface temperature based on geology and geothermometry, and on geophysics and downhole measurements where available. (Subsurface temperatures derived from silica mixing models are not used in estimating reservoir temperatures in this report unless corraborative evidence for mixing exists e.g., chloride-enthalpy analyses or water-oxygen isotope analyses.)

Estimates of reservoir volume are made from available geologic, geophysical, and bore-hole data. Few thermal sites in Alaska, however, have had even cursory geophysical exploration and only two sites, Pilgrim Springs (Turner and others, 1980) and Summer Bay on Unalaska Island (DGGS, unpub. data), have exploratory wells.

6. Comments: (speculates on the cause of the thermal springs; the potential usefulness of the geothermal resource; unusual characteristics; and other miscellaneous items)

7. Tables:

a) (physical properties and chemical composition of thermal waters, including sample source, collection date, major-element chemical composition, discharge rate of spring sample, temperature, etc.)

b) geothermometry, including all cation, all silica, and mixing models where applicable.

8. Figures:

a) geologic map generalized from available literature.

b) sketch of site.

NORTHEAST ATKA ISLAND

Background

Atka Island is located in the Andreanof group of the central
Aleutian chain, at approximately 52°15' latitude and 174°15' longi-
tude (fig. 1 and 3). Intense Pleistocene glaciations have rendered a spec-
tacular and rugged landscape: broad glacial valleys, numerous cirques,
hanging valleys, glacial lakes, and several deep fjord like embay-
ments on both the Bering and Pacific coastlines. Sea mammals, particu-
larly sea otters, abound in the protected inlets of the island. The
glacial topography has been carved into the Tertiary and Quaternary
(basaltic and andesitic) volcanic rocks that constitute the 100-km-long
southwest-trending island. Lush and verdant tundra vegetation blankets
the lower elevations over most of the island.

Quaternary volcanism has been concentrated exclusively in the north-
east part of the island principally at two major stratovolcanoes, Mount
Kliuchef (1,460 m) and Korovin Volcano (1,530 m) the latter of which is
still very active (fig. 5). Northeast Atka is separated from the rest of the
island by a narrow lowland lying between Korovin Bay and Nazan Bay.
Northeast Atka is roughly circular, with a diameter of about 20 km.
Unlike the rest of the island, there are relatively few embayments in
northeast Atka, probably as a result of late Quaternary volcanism. All
the known active thermal areas and hot-springs sites on the island occur
in the northeast part.

The native village of Atka, the only settlement on the island, is
located on the southwest shore of Nazan Bay near a deep, protected
anchorage. Atka served as a staging area and a small military base
during World War II. The old military airstrip and boat dock are pre-
sently in disrepair, but the village corporation is seeking funds to
renovate both facilities. An old military jeep road connects the village
of Atka to Korovin Bay, where a summer fishing camp is maintained.

The village has a population of 120 people and is the western-most
Aleut settlement in the Aleutians. Atka is presently based on a sub-
sistence economy, but the village council has expressed a strong desire
to develop an energy base to attract fishing industries to the area.
Power is presently supplied by diesel generators.

The village is remote and not easily accessible. Biweekly amphibious
air service is maintained between Atka and Adak Island, a U.S. Naval base.
Adak can be reached from Anchorage by commercial airlines. Most of the
village's supplies are brought in by barge in the spring; smaller shipments
and mail are flown in from Adak. If the airstrip is renovated, scheduled
commercial air service to Atka should improve. Lands on northeast Atka
have been selected by the Atka Native Village Corporation under terms of
the Alaska Native Claims Settlement Act.
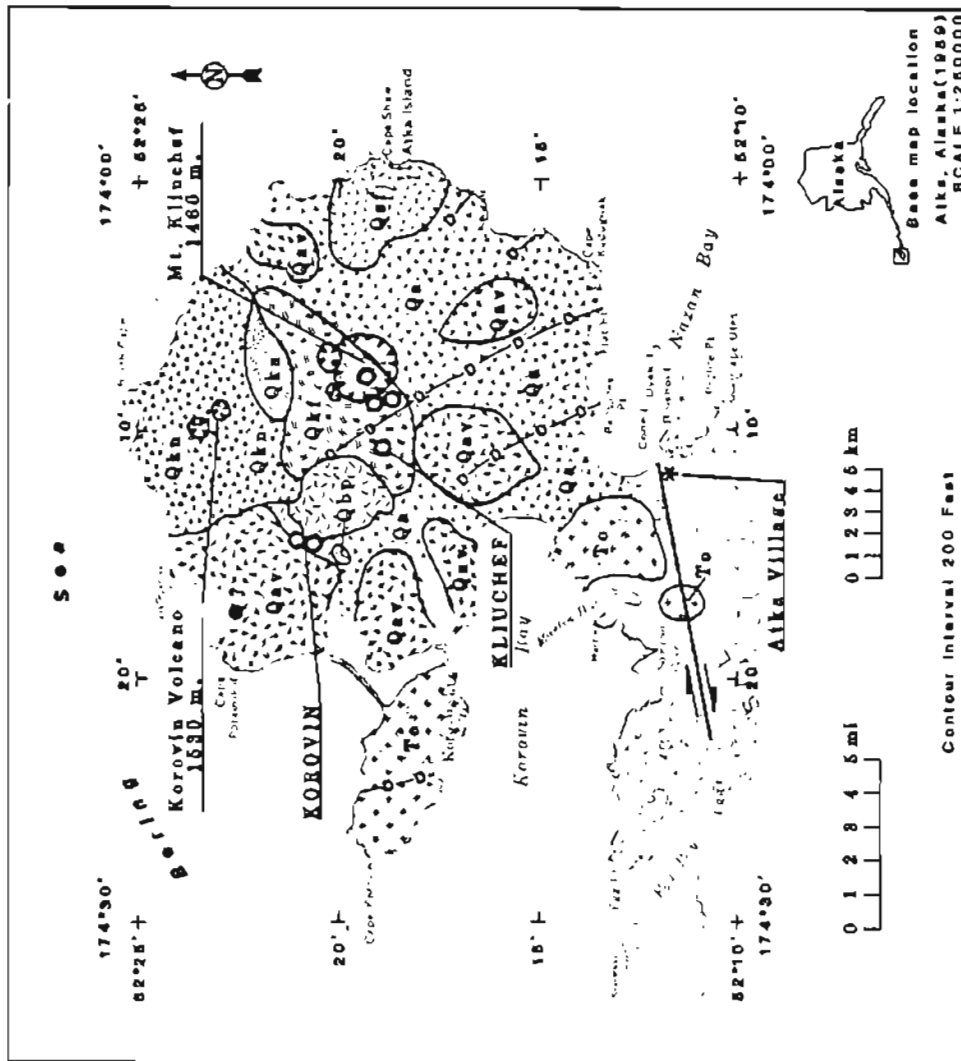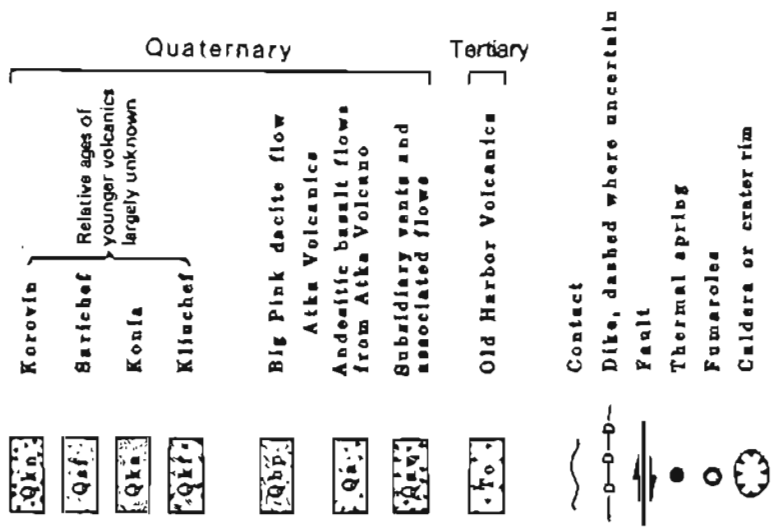
Figure 5. Generalized geology for northeast Atka Island and locations of Kliuchef and Korovin thermal fields.

Geology

Northeast Atka Island consists of a thick sequence of late Tertiary and Quaternary effusive flows, tuffs, breccias, and associated sedimentary rocks. The assemblage records an extensive and on-going period of calc-alkaline volcanism that is coeval with volcanic activity around much of the Aleutian Range. This volcanism is associated with the subduction of the Pacific lithospheric plate under the margin of the North American plate along the Aleutian Trench.

The geology and volcanic history of northeast Atka has been under investigation by B. Marsh at Johns Hopkins University, and the geologic discussion that follows is based on personal communication with him. A preliminary generalized geologic map based on Marsh's work is given in fig. 5. According to Marsh (pers. comm.) the oldest episode of volcanism found in the region is represented by the Old Harbor volcanic series, which crops out around Korovin Bay and consists of basaltic-andesitic to dacitic lava flows, pyroclastic flows, and lahars. These volcanics are thought to be derived from a large shield volcano located in what is now Korovin Bay. On the basis of a preliminary K-Ar age date on a volcanic plug, the Old Harbor series is 6.6 m.y. old.

A second episode of volcanism began about 1.5 to 2.0 m.y. ago with activity near what is now the center of the exposed volcanic field. Atka Volcano, a large ancestral stratocone, developed with a series of at least six subsidiary or satellite vents on its outer flanks. Nearly every flow from the older Atka volcanic complex was found to be an andesitic basalt with a silica content of about 50 percent by weight (Marsh, pers. comm.). A 750-m-thick dacitic flow (Big Pink, fig. 5) is associated with the formation of a 5-km-dia. caldera at Atka Volcano. A hydration date on the dacite suggests caldera formation occurred 300,000 to 500,000 years ago.

Mount Kliuchef developed on the west rim of the caldera and was active in Holocene time. Korovin Volcano, 5 km north of Mount Kliuchef, shows little sign of glacial erosion and probably was formed after Pleistocene time. Aerial photos taken July 21, 1951 show Korovin capped with a 2.5-km-dia. explosion crater that is over 1000 m deep. Korovin Volcano has been active in historic times, with reports of eruptions occurring in 1951, 1974, and 1976. In 1977 Marsh found a recent mudflow at the base of Korovin that was probably related to the 1974 eruption. He also noted changes in summit morphology.

Mount Sarichef (825 m), a dissected subsidiary volcano located 5 km south-southeast of Mount Kliuchef, was reported to have had an ash eruption in 1907 (Dall, 1870), but field observations by Marsh show this to be doubtful. These youngest volcanoes are also primarily andesitic basalt.

Those parts of northeast Atka not covered by recent volcanic flows show the deep erosional effects of the Pleistocene glaciations. Field studies recently done by R. Black (pers. comm.) indicate a post-Wisconsinan glacier advance that reached tidewater occurred in at least two of the major valleys on the west side of northeast Atka. If these neoglacial advances were contemporaneous with those documented on Umnak Island (R. Black, 1975), the advance would have taken place about 3,000 years ago. A small ice cap and alpine glaciers still mantle the higher elevations of Atka caldera and summit region of Mount Kliuchef. Korovin Volcano, although higher than Kliuchef, is nearly devoid of glaciers. Probably this is a consequence of recent volcanic activity.

Thermal areas

Several active thermal areas have been identified on northeast Atka Island (fig. 5). Early reports of some of these sites are summarized in Dall (1870) and Waring (1917). Other sites were investigated by B. Marsh in 1973, 1976, and 1977 or identified from aerial photos. Because of time constraints and weather conditions the DGGS field party was able to investigate only the two most accessible sites, the Kliuchef and Korovin thermal areas (fig. 5).

Of the other thermal areas, most are associated with Mount Kliuchef and occur on the summit and flanks of the stratovolcano. Aerial photos taken on July 21, 1951 show the 0.75-km-dia summit crater to have a deep snow depression in the center of it, which suggests thermal activity. A much smaller crater (0.25 km in dia), west and adjacent to the summit crater may also be thermally active; it has a small crater lake at its bottom.

About 1.5 km southeast of the main summit, a large thermal field is marked by a prominent 0.75-km-dia depression that occurs in the glacier ice cap near its southwestern edge. The hole, which is at least 50 m deep, is surrounded by numerous concentric crevasses. Ice can be seen collapsing onto the exposed thermal field at the bottom of the hole. Another much smaller depression in the glacier occurs about 0.5 km farther southwest and probably marks the location of yet another thermal vent.

A 2-km-dia ice-filled crater is located east of the summit of Mount Kliuchef. The rim of the crater, which does not appear to be thermally active, has been breached by glacier flow. A thermal area reported by B. Marsh (pers. comm.) is located on a south-facing steep glacier valley wall on the south flank of Mount Kliuchef at an elevation of about 915 m. The site is described as highly colored and is visible from the village of Atka on a clear day. The area does not show much vapor but was very active at one time.

One additional thermal field, 'Atka north' (fig. 5), was reported to B. Marsh and has been tentatively identified on aerial photos. This site occurs near the northern part of the island on an east-facing cliff overlooking a lagoon near the Bering Sea east of Cape Potainikof. An attempted field verification of this site by DGGS was thwarted by deteriorating weather conditions.

Location

Latitude: 52°16.0'N, Longitude: 174°11.0'W;
Atka 1:250,000 Quadrangle (1959)

General description

The Kliuchef thermal field is located 12 km north of the village of Atka on the west flank of Mount Kliuchef (fig. 5). The thermal field can be reached from Korovin Bay, which is accessible from the village of Atka by jeep trail. The field occurs at an elevation of about 600 m in a small cirque or amphitheater at the head of a glacier valley that trends westward to an inlet of Korovin Bay. The site consists of numerous fumaroles, steam vents, vigorously boiling springs, and zones of intense hydrothermal alteration covering an area of about 50,000 m^2 (figs. 6-8). Thermal waters from the bowl drain westward into a cold stream channel. Stream waters measured 15°C about 0.5 km downstream from the thermal field despite heavy dilution with snow-melt runoff.

Geology

The thermal field lies in a small glacial bowl about 500 m in diameter that has been carved into shallow-dipping lava flows. The flows near the thermal field were found to be hypersthene-augite andesitic basalts and were probably derived from the summit region of Mount Kliuchef or the earlier Atka volcano. The ground immediately surrounding the thermal vents is intensely altered into multihued hydrothermal clays. Local bedrock is often veneered with red oxidation.

Morainal debris from recent glacial activity blankets much of the surrounding bedrock. One group of boiling springs and fumaroles was found to be actively cutting into a bank of glacial drift that is at least 5 m thick. The site was obviously covered with ice during the last advance. R. Black (pers. comm.) found fragments of cemented hydrothermal clays near tidewater in morainal deposits believed to be associated with a neoglacial advance in the valley containing the thermal site. If the fragments were derived from the Kliuchef thermal field this would indicate the site was active before and perhaps during the ice advance of possibly 3,000 years ago.

Thermal-vent characteristics

The thermal vents lie in two adjacent areas separated by a small knoll of hydrothermal clays (fig. 6). The southwestern series of vents, A, are about 10 m higher than series B. Series A consists of a 50-m-wide, 150-m-long semicircular band of fumaroles, steam vents, hot ground, violently boiling acid springs, and mudpots located on a 25° slope below a
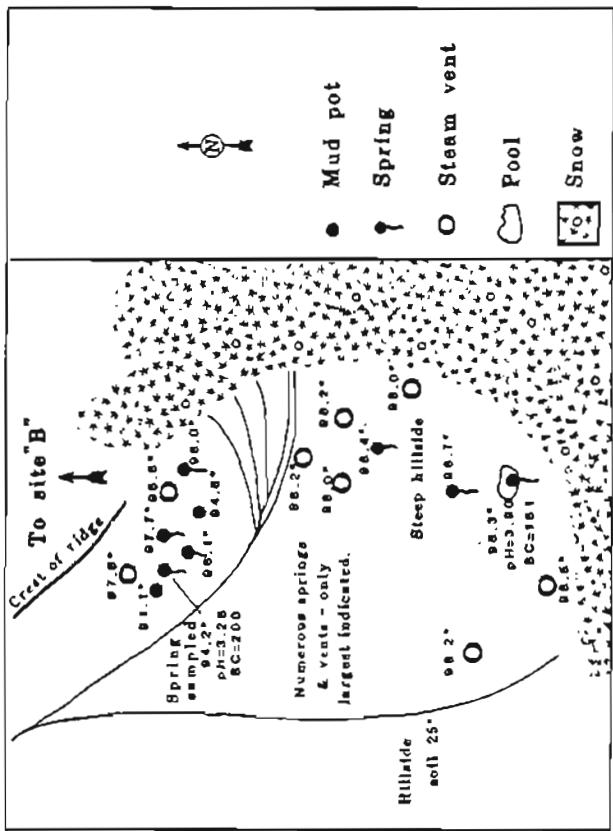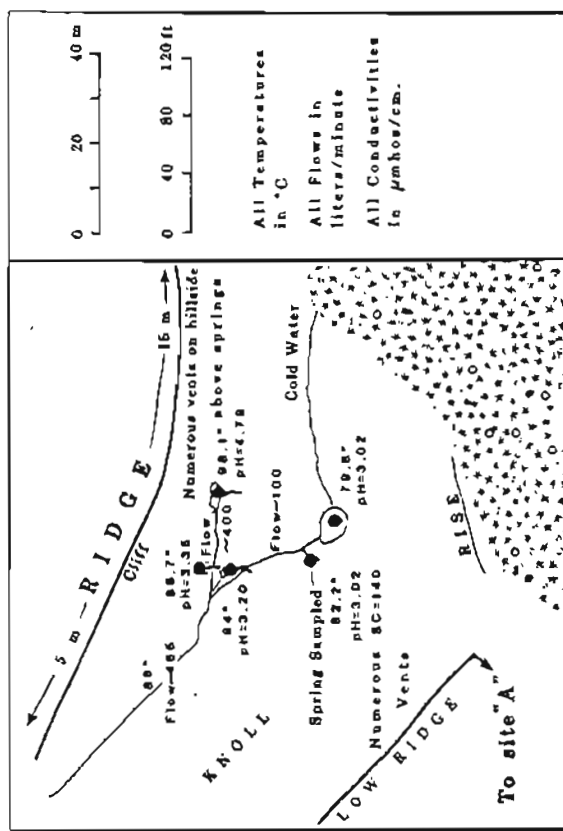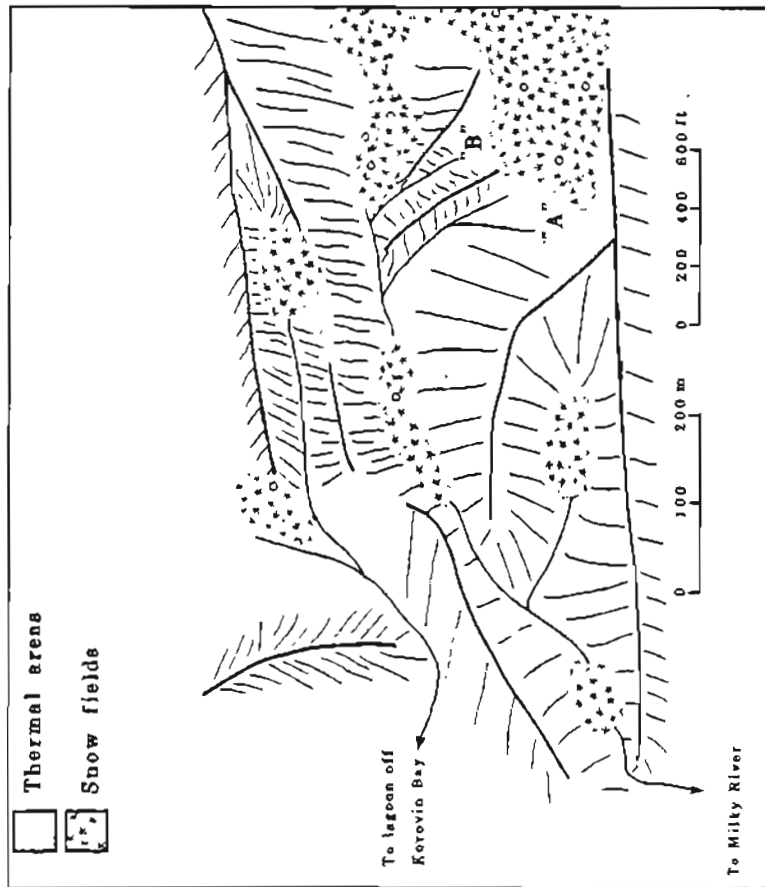
Figure 6. General location diagram showing relationship between Kliuchef
sites A and B on Atka Island. Figure 7. Detail at Kliuchef site A.
Figure 8. Detail at Kliuchef site B.

snow field, in a small basin at the foot of this slope. Fumarole vents are commonly 1-5 cm in diameter and slightly to moderately pressurized, and surrounded by sublimates. Dry outflow channels from several of the fumarole orifices indicate that waters occassionally drain from the vents, perhaps during periods of high precipitation and spring melt. Mudpots were formed only at the base of the slope and usually in funnel-shaped caverns, 0.5 m to 1 m in diameter. The mudpots were commonly at or near boiling temperatures. Thermal waters were all acidic and generally turbid. Several springs were boiling violently, in pools 0.5 to 1 m in diameter, located among hematite-stained volcanic boulders and cobbles.

Series-B thermal vents are located in a shallow trough adjacent to a small moraine. The trough acts as a catch basin for snow-melt runoff above the thermal field. These meltwaters apparently are being heated by a high flux of steam resulting in several violently boiling, shallow, turbid pools, up to 4 m in diameter, nested in glacial boulders and cobbles. The small morainal ridge above the springs is dotted with small steaming vents.

The combined flow of heated water leaving the series-A hot pools was measured in a surface channel at 465 lpm. Much of the outflow, however, was seen and heard discharging through subsurface channels, beyond the reach of measurement.

Table 2 gives the chemical and physical properties of thermal waters obtained from both thermal areas. The waters are conspiciously low in cations and dissolved solids, have little or no chloride, and are relatively rich in sulfate. The waters are undoubtedly locally derived surface meteoric waters that are heated by a huge flux of steam and hot gases at and near the ground surface. An analysis of gases present in a sample obtained from area A is given in table 3. The gas is rich in CO_2 but also moderately high in H_2 and H_2S, the presence of which indicates a high-temperature reservoir at depth.

The high nitrogen level in the sample indicates air, perhaps dissolved in ground water, enters the system, with oxygen being selectively removed in oxidizing reactions.

The high acidity and sulfate content of the waters is probably derived from the oxidation of H_2S in hot surface waters. The hot acid waters in turn attack and leach the local bedrock and probably account for most of the dissolved solids present. The low concentration of cations and silica indicates the heated waters have a short residence time and are rapidly flushed from the area.

A minimum estimate of the steam flux can be obtained by considering the outflow of hot waters from the area. The only flow measurement available is for the lower set of hot pools, where a considerable part of the discharge occurs underground. A minimum estimate of over 1,000 lpm for the combined outflow of hot waters from the area does not appear unreasonable. To obtain a rough estimate of heat loss, the waters are presumed to be initially at $0°C$ and then heated to $100°C$. The rate of

steam condensation required to obtain this amount of temperature change for 1,000 lpm of water is approximately 3 kg/s, equivalent to an energy exchange of about 1.67×10^6 cal/s, or 7 MW. The amount of steam and hot gases discharging directly to the atmosphere is unknown, but is probably at least as much as that being condensed at the ground surface.

Table 2. Chemical composition and physical properties of Mount Kliuchef hot springs (all chemical analyses in mg/1).

	Series A	Series B
SiO_2	12.5	10
Al	nd	nd
Fe	1.43	nd
Ca	6.4	3.6
Mg	2.6	1.3
Na	1.87	3.82
K	0.75	0.47
Li	.01	.01
HCO_3	---	---
SO_4	39.5	24.9
Cl	5	5
F	0.01	0.01
Br	nd	nd
I	nd	nd
B	0.5	0.5
H_2S	nd	0.15
Sr	0.01	0.02
pH, field	3.28	3.28
Dissolved solids	65.06	49.77
Hardness (mg/1 $CaCO_3$)	26.7	14.3
Sp conductance (μmho/cm at 25°C)	200	140
T, °C	94.2	82.2
Flow rate, lpm	nd	465
Date sampled	7/14/80	7/14/80

nd = not determined.

Reservoir properties

The high flux of steam, the large area of intense hydrothermal alteration, and the associated occurrence of boiling low-chloride acid-sulfate springs are all evidence for the presence of at least a shallow vapor-dominated system. The source of steam and hot gases could be a deeper vapor-dominated system or perhaps a deep, subsurface boiling-hot-water convective system.

Table 3a. Chemical composition of gas sample from
Mount Kliuchef thermal field.*

	Volume (%)
He	0.01
H_2	5.87
Ar	0.46
O_2	3.26
N_2	22.03
CH_4	0.07
CO_2	67.40
C_2H_6	0.01
H_2S	1.63

*W. Evans, analyst, U.S. Geological Survey,
Menlo Park, Calif.

Table 3b. Gas geothermometry,* Mount Kliuchef thermal field.

B	T (^{o}C)
-7	477
0	325
7	239

*Equations from D'Amore and Panichi (1980):

$$T = \frac{24775}{A + B + 36.05} - 273.15$$

where

$$A = 2 \log \frac{CH_4}{CO_2} - 6 \log \frac{H_2}{CO_2} - 3 \log \frac{H_2S}{CO_2}$$

(gases expressed in volume percent)

and B = -7 for $CO_2 > 75\%$ and CH_4 $2H_2$, H_2S $2H_2$
    B = 0 $CO_2 > 75\%$
    B = 7 $CO_2 < 75\%$

-33-

The analysis of a gas sample from the thermal field allows an estimate to be made of the deep reservoir temperature (table 3b). The volume percentage of CO_2 is less than 75 percent, which yields an estimated reservoir temperature of 239°C for application of the geothermometer described by D'amre and Panichi (1980). This temperature is similar to maximum temperatures found in deep parts of known vapor-dominated systems elsewhere in the world. This geothermometer, however, is still under evaluation, and the above estimate must be used with caution. Nevertheless, the large volume of steam escaping from the system and the high levels of H_2 and H_2S present in the gases indicate the deep reservoir exceeds 150°C, regardless of whether it is a hot-water or vapor-dominated system.

No geophysical exploration or exploratory drilling has been done at the site. The depth to water table (if any exists), the subsurface lateral extent of the thermal anomaly, the porosity and permeability of the host volcanic rocks, and the degree of silicification in the reservoir all need to be determined.

Comments

The thermal waters issuing from the Kliuchef thermal field are locally derived surface waters being heated to boiling at or near the ground surface by a voluminous upflow of steam and hot gases. The extent and depth of the vapor-dominated zone at Kliuchef is unknown.

Such localized zones of fumarolic activity are not an uncommon occurence on the upper flanks of active volcanic systems. Various models have been proposed for the deep geothermal systems of volcanoes exhibiting similar thermal activity (Oki and Hirano, 1970; Mahon and others, 1980). A cooling magma body, presumed to be at a depth of no more than a few kilometers, is commonly invoked as the primary source of heat driving the hydrothermal system. For the Kliuchef thermal field the magma could be associated with Kliuchef volcano or perhaps the older Atka caldera.

Evidence acquired from drilling of similar volcanic geothermal systems elsewhere in the world indicates that a deep Na-Cl hot brine normally develops and overlies the cooling hot rock. This brine is thought to become isolated from shallower levels by a process of silica deposition on the outer boundary of the reservoir and because the brine has a greater density than the infiltrating cold surface waters. Secondary reservoirs, lower in density, can then develop over the brine system. Waters normally sampled at the surface probably reside in secondary reservoirs overlying and being heated by dense fluids escaping from the deeper brine reservoir.

If waters in the secondary reservoir become hot enough, subsurface boiling can occur, causing fumarolic activity at the surface. Alternatively, if cold-water recharge is insufficient to develop a hot-water reservoir, a vapor-dominated system could evolve. Recharge of the

deeper system could be restricted by silica cementation; with continued boiling and lack of recharge a vapor-dominated system can slowly develop, heated by dense gases escaping from the deeper brine reservoir.

The conduits for escape of hot fluids to the surface are commonly fractures, and this is probably the case with Mount Kliuchef. Although hydrothermal alteration and silica deposition can restrict flow, seismic activity coupled with subsurface gas pressures in the reservoir often open channels and keep them free.

Volcanic flows are usually highly porous and permeable, and this could explain the lack of hot-springs activity elsewhere, such as at lower elevations on the flanks of the volcanoes. The hot fluids discharge directly into meteoric waters infiltrating the porous rocks, and are flushed from the system at subsurface levels.

The site appears to be particularly attractive for further exploration and eventual development on two counts: a) the strong evidence for a high-temperature geothermal reservoir underlying Mount Kliuchef and b) the proximity of this resource to potential users who are actively seeking an energy base. The estimated reservoir temperatures should be more than adequate for generation of electrical power and for a variety of other applications including direct heating and industrial processing.

KOROVIN THERMAL AREAS

Location

Latitude 52°17.8' N, longitude 174°147' W

Atka 1:250,000 (1959)

General description

The Korovin thermal areas lie 17 km north of the village of Atka in the north-central part of northeast Atka Island. There are two sites, 0.5 km apart, located near the head of a broad verdant glacier valley 6 km southwest of Korovin Volcano (figs. 5 and 9). The fields cover an area of about 50,000 m^2 and consist of steam vents, mudpots, boiling springs, and warm ground. In addition, site A has two small explosion craters, one of which contains a red-colored acid-sulfate lake. The waters are perched above and lie adjacent to the main cold stream channel, which drains the central part of the upper valley. Site B is about 30 m higher than A, and is located in a 500-m-dia bowl set between a small knoll on the north and steep volcanic slopes to the south (fig. 9).

The thermal fields are accessible from the village of Atka by jeep trail to Korovin Bay, thence along the beach and overland for about 10 km to the sites, or by small boat to the head of either one of two inlets and thence overland for about 5 km. The springs site is briefly mentioned in Dall (1870) and was apparently used by Russians and Aleuts during the tenure of Russian settlement.

Geology

The ridge southeast of the thermal fields is composed of a massive dacitic flow that is in places up to 750 m thick (fig. 5). The flow is frothy or pumaceous in its upper part but has the characteristics of a lava in its middle and lower sections (B. Marsh, pers. comm.). The dacite is thought to be part of the eruption that formed the Atka caldera; a hydration date suggests an emplacement of 300,000 to 500,000 years ago. The dacite overlies a thick sequence of andesitic-basaltic flows derived from the ancestral Atka Volcano. The Atka flows probably underlie the valley containing the thermal fields.

Outcrops exposed in the 700-m-high valley wall and ridge north of the thermal sites consist of a series of interbedded andesitic-basaltic flows collectively mapped as Potainikof volcanics (fig. 5). This volcanic sequence appears to overlie flows from Atka Volcano and may be contemporaneous with postcaldera volcanic activity farther south.

The area has been heavily glaciated, and the valley is floored with glacial drift and postglacial alluvium. Neoglacial advances may have affected this part of the island.
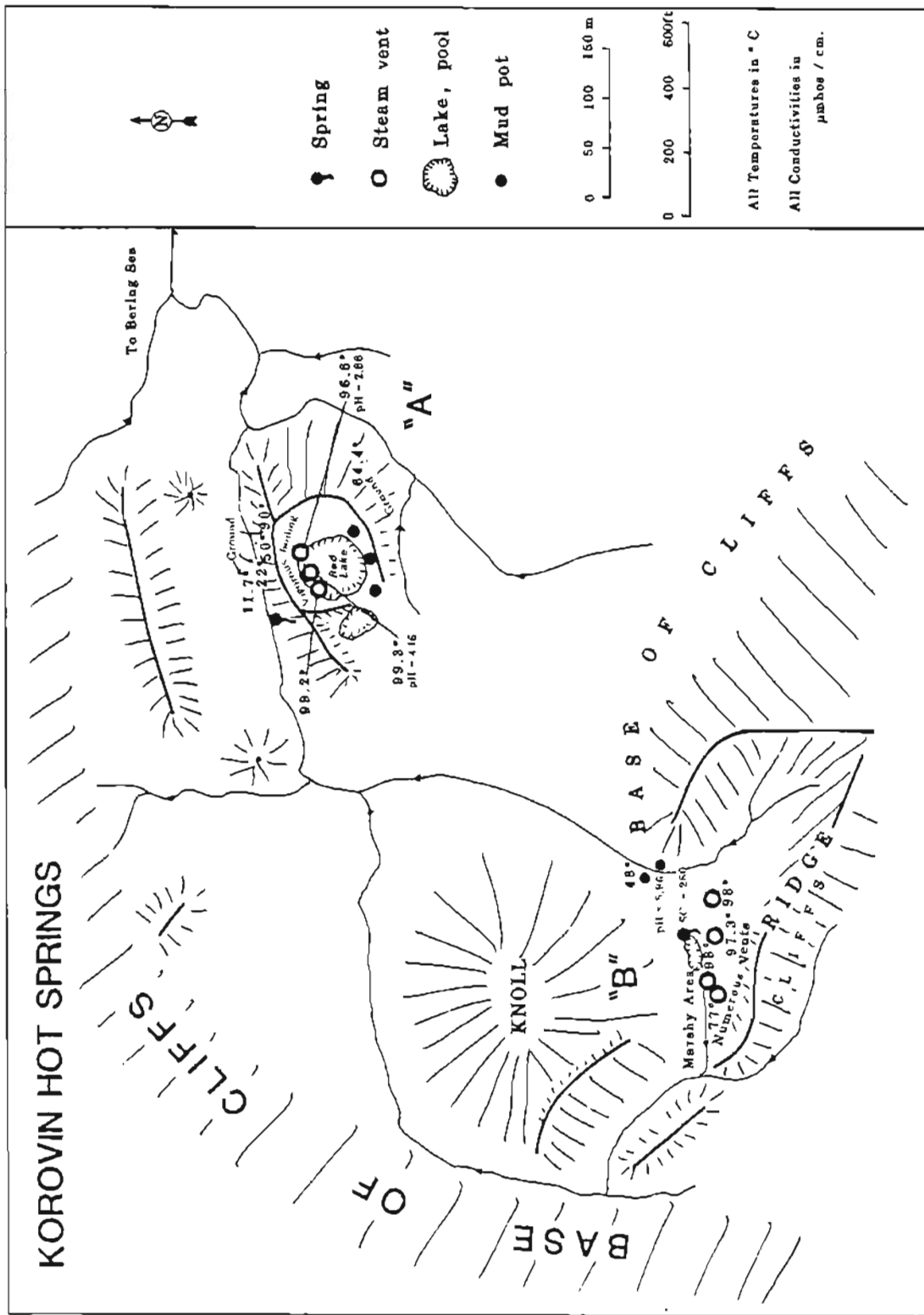
Figure 9.   Sketch map of Korovin A and B thermal areas on Atka Island.

At site A are two small, oblong explosion craters, oriented about
S30°E (fig. 9). The larger is 60 m long and 30 m wide, and has a shallow,
red turbid lake. Gouging by fumarolic and boiling-spring activity has
exposed strata in the north wall of the crater, which rises 7 m above
the lake bed. The crater rim is mantled with a 1.5-m-thick ring of
well-bedded ejecta. The beds vary from 0.5 cm to several cm thick and con-
sist of poorly sorted silt, sand, and pebble-sized lithic fragments
cemented by hydrothermal alteration. The tephra beds in turn overlie what
appears to be glacial drift exposed in the crater wall. Lack of surface
erosion indicates the craters are postglacial features. The craters
probably formed as a result of a series of phreatic explosions that may
have occurred during the waning stages of valley deglaciation. Explosion
craters in geothermal fields have been correlated with deglaciation else-
where, e.g. Yellowstone National Park (Muffler and others, 1971).

Thermal-vent characteristics

The most distinctive feature at site A is the small, red-stained
crater lake measuring about 30 m long and 15 m wide. The principal
thermal vents occur at the northwest end of the lake, where several vigor-
ously boiling springs and steam vents are carving a cavern into the side
of the hematite-stained crater wall. The crater wall and rim are pock
marked with numerous small vapor vents that are often ringed with yellow-
colored sublimates. Most of the ground surrounding the lake has been
hydrothermally altered to red, yellow, and gray clays.

Several meters south of the lake are several 0.5-m-dia steam caverns,
some filled with bubbling mud. Parts of the adjacent smaller crater are
also thermally active, again consisting of small mudpots and steam
vents. The hollow of this smaller crater contains a warm, marshy
area.

The northwest flanks of the craters are steep and drop about
15 m to a cold stream channel. Temperatures in the soil at 10 cm
depth measured 50° to 98°C near the crater rim and 22°C near the stream
channel. Several warm seeps and small hot springs measuring up to 75°C
were observed issuing from the stream bank below the crater. The area
southeast of the craters is also warm, measuring 64°C at a depth of
10 cm at a distance of 20 m from the larger crater rim.

Thermal activity at site B is much less intense than at A. The
site consists of a series of hot mudpots, turbid pools, bubbling warm
springs, several small steam vents and generally warm marshy ground
(fig. 9). This activity occurs in a bowl like feature with the thermal
waters and steam emanating from the alluvial and colluvial cover, which
may be underlain by glacial deposits. The warm waters drain from the
bowl to both the east and west.

Table 4 gives the chemical composition and physical properties of
thermal waters obtained from the two Korovin sites. The water sample
from site A was obtained from a vigorously boiling pool at the northwest
end of the crater lake. The water sample from site B was taken from a

small hot spring pool, measuring 48°C with a low discharge. Both spring samples are distinguished by very low concentration of chlorides. Spring water from B is much more dilute, much lower in sulfate, and nearer neutral pH than water from site A. The higher concentration of cations at site A---particularly Ca and Mg---is probably partially due to hot acid waters attacking and leaching the surrounding rocks. The acidity probably results from the oxidation of H_2S to form sulfuric acid. The odor of H_2S was noticeable at site A and a trace amount was detected in the water.

Table 4. Chemical composition and physical properties of
Korovin Bay hot-springs sites A and B
(all chemical analyses in mg/l).

	Site A	Site B
SiO_2	140	62
Al	6.0	nd
Fe	1.42	2.64
Ca	60.0	26.8
Mg	19.0	9.2
Na	15.5	15.5
K	10.0	4.1
Li	0.01	0.01
HCO_3	---	nd
SO_4	300	8.6
Cl	5	10
F	0.2	0.01
Br	nd	nd
I	nd	nd
B	2.0	0.5
H_2S	0.29	nd
Sr	0.23	0.11
pH, field	4.16	5.96
Dissolved solids	554.6	138.95[a]
Hardness (mg/l $CaCO_3$)	244	104.92
Sp conductance (µmho/cm at 25°C)	750	280
T (°C)	99.3	48
Flow rate (lpm)	nd	nd
Date sampled	7/15/80	7/15/80

nd = not determined
[a]Does not include HCO_3 data.

Table 5 is an analysis of a gas sample obtained from a warm-spring pool at site B. The dominant gas is CO_2, with H_2 and H_2S notably absent, perhaps as a result of extensive interaction with waters in a shallow low-temperature reservoir. The high N_2 content suggests the infiltration of air into the subsurface system and perhaps dissolving in downward-percolating meteoric waters; residual oxygen would be removed by water-rock interactions.

Table 5. Chemical composition of gas sample from
Korovin Bay thermal site B.[a]

	Volume (%)
He	0.01
H_2	0.03
Ar	0.62
O_2	0.69
N_2	32.05
CH_4	0.28
CO_2	66.92
C_2H_6	0.01
H_2S	---

[a]W. Evans, analyst, USGS, Menlo Park, CA.

The surface manifestations in both locations---the low chloride level, acid springs, numerous steam vents, and mudpots---all suggest that a vapor-dominated zone underlies the area. The thermal waters are probably locally derived meteoric waters being heated in a shallow reservoir by condensing steam and hot gases with acidity caused by oxidation of H_2S.

Reservoir properties

The steam vents, boiling acid springs, mudpots, and low-chloride thermal waters all indicate a vapor-dominated zone underlies the thermal fields. Water and gas chemistry suggest that steam is condensing into and heating a shallow-water reservoir that is probably being fed by local meteoric waters. The extent and depth of the vapor-dominated zone is unknown. Isolated pockets of steam may underlie the two sites, or the sites could be an indication of a much broader vapor-dominated thermal reservoir beneath the area.

The silica content of both thermal waters suggests temperatures in the shallow reservoir are warm, ranging from 100° to 150°C. The variation in silica levels between the two waters could represent differences in residence time for the individual thermal waters sampled, acid water-rock interaction, or perhaps differences in cold-water dilution.

To use the D'Amore-Panichi gas geothermometer two conditions should be met: a) the gases should not be in contact with a large, low temperature water table above the main reservoir and b) the spring and fumarole sampled should have a high gas flow rate because H_2S and

H_2 are strongly affected by near-surface alteration through water-rock reactions. Both these conditions are probably violated at the Korovin sites, and therefore application of the gas geothermometer is inappropriate. The high steam flux, however, does suggest a deep reservoir temperature exceeding 150°C.

No geophysical exploration or exploratory drilling has been done at the two sites. The dimensions of both the shallow water table and the underlying vapor-dominated zone, and the nature of the deep system have yet to be determined.

Comments

Unlike the Kliuchef site, the Korovin thermal fields do not occur on the flank of an active volcano. Rather, the sites occur at a relatively low elevation in an open valley, a situation in which a substantial water table would be expected. The surface manifestation of the thermal activity and fluid chemistry, however, indicate the presence of a vapor-dominated zone under a shallow water table. Despite the distance from active volcanoes, the source of heat driving the hydrothermal system at Korovin could still be magmatic.

Evidence exists that fractures and volcanic dikes tend to develop normal to the minimum compression or parallel to the maximum horizontal compression of regional origin, in this case the convergence of two major tectonic plates (Nakamura and others, 1977). Marsh (pers. comm.) reports that the predominent trend of dikes exposed at the surface on northeast Atka are in the general direction of plate convergence. The Kliuchef and Korovin thermal sites lie on a trend of N. 50° W., the direction of plate convergence in this part of the Aleutians.

The sites may overlie a dike or dike swarm---or perhaps even a large magmatic system with fracture zones providing conduits for the escape of thermal fluids from a deep geothermal reservoir. If a single large geothermal reservoir does underlie the entire area, the potential for energy development will be enormous. The system is probably high temperature, i.e., greater than 150°C and therefore attractive for the generation of electrical power and for most direct-heat applications. The proximity of the thermal sites to users who are actively seeking an energy base to attract fishing industries makes the northeast Atka sites prime candidates for further exploration and development.

UMNAK ISLAND

Background

Umnak Island is located in the eastern Aleutian Chain southwest of Unalaska Island and separated from it by Umnak Pass, 360 km from the end of the Alaska Peninsula (figs. 1 and 3). Most of the island is between the meridians 168°-169^oW. and 53°-54^oN. The 120-km-long island, which follows the trend of this part of the Aleutian arc, N. 45° W., is divided into northeastern and southwestern parts at the narrow isthmus formed by the indentation of the island by Inanudak Bay (fig. 10). Northeastern Umnak Island is dominated by Okmok Caldera, a low (1,070-m) shield volcano capped by a 10-km-dia collapse caldera. Southwestern Umnak is much more rugged, with two large glacier-clad stratovolcanoes, Mount Vsevidof and Mount Recheshnoi, each rising to nearly 2,150 m. Most of the coastline of Umnak is directly exposed to either the Bering Sea or Pacific Ocean and is characterized by rugged sea cliffs and dark sandy beaches.

Three areas of thermal springs occur south of Inanudak Bay in alluvium-floored valleys: south of Hot Springs Cove, southeast of Geyser Bight, and in a small unnamed valley that drains eastward across the narrowest part of Umnak (fig. 10). The Geyser Bight springs are the most widespread, hottest, and probably best known thermal springs in the Aleutian Islands. The existence of the Hot Springs Cove and Geyser Bight thermal spring areas were reported in Grewingk (1850) and in Waring (1917). Byers and Brannock (1949) performed an extensive survey of the thermal spring areas on the island during their geologic mapping of Umnak in 1946-48. More recently the geochemistry of the thermal waters was reexamined by I. Barnes of the U.S. Geological Survey, Menlo Park (pers. Comm., unpub. data) and by DGGS (this report).

The only areas of habitation occur at either end of the island. A sheep ranch run by a single individual is located near an airstrip at the abandoned WW-II Fort Glenn Air Force Base on the northeast end of the island. An abandoned jeep trail at the base of Okmok Caldera leads from Fort Glenn along the Pacific coast then crosses the island to Inanudak Bay on the Bering seacoast. Nikolski, a native village of about 60 Aleuts, lies at the southwest end of the island near a small sheltered harbor on the Bering seacoast. Village economy is based on subsistence and a few small sheep farms. Much of the land surrounding the hot-spring sites has been selected by the Aleutian Pribiloff Native Corporation and the St. George Native Association under terms of the Alaska Native Claims Settlement Act (ANCSA).

General geology

The hydrothermal activity on the island is probably associated in large part with on-going volcanism. Three active volcanoes dominate the island, the largest of which is Okmok Caldera.

Figure 10. Generalized geology of Umnak Island.

Okmok Caldera, located on the northeast end of Umnak Island
(fig. 10), is a large shield-form stratovolcano with a 10-km-dia
central collapse caldera. The volcano is composed of gently out-
ward-dipping basaltic flows and interbedded pyroclastic rocks (Byers,
1959). Numerous subsidiary cinder cones and small parasitic (mostly
basaltic) volcanoes occur on the flanks and within the caldera.
Rocks of andesitic to latitic composition form a few dikes, plugs,
and stubby lava flows and occur as fragments in the pyroclastic rocks
of the Okmok Volcanics (Byers, 1959). Rhyolite appears to be
restricted to one elongated dome on the outer northwestern slope of
Okmok Caldera.

Lack of any significant glacial erosion indicates Okmok Caldera
formed since the last major glaciation on Umnak Island. On the basis
of volcanic ash-soil stratigraphy and carbon-14 dating of soil hori-
zons from the southwest end of Umnak Island, Black (1975) placed
caldera formation at 8,250 yr B.P. Okmok Caldera has remained very
active, erupting at least 10 times since 1700 (Coats, 1950). According
to local informants, several eruptions occurred during the last decade.
An enormous steam plume emanates from the west end of the caldera and
new lava flows, erupted since 1945, cover parts of the caldera floor
(C. Nye, pers. comm.).

Mount Vsevidof, a 2,150-m-high stratovolcano lying southwest of
Okmok Caldera, has erupted at least five times since 1700 (Coats, 1950).
The dominant lithologies of Vsevidof are basaltic andesite and andesite
with subordinate basalt and rhyolite (Byers, 1959). Mount Recheshnoi,
a deeply eroded 1,985-m-high stratovolcano east of Mount Vsevidof, has
no historically recorded eruptions. It was the source of a least one
lava flow that reached the sea as recently as about 3,000 years ago
(Black, 1975). The volcano is composed chiefly of andesitic flows
interlayered with pyroclastics (Byers, 1959).

The volcanic rocks of central Umnak mark a fourth much-older center
of volcanism on the island. The initial forms of the volcanoes have
been completely obliterated by subsequent erosion. The rocks are com-
posed of middle Tertiary to early Quaternary lava flows, vent breccias,
and associated irregular shallow intrusive bodies that are hydrothermally
altered in places. The areal extent of the central Umnak Island volcanics
is unknown because they are covered both to the northeast and to the
southwest by Quaternary lavas of Okmok Caldera and Mount Recheshnoi,
respectively. The volcanics appear to be underlain by Tertiary plutonic
rocks and albitized sedimentary rocks.

Thermal areas

Numerous thermal springs, geysers, and fumaroles occur on Umnak
Island. Thermal springs in three areas of central Umnak Island were
examined by Byers and Brannock (1949): south of Hot Springs Cove,
southeast of Geyser Bight, and in the small unnamed valley that drains
eastward across the narrowest part of Umnak Island (fig. 10). The

Figure 10. Generalized geology of Unmak Island.

Okmok Caldera, located on the northeast end of Umnak Island (fig. 10), is a large shield-form stratovolcano with a 10-km-dia central collapse caldera. The volcano is composed of gently outward-dipping basaltic flows and interbedded pyroclastic rocks (Byers, 1959). Numerous subsidiary cinder cones and small parasitic (mostly basaltic) volcanoes occur on the flanks and within the caldera. Rocks of andesitic to lacitic composition form a few dikes, plugs, and stubby lava flows and occur as fragments in the pyroclastic rocks of the Okmok Volcanics (Byers, 1959). Rhyolite appears to be restricted to one elongated dome on the outer northwestern slope of Okmok Caldera.

Lack of any significant glacial erosion indicates Okmok Caldera formed since the last major glaciation on Umnak Island. On the basis of volcanic ash-soil stratigraphy and carbon-14 dating of soil horizons from the southwest end of Umnak Island, Black (1975) placed caldera formation at 8,250 yr B.P. Okmok Caldera has remained very active, erupting at least 10 times since 1700 (Coats, 1950). According to local informants, several eruptions occurred during the last decade. An enormous steam plume emanates from the west end of the caldera and new lava flows, erupted since 1945, cover parts of the caldera floor (C. Nye, pers. comm.).

Mount Vsevidof, a 2,150-m-high stratovolcano lying southwest of Okmok Caldera, has erupted at least five times since 1700 (Coats, 1950). The dominant lithologies of Vsevidof are basaltic andesite and andesite with subordinate basalt and rhyolite (Byers, 1959). Mount Recheshnoi, a deeply eroded 1,985-m-high stratovolcano east of Mount Vsevidof, has no historically recorded eruptions. It was the source of a least one lava flow that reached the sea as recently as about 3,000 years ago (Black, 1975). The volcano is composed chiefly of andesitic flows interlayered with pyroclastics (Byers, 1959).

The volcanic rocks of central Umnak mark a fourth much-older center of volcanism on the island. The initial forms of the volcanoes have been completely obliterated by subsequent erosion. The rocks are composed of middle Tertiary to early Quaternary lava flows, vent breccias, and associated irregular shallow intrusive bodies that are hydrothermally altered in places. The areal extent of the central Umnak Island volcanics is unknown because they are covered both to the northeast and to the southwest by Quaternary lavas of Okmok Caldera and Mount Recheshnoi, respectively. The volcanics appear to be underlain by Tertiary plutonic rocks and albitized sedimentary rocks.

Thermal areas

Numerous thermal springs, geysers, and fumaroles occur on Umnak Island. Thermal springs in three areas of central Umnak Island were examined by Byers and Brannock (1949): south of Hot Springs Cove, southeast of Geyser Bight, and in the small unnamed valley that drains eastward across the narrowest part of Umnak Island (fig. 10). The

springs are located in alluvium-covered valleys that are underlain by the central Umnak volcanics. Spring temperatures were reported to range from 47° to 101°C, with most of the springs having temperatures above 85°C. Byers and Brannock (1949) estimated the total heat carried away by these thermal springs at 6,350 kcal/sec (26 MW).

A series of east-west-trending thermal springs located at the base of a volcanic cone within Okmok Caldera were also examined by Byers and Brannock (1949). Heat carried away by these springs was estimated at 21,000 kcal/sec (88 MW).

Byers and Brannock (1949) reported the existence of numerous fumaroles associated with outgassing from recent volcanic eruptions within Okmok Caldera. Two fumaroles were also reported near the head of Geyser Creek, apparently unrelated to any recent eruption.

Although much of the present surficial thermal activity within Okmok Caldera is probably derived from recent volcanic lava flows, some of the inner-caldera activity and probably all the surficial thermal activity located in the central part of Umnak Island comes from deeper hydrothermal systems.

Avenues to such subsurface systems are commonly fractures and fault systems. In Okmok Caldera, these fractures and faults probably developed during caldera formation. In the central part of the island, fractures are probably the result of tectonic stress. On the basis of orientations of volcanic features, dikes, and faults, Nakumura and others (1977) suggested an azimuth of maximum horizontal compressive stress for Umnak Island of N. 65 ± 20° W. This trend is roughly in the direction of convergence between the North American and Pacific tectonic plates (N. 45° W.) in this sector of the Aleutian Chain as determined by Nakamura and others (1977). Interestingly, Geyser Creek valley, which contains over 15 thermal springs and geysers, is also oriented N. 45° W. These similarities suggest that fractures created by tectonic stresses extend to great depths and thus provide conduits for the circulation of surface waters through deep-seated hot rocks.

The source of heat driving the hydrothermal system probably comes in large degree from shallow magma chambers and the hot rocks surrounding them. Evidence for at least one such chamber comes from the size and youth of the Okmok Caldera. Such calderas imply the existence of large shallow magma chambers with immense amounts of residual heat.

During the summer of 1980 the DGGS field party examined three of the thermal areas on Umnak: Geyser Bight, Hot Springs Cove, and Partov Cove.

Location

Latitude 53°13' N., longitude 168°28' W.; Umnak 1:250,000 Quadrangle (1951); T. 80 S., R. 133 W., Seward Meridian.

General description

The thermal area consists of five thermal spring sites that are dispersed over about 4 km^2 on the floor and at the head of a prominent glacial valley that trends southward from Geyser Bight (fig. 11). The springs mostly occur along Geyser Creek and its tributaries, and emerge from alluvium and colluvium at the base of steep valley walls. In addition, two small fumarole fields are situated at elevations of 240 m and 300 m in a small tributary valley at the headwaters of the west fork of Geyser Creek. The Geyser Bight hot-spring site is the hottest and most extensive thermal-springs area in Alaska.
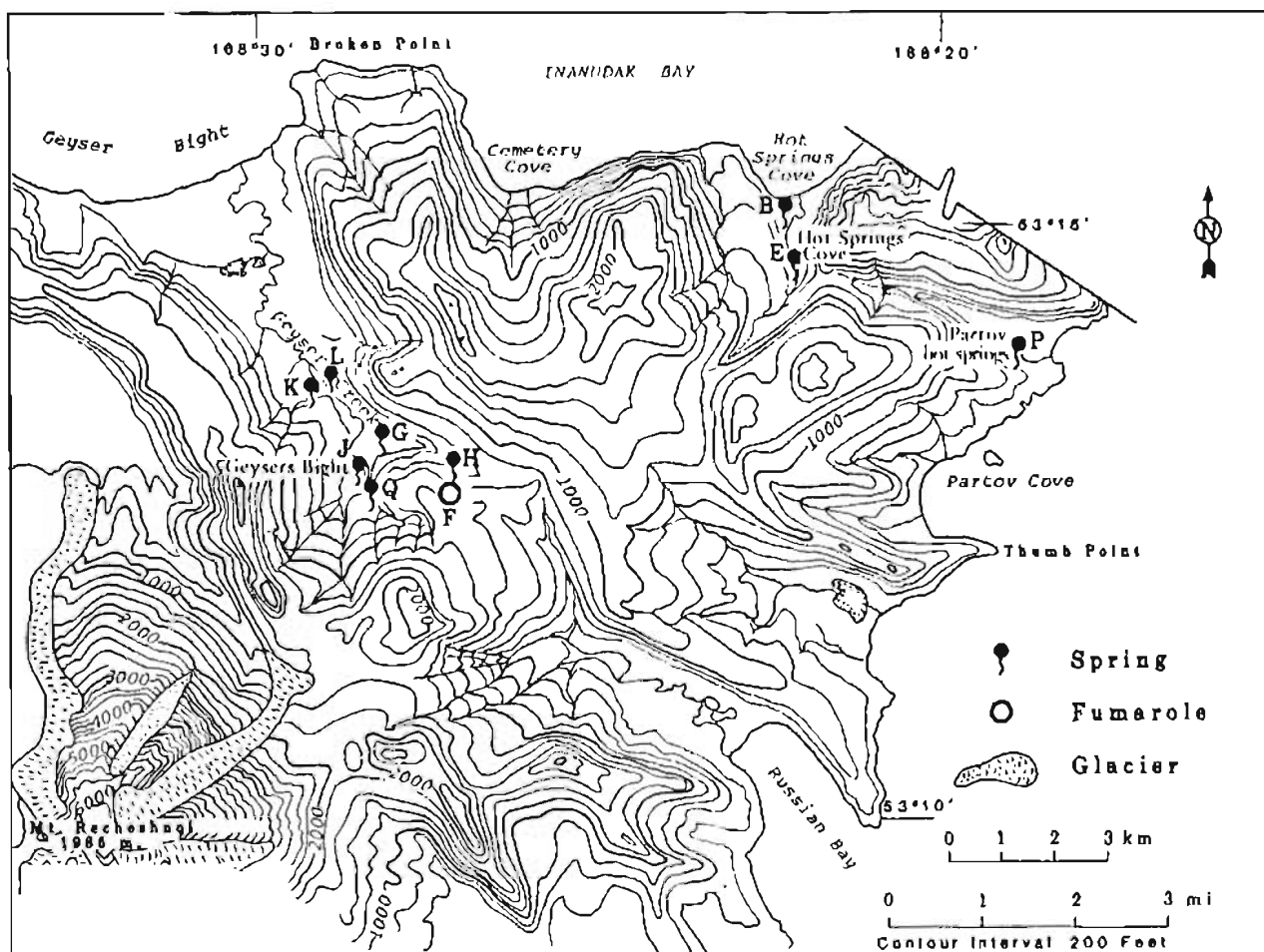
Figure 11. Location map for Geyser Bight, Hot Springs Cove, and Partov hot springs.

The glaciated rugged ridges that flank the U-shaped valley rise to 610 m; the adjacent regions not covered by recent volcanic rocks show additional signs of intense glacial erosion. The two large stratovolcanoes, Mounts Vsevidof and Recheshnoi, lie southwest of the springs site and are partially mantled by glaciers that fill erosional ravines cut into the flanks of the volcano. Two of these narrow ribbons of ice descend to an elevation of about 90 m.

The floor of the valley is marshy and contains several small ponds, mostly located behind a series of beach dunes that occur near the seacoast. Lush, thick tundra vegetation blankets the valley up to elevations of about 300 m.

The Geyser Bight hot-springs site is very remote and access is difficult. The DGGS field party reached the area via chartered vessel from Unalaska. High surf conditions can sometimes render the Geyser Bight beach unsafe for small boat landings. The springs area can alternatively be reached by long overland treks from either Fort Glenn or Nikolski, located at either end of Umnak Island.

Geology

Tertiary bedded volcanic rocks of central Umnak, hydrothermally altered in places, are exposed along the lower sections of the valley walls surrounding the hot-springs sites (Byers, 1959). These volcanics overlie Tertiary diorites that outcrop at the base of the west valley wall at its northern end and along the Bering seacoast east and west of Geyser Bight. The late Tertiary and Quaternary volcanic rocks of Mount Recheshnoi unconformably overlie the central Umnak volcanics. The Recheshnoi volcanics, exposed in the upper parts of the valley walls and on the flanks of the volcano, consist of a thick sequence of hypersthene andesitic flows containing minor interbedded pyroclastic deposits.

The U-shaped Geyser Bight glacial valley is floored with an unknown thickness of alluvial and colluvial deposits. A 1-km-wide band of older dune sands spans the mouth of the valley and occurs immediately south of the present coastline.

Spring characteristics

The thermal-spring sites occur in Geyser Creek Valley 4 to 7 km southeast of Geyser Bight at elevations ranging from 45 to 150 m (figs. 11-16). Steam fumarole fields are situated on the west side of the east fork of Geyser Creek at elevations of 240 and 300 m (figs. 11, 17, and 18). Measurements of discharge were possible for only a few of the thermal spring vents, but where performed the measured flow rates were substantially lower (one-half or less) than flow rates reported for the same springs by Byers and Brannock (1949) (table 6). Visual estimates of discharges at other thermal springs tended to verify the conclusion that the flow of thermal waters in the valley has diminished substantially since 1947. Although Byers and Brannock (1949) did not report the method or accuracy of their measurements, the differences in flow rate appear to be too large to be explained by differences in measuring techniques.

-47-
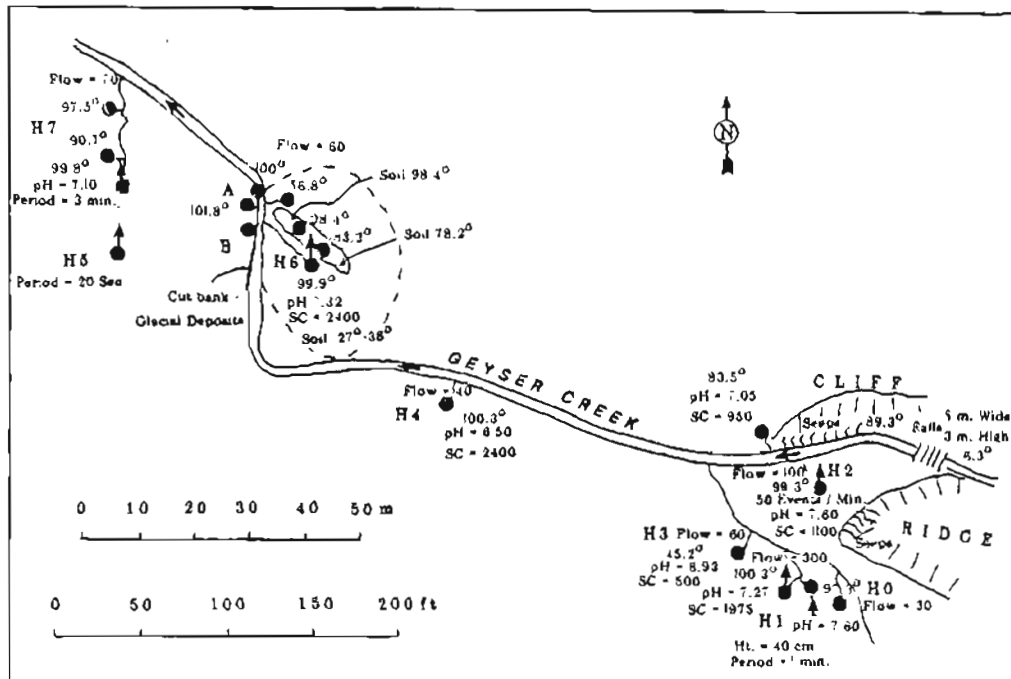
Figure 12. Detail at Geyser Bight site H.

Temperatures at the individual spring vents were similar to those measured in 1947. However, although slightly superheated temperatures were measured at the several small geysers that occur in the valley, the level of geysering activity seemed much more subdued than that reported in 1947.

Site H occurs in a narrow valley at an elevation of about 150 m, situated below a beautiful 3-m-high waterfall near the head of the west fork of Geyser Creek (fig. 12). The site consists of two groups of thermal springs about 100 m apart. The thermal waters issue from fissures and pools in the cemented alluvium, colluvium, and glacial debris on both sides of the creek and from fractures in volcanic bedrock exposed at the base of the waterfalls. Temperatures at many of the spring orifices are at or slightly above boiling point. Several vents exhibit considerable ebullition and fountaining; mild geysering activity occurs at two or three of the vents. Thermal-spring basins and outflow channels were frequently coated with siliceous sinter deposits. The flow rates measured for several of the springs are given in table 6 with 1947 rates of discharge included for comparison.

Table 7 gives the chemical composition and physical properties of thermal waters obtained from springs H1 and H6. The waters are moderately concentrated in sodium and chloride. Equipment malfunction prevented determination of bicarbonate. The slighly more dilute H1 waters may have resulted from mixing with ground waters. The springs have similar ratios (table 8) of sodium to chloride and of the conservative elements boron and chloride.
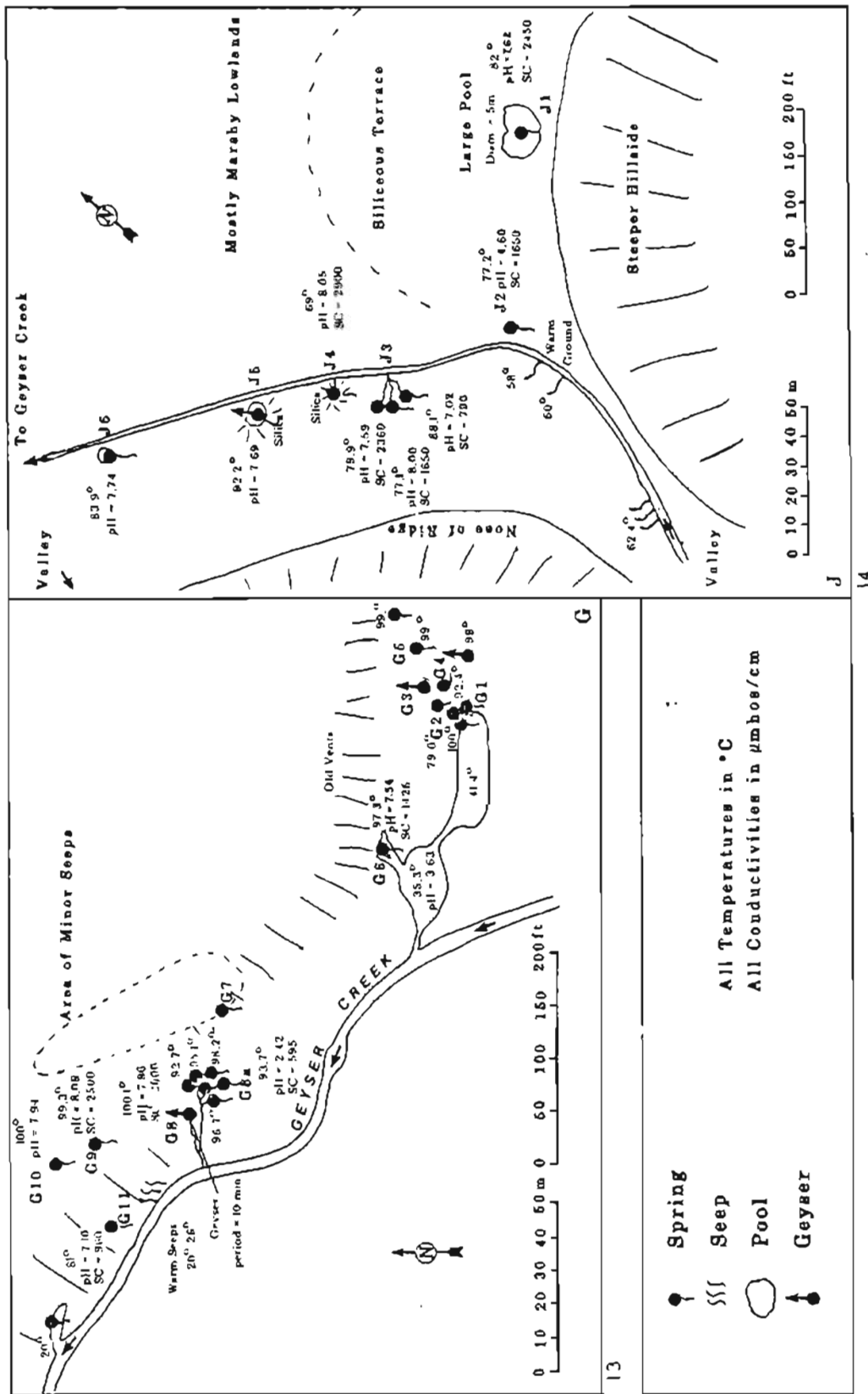
Figure 13. Detail at Geyser Bight site G. Figure 14. Detail at Geyser Bight site J.

Figure 15. Detail at Geyser Bight site K. Figure 16. Detail at Geyser Bight site L (at right).
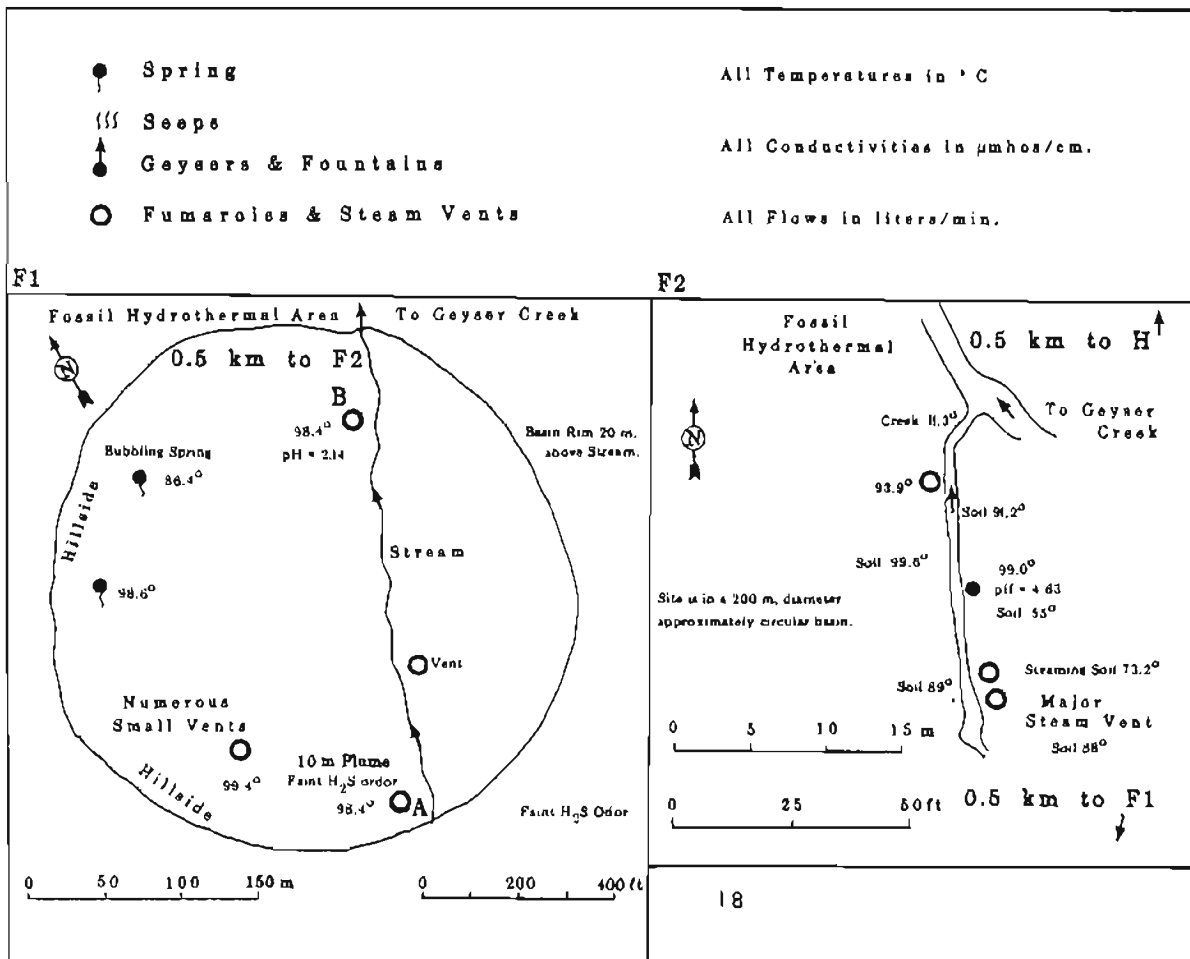
Figure 17. Detail at Geyser Bight site F1. Figure 18. Detail at Geyser Bight site F2.

Table 6. Data on thermal springs, Geyser Bight. DGGS discharge measurements made with standard pygmy flowmeter; flows visually estimated are in parentheses.

Thermal spring	Activity[c]	1980			1947[a]	
		T (^{o}C)	Flow (lpm)	Quality of Flow measurement	T (^{o}C)	Flow (lpm)
HO	sp	97.3	(30)	vis. est.	nr	nr
H1	g	100.3	300	good (5%)	101.5	660
H2	f, eb	99.3	100	poor (10%)	101	600
H3	sp	45.2	(60)	vis. est.	53	none
H4	eb	100.3	45	poor (10%)	101	340
H5	g	101.8	within a small cavern		101	85
H6	f, eb	99.9	30	poor (10%)	100	66
H7	eb	99.8	70	fair (10%)	90	260
G1	g	100.0	(20)	vis. est.	101	260
G2	s	79.0	(5)	vis. est.	88	6
G3	g	100.1	16	poor (10%)	100.5	18
G4	s	92.4	(5)	vis. est.	98	36
G6	eb	97.3	20	poor (10%)	95	80
G7			not found		82	85
G8	g	100.1	75[b]	poor (10%)	100.5	170
G9	sp	99.3	nd	nd	100.5	6
G10	sp	100	nd	nd	99	170
G11	sp	81	nd	nd	77	170
J1	p	82	not possible		88	720
J2	s	77.2	seeps	vis. est.	nr	nr
J3	sp, s	77-88	(10)	vis. est.	nr	nr
J4	p	69	(5)	vis. est.	nr	nr
J5	g	92.2	(15)	vis. est.	nr	nr
J6	p	83.9	(15)	vis. est.	nr	nr
K	p	59-62	nd	nd	58-70	250
L	p	80-85.5	200	poor (10%)	67-69	170
Q	sp, s	70-75	(25)	vis. est.	nr	nr

[a]Byers and Brannock, 1949
[b]measured at height of geyser cycle
[c]g, geyser; f, fountaining; eb, ebullient boiling; p, pool; sp, spring; s, seep
nr = not reported; nd = not done; vis. est. = visually estimated

Table 7. Chemical composition and physical properties of
Geyser Bight thermal springs
(all chemical analyses in mg/l).

	Site							
	H1	H6	G6	G8	G8A	J	K	L
SiO$_2$	170	190	178	270	63	272	148	160
Al	nd	nd	nd	nd	nd	nd	nd	nd
Fe	0.03	0.04	0.05	0.05	0.09	0.05	0.07	0.08
Ca	33.2	36.2	22.9	19.3	9.8	19.1	25.1	39.7
Mg	0.26	0.07	1.2	0.15	3.8	0.01	2.8	1.4
Na	355	442	248	487	28.5	447	179	280
K	16.3	19.9	17.1	30.9	3.6	31.7	13.9	20.1
Li	2.8	3.4	1.78	3.9	0.13	3.5	1.18	1.78
HCO$_3$	nd	nd	nd	146	nd	113	266	262
SO$_4$	131	154	96.5	170	132	168	63.6	90.3
Cl	492	591	339	630	35	591	225	370
F	1.27	1.55	0.9	2.3	0.13	2.4	0.9	1.6
Br	1.68	1.92	1.09	2.20	nd	2.13	1.22	1.07
I	1.1	1.2	0.7	1.1	nd	1.0	0.5	0.7
B	51.5	58.3	15	60	2.3	50	18.8	30
H$_2$S	0.29	nd	nd	nd	nd	nd	nd	0.5
Sr	0.23	0.21	0.07	0.3	0.04	0.08	0.13	0.24
pH, field	7.30	7.32	7.54	8.00	2.80	7.62	7.83	6.85
Dissolved solids	1254.8	1499.8	922.3	1823.0	278.4	1701.0	946.2	1259.0
Hardness (mg/l CaCO$_3$)	84.3	90.9	62.2	48.9	40.16	47.8	74.4	105.2
Sp conductance (μmho/cm at 25°C)	1975	2400	1425	2500	595	2450	1080	1600
T (^{o}C)	100.3	99.9	97.3	100.1	98.2	82.0	62	85.5
Flow rate (lpm)	300	30	20	75	nd	nd	nd	200
Date sampled	7/25/80	7/25/80	7/26/80	7/26/80	7/28/80	7/26/80	7/25/80	7/25/80

nd - not determined.

Table 8. Ratios of selected chemical constituents to chlorides
in Geyser Bight thermal springs

Ratio	H1	H6	G6	G8	J	K	L	G8A
				Site				
Na:Cl	0.72	0.76	0.73	0.77	0.76	0.80	0.76	0.814
K:Cl	0.033	0.034	0.050	0.049	0.54	0.062	0.054	0.103
SO_4:Cl	0.27	0.26	0.29	0.27	0.28	0.28	0.24	3.77
B:Cl	0.10	0.10	0.044	0.10	0.09	0.08	0.08	0.07

Site G is located in the northeast corner of the main glacial valley above the east bank of Geyser Creek (fig. 11). Two groups of thermal springs emerge at the base and on the lower slopes of the east valley wall (fig. 13). The thermal waters emanate from numerous small pools, orifices and seeps in the cemented alluvium and colluvium. Several small steam vents also occur in the area, which indicates steam is separating below the surface. The most prominent thermal spring, G8, is a geyser whose eruption cycle is about 10 to 11 min. long. Waters fill a 20-cm-deep, 1-m-dia basin coated with siliceous sinter. Ebullition rises to 10-15 cm above average water level during the period of maximum activity.

Thermal waters from G6 and G8 are chemically similar to those at site H (table 7). The silica content of G8, however, is conspicuously higher. The acid spring G8A is low in chloride and probably results from the condensation of steam separating from waters rising in the conduits feeding G8. The high acidity probably results from the near-surface oxidation of hydrogen sulfide.

An analysis of gases obtained from spring G6 appears in table 9. The high nitrogen content indicates a considerable amount of air contamination, perhaps from air dissolved in the circulating ground water. The oxygen is probably selectively removed in oxidation reactions of H_2S and other constituents; the pool adjacent to G6 has a pH of 3.63. Carbon dioxide is the major active gas, but a measurable amount of hydrogen emerges with the spring waters.

Site J occurs in the southwest corner of the valley across from site G. The most prominent thermal spring at the site, J1, emanates from a 5-m-deep funnel-shaped aquamarine blue pool set into the valley alluvium (fig. 14). Small mounds of fresh silica sinter rim the perimeter of the 3-m-dia 82°C pool, with outflow cascading over a broad apron of siliceous sinter east of the pool. The size of the silica apron suggests that spring flow from the pool was much greater at one

time. Low rumbling concussions could be heard beneath the ground surface in the vicinity of J1. The chemistry of waters from J1 are strikingly similar to that of G8 and indicates a common source (table 7).

Table 9. Chemical composition of gas sample from
Geyser Bight thermal spring G6
(analyses in volumer percent).[a]

	Volume (%)
He	0.01
H_2	0.09
Ar	0.78
O_2	0.70
N_2	85.25
CH_4	0.04
CO_4	13.45
C_2H_6	0.01
H_2S	---

[a]W. Evans, analyst, USGS, Menlo Park, CA.

Other springs in the vicinity of J1 occur along the slope break at the base of the southwest valley wall dispersed over a distance of 250 m. The springs typically emerge from pools ranging from 0.5 to 2.5 m in diameter with deep funnel-shaped bottoms set into valley alluvium. Several additional small springs and seeps occur in a small tributary valley located about 0.5 km above site J and are labeled Q in fig. 11.

Site K is located 4.75 km inland from Geyser Bight in the alluvium of Geyser Creek valley. The springs lie near the center of the valley and appear to flow directly out of the alluvium. Thermal waters, 62°C, emerge in an oval-shaped pool, 2.5 m wide, 4 m long, and up to 1.5 m deep, and flow down a straight, narrow channel 20 m long and 0.3 m wide into two successive large oval pools (fig. 15) that were covered with a thick layer of dark algal growth. Overflow from these pools spills into a nearby cold stream. A fourth irregularly shaped small pool with 43°C water also drains into the cold stream at the same point. The main pool and the rest of the drainage system was clogged with thick, dark algal growth. A temperature of 59°C for the first of the larger oval pools indicates additional influxes of hot water here.

Almost directly across from site K, tucked in an indentation of the northeast side of the valley, is hot-spring-site L (fig. 11). The concavity of the hollow in which the site is located, plus the warmth, softness, and muddiness of the soil in and around the springs suggest the area is the site of a small shallow slump or landslide due to loosening of subsurface material by the injection of warm water. Several small springs

occur around the upper back wall of the depression and a few muddy seeps occur at its center (fig. 16). Nine vents that emitted 44.5° to 92.2°C water were distinguished. The spring of greatest activity was located at the far south side of the site. From it 85.5°C water bubbled up and flowed down a narrow channel to a pool 20 m long, 7 m wide, and up to 1 m deep. The pool supports abundant bacteria and algal flora. Discharge from the nine vents totaled 200 lpm.

The chemistry of thermal waters from sites K and L are similar (table 7). Both are mildly concentrated in sodium chloride and have a high level of bicarbonate.

The chemical analyses of Geyser Bight thermal waters given in table 7 compare well with analyses on waters from two of the springs reported by Byers and Brannock (1949) and to more recent USGS analyses of waters collected from several of the springs in 1973 (I. Barnes, unpub. data). The thermal waters are all moderately concentrated in sodium and chloride and are notably high in boron. The ratios Na:Cl, SO_4:Cl, and B:Cl are similar for all thermal waters sampled in 1980 except for the acid spring G8A and the B:Cl in G6 (table 8). These similarities in the more conservative constituent ratios suggest the thermal waters, although occurring in different localities, originate from a common deep reservoir. The K:Cl ratios are similar for thermal springs occurring within the same group, but vary slightly between groups. These differences may reflect reequilibration of the waters on ascent or perhaps varying residence times in intermediate reservoirs.

The striking similarity in chemistry of G8 and J1 indicates these springs are being fed directly from a common reservoir. The springs lie on opposite sides of the upper valley, which suggests that such a reservoir may underlie the entire valley floor in this vicinity. The differences in the amount of silica and other constituents between the springs could be due to varying amounts of boiling within individual systems, dilution with cold ground water, or differing intermediate reservoirs.

Reservoir properties

Table 10 summarizes the application of silica and cation geothermometry to the DGGS chemical analyses of various thermal springs of Geyser Bight. A sulfate-water oxygen isotope geothermometer, also given in table 10, is available from a previous USGS analysis (Nehring and others, 1980; I. Barnes, unpub. data). Because most springs are at boiling, $T_2 = 264°C$ is selected as the appropriate thermometer under conditions prescribed in McKenzie and Truesdell (1977). Because of its much longer reequilibration time than either silica or cation geothermometers, the sulfate geothermometer is often a good indicator of the deep reservoir temperature. However, because there is no other concordant geothermometer and because additional sulfate-water oxygen-isotope data are lacking for Geyser Bight, the T_2 temperatures are

taken as the maximum in estimating the deep reservoir system. The quartz adiabatic and the Na-K-Ca (1/3) temperatures for J1 are taken as the most likely and minimum estimates, respectively:

	Min	Max	Most Likely	Mean
Subsurface temp (^{o}C)	180	264	186	210

Table 10. Geyser Bight thermal springs geothermometry
(all temperatures are in ^{o}C).

	Site						
	H1	H6	G6	G8	J	K	L
Surface temperature	100.3	99.9	97.3	100.1	82.0	62.0	85.5
Cation geothermometers							
Na-K	158	157	187	182	189	196	190
Na-K-Ca (1/3)	149	151	166	175	180	166	166
Na-K-Ca (4/3)	122	131	129	173	174	114	122
Silica geothermometers							
Adiabatic	159	165	162	185	186	152	156
Conductive	169	176	172	201	202	160	165
Chalcedony	146	155	150	184	184	136	142
Christobalite	119	127	122	153	153	110	115
Opal	46	53	49	77	77	38	43

Sulfate-water oxygen isotope geothermometer, thermal spring G8[a]

$\delta^{18}O$-SO_4 $^o/oo$	$\delta^{18}O$-H_2O $^o/oo$	T1	T2	T3
-4.05	-8.06	322	264	282

[a]From Nehring and others, 1980. Temperature estimates are based on three different end member cases of water cooling as discussed on page 19 of this report.

Variations in the chemistries and corresponding reservoir geothermometers for the different spring systems may be due to the degree of reequilibration of the deep thermal waters on ascent through the feeding conduits or to the degree of dilution with ground waters. Inter-

mediate reservoirs fed by a parent deep reservoir may also underlie the
three geographically separate groups of springs (H; G and J; K and L).
Such tiered reservoir systems are not uncommon in other geothermal systems.
Geothermometry for the individual spring groups suggests temperatures of
155°C, 185°C, and 165°C for the three secondary reservoirs.

The host rocks for the reservoirs may be the Tertiary central Umnak
volcanic rocks, or the Tertiary diorites that appear to underlie the
central Umnak volcanics, or both. No geophysical exploration or explora-
tory drilling has been done, and the thickness of valley sediments and
depth to bedrock are unknown.

Comments

The Geyser Bight hot-water system constitutes the hottest and most
extensive hydrothermal convective system known to exist in Alaska. Deep
reservoir temperatures, conservatively estimated at 210°C, may be as hot
as 264°C. The surface expression of thermal springs, geysers and fuma-
roles suggests the subsurface reservoir is large. The system could be
used for large-scale flash-steam electric power production and for a
variety of other applications. However, there are no protected deep-water
harbors in the area and few potential users for such a large energy
resource.

The origin of the thermal energy driving the hydrothermal convective
system may be associated with the active volcanism that occurs on Umnak
Island. Deep fractures may provide conduits to high-temperature reser-
voirs overlying cooling bodies of magma.

HOT SPRINGS COVE

Location

Latitude 53°14.3' N., longitude 168°21.6' W.; Umnak 1:250,000
Quadrangle (1951); T. 80 S., R. 132 W., Seward Meridian.

General description

Thermal springs in the vicinity of Hot Springs cove occur at the
beach and about 1 km inland, south of the beach at the base of the west
slope of the valley that drains northward into the cove (fig. 11). The
thermal springs at the beach emerge along the western shoreline during
periods of low tide. Old beach dunes, about 0.5 km wide, span the 1-km-
wide mouth of the valley at Hot Spring Cove.

The shallow valley, roughly 0.5 km deep and 0.75 km wide, contains
a broad open marsh located behind the beach dunes, lushly vegetated with
grasses and muskeg and surrounded by ridges rising to 600 m. Reindeer
were observed grazing in the valley and in the 180-m-high pass that leads
from the southeast corner of the valley to an unnamed valley that drains
to the Pacific coast. These valleys and the surrounding countryside
show the erosional effects of intense glaciation. The Pacific side
valley contains another thermal spring site, "Partov" hot springs.

Hot Springs Cove and adjacent Stepanof Cove offer the only protected
anchorages along this portion of the Umnak Island Bering Seacoast. DGGS
reached the site via chartered vessel from Unalaska. An old military
road, washed out in several places and in a general state of disrepair,
leads from an airstrip at Fort Glenn on the northwest end of the island
over a 100-m-high pass to Stepanof Cove. The 35-km-long road is a poten-
tial means of access to the site.

Land status in the vicinity of the site is unclear. The lands may
have been selected by the St. George Village Association and the Aleutian
Pribilof Native Association under terms of ANCSA.

Geology

Bedrock exposed in valley walls adjacent to the thermal site consist
of late Tertiary central Umnak volcanic rocks overlain by Quaternary
hypersthene andesitic flows of Mt. Recheshnoi (fig. 10) (Byers, 1959).
These volcanic units appear to rest on a basement complex composed of
probable early to middle Tertiary plutonic and low-grade metamorphic rocks
that are exposed along the coastline of Umnak Island. An isolated outcrop
of a quartz-bearing olivine andesite flow overlying the Recheshnoi vol-
canics lies directly south of the valley at an elevation of 500 m.

Okmok Caldera, a huge active shield volcano, lies 20 km NE of the thermal-springs site. A recent cinder cone and associated lava flows occur across Hot Springs Cove at Cinder Point (fig. 11).

Spring characteristics

The upper series of thermal springs occur along a 300-m linear zone west of Hot Springs Creek at the base of the west valley slopes (fig. 19). Spring E5, the most southerly in the series, flows from a small cavern located at slope break at the base of the valley wall at the entrance of a steep SW-trending tributary valley. The thermal waters issue from a nest of cemented boulders, cobbles, and soil inside the 1-m-dia cavern. Discharge measured 100 lpm; spring temperature was 71.8°C. The only other spring exhibiting any significant flow in 1980 was E1, which emerges from a 30-cm-deep, 70-cm-dia pool ringed by boulders and cobbles. Temperature at the vent located at the pool bottom was 93.5°C; discharge from the pool measured 60·lpm. Sinter coats ·rocks in the outflow channel; bacteria and algae mats occur further downstream.

In contrast to the earlier investigations of Byers and Brannock (1949), the springs E2 and E4 were found to be dry and only a trickle of flow occurred at E3 (table 11). The flow at E5 was also much lower than that reported for 1947. However, the spring temperatures at E1 and E5 were notably higher in 1980, which suggests that the differences in measured flow rates may be due to a greater degree of ground water mixing during the 1947 measurements.

Table 11. Temperatures and flow rates, thermal springs south of Hot Spring Cove. Data from Byers and Brannock (1949) included for comparison.

Thermal spring	1980		Quality of measurement	1947	
	T (°C)	Flow rate (1pm)		T (°C)	Flow rate (1pm)
E1	93.5	60	Fair (10%)	87	54
E2	31.8[a]	dry	---	47	54
E3	61.2	trickle	vis. est.	65	6
E4	38.9[a]	dry	---	35	36
E5	71.8	100	Fair (10%)	67	200

[a]Ground temperature.

Springs E1 and E5 are moderately concentrated in sodium and chloride and have a notably high level of boron (table 12). The hotter spring, E1, has the greater concentration of constituents. The difference in temperature and the similarity in the $Na:Cl$, $Li:Cl$, $SiO_2:Cl$, and $B:Cl$ ratios of
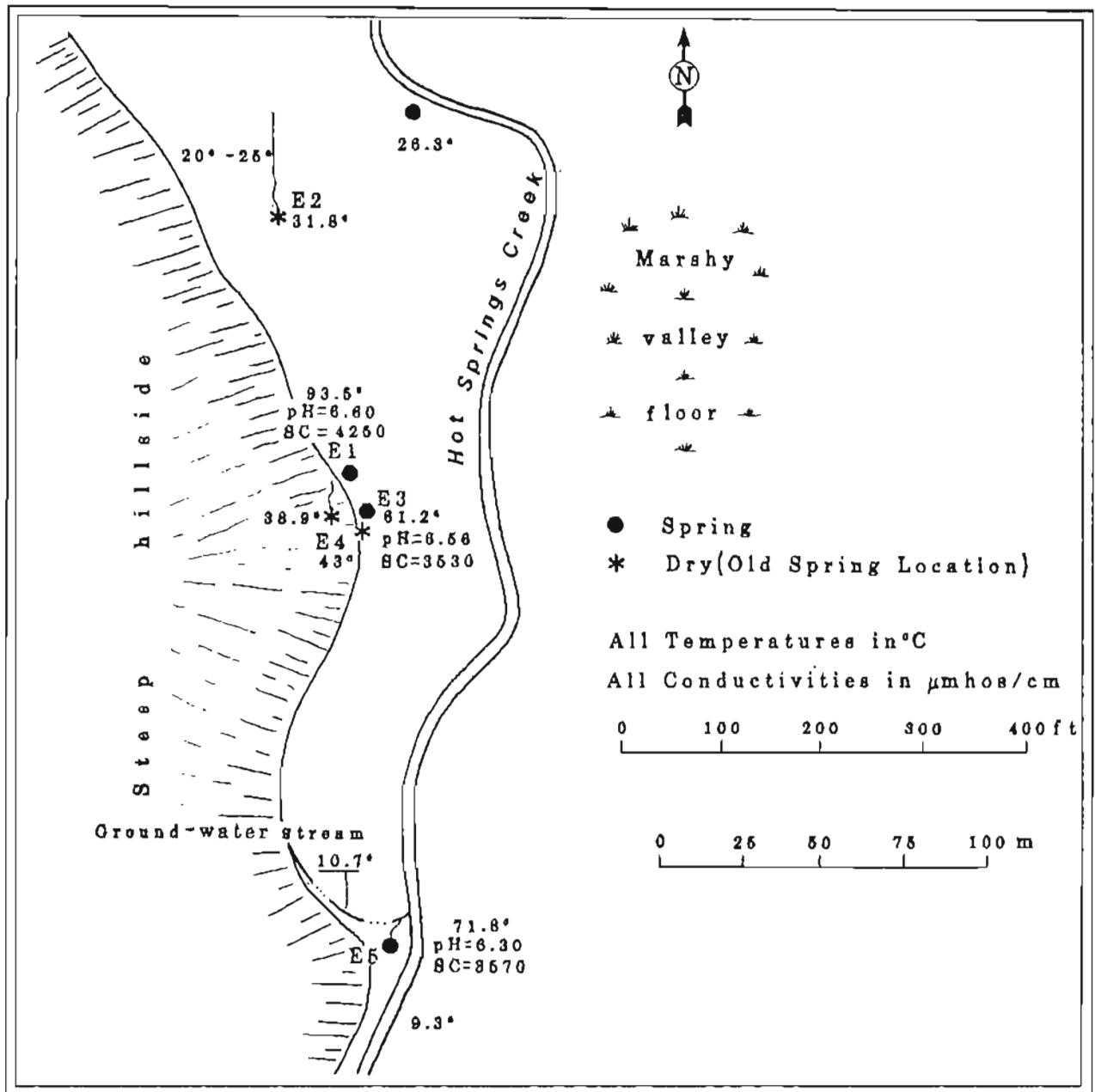
Figure 19. Detail at Hot Springs Cove site E.

the two waters suggests they are derived from a common thermal reservoir and undergo differing degrees of ground-water dilution. The chemistries and temperatures of springs E1 and E5 in 1980 were similar in all respects to a previous chemical survey of the springs made by the USGS in 1973 (I. Barnes, unpub. data). However, both the DGGS and USGS water samples were significantly higher in dissolved constituents than the water sampled in 1947, further suggesting that a greater amount of ground-water dilution occurred in 1947.

Table 12. Chemical composition and physical properties of
Hot Springs Cove hot springs E1 and E5.
(all chemical analyses in mg/l).

	Site E1	Site E5
SiO_2	120	91
Al	nd	nd
Fe	0.08	0.13
Ca	164	134
Mg	1.1	1.2
Na	664	531
K	34.2	24.5
Li	2.62	2.26
HCO_3	142	133
SO_4	91.4	83.2
Cl	1255	1010
F	0.86	0.72
Br	3.98	3.29
I	0.74	0.60
B	31.3	23.8
H_2S	0.15	nd
Sr	1.56	1.28
pH, field	6.47	6.36
Dissolved solids	2513.0	2040.0
Hardness (mg/l $CaCO_3$)	416	341
Sp conductance (μmho/cm at 25°C)	4250	3300
T (°C)	93.5	71.8
Flow rate, lpm	62	101
Date sampled	7/29/80	7/29/80

nd = not determined.

The shoreline thermal waters emerge at lowest tide along a 800-m linear zone at the west end of the beach. Maximum sand temperatures in 1980 measured 45°C. Byers and Brannock (1949) reported temperatures as high as 70°C. Because the biweekly cycle of variations in tidal

amplitude was at its minimum during the DGGS visit to Hot Springs Cove, the shoreline thermal waters were nearly always covered with sea water and we could not obtain a sample.

Reservoir properties

Table 13 summarizes the application of silica and cation geothermometry to thermal springs E1 and E5. The quartz-conductive temperatures differ by 16°C, whereas the applicable cation temperatures differ by only 7°C. This trend is consistent with a hypothesis of ground-water mixing. The cation geothermometers, particularly Na-K, are less susceptible to dilution effects than the silica geothermometers, and are therefore probably more representative of the deep reservoir temperatures. Two different ground-water samples obtained near the hot springs each had temperatures and silica contents of about 10°C and 20 ppm. These values lie on the same linear trend as the values for the thermal springs, E1 and E5. Following the method of Truesdell and Fournier (1977), application of the quartz-conductive mixing model results in a deep reservoir temperature estimate of 198°C. This corresponds to a parent thermal-water silica content of about 240 ppm and hot-water mixing fractions of 45 and 33 percent for springs E1 and E5, respectively.

Table 13. Hot Springs Cove geothermometry
(all temperatures in °C).

	Site E1	Site E5
Surface temperature	93.5	71.8
Cation geothermometers		
Na-K	166	159
Na-K-Ca (1/3)	152	145
Na-K-Ca (4/3)	117	107
Silica geothermometers		
Adiabatic	141	128
Conductive	148	132
Chalcedony	122	105
Cristobalite	97	81
Opal	26	12

In estimating the deep reservoir temperature, the quartz-conductive mixing-model temperature is chosen as the maximum, the Na-K temperature for spring E1 as the most likely, and the quartz-conductive temperature for E1 as the minimum:

	Min	Max	Most likely	Mean
Subsurface T (°C)	148	198	166	171

Although the evidence for mixing is strong, the maximum temperature estimate must still be viewed as speculative. The host rocks for the reservoir are probably the underlying basement Tertiary plutons and low-grade metamorphic rocks. No geophysical exploration or exploratory drilling has been done, and the depth and extent of any deep thermal reservoir are unknown.

Comments

The estimated deep-reservoir temperatures would be sufficient to power a small- to medium-scale, binary, Rankine-type, wellhead, electrical-generation system. The thermal waters, if in sufficient supply, could also be used for a variety of other geothermal applications. However, the remoteness of the site and the lack of a good, protected deep-water anchorage probably precludes any development in the foreseeable future.

The source of thermal energy driving the hydrothermal system may be related to the active volcanism that occurs northeast and southwest of the site. Ground waters may be penetrating via fracture system into rocks heated by nearby magma systems.

Location

Latitude 53°13.7' N., longitude 168°18.5' W.; Umnak 1:250,000
Quadrangle (1951); T. 80 S., R. 132 W., Seward Merdian.

General description

Partov hot springs[*] is located about 6 km southeast of Hot Springs
Cove on the Pacific side of Umnak Island. The thermal springs occur in
an unnamed stream valley that drains into an unnamed cove 4 km northeast
of Partov Cove. The springs are situated about 3/4 km from the Pacific
Ocean on the northern banks of the main stream drainage in the valley
that trends S. 65 E. The site was reached by crossing a 180-m-high pass
that connects this valley with Hot Springs Cove.

Geology

The geology in the vicinity of Partov hot springs is similar to that
discussed under Hot Springs Cove (preceding section).

Spring characteristics

Five areas of springs and seeps are found in a 200-m linear zone
adjacent to the north bank of the main valley creek. The springs and
seeps emerge from valley alluvium 2 m above stream level (fig. 20). The
combined flow from the five springs was visually estimated at about 200 lpm.
Spring temperatures ranged from 45°-85°C. Flows from three of the springs
feed a large pool, 15 by 10 m, that is covered with rust-colored scum.
White calcite coating was observed on rocks in outflow channels below the
springs. A small amount of gas bubbling occurs from the main pool; no
odor of H_2S was detected.

Table 14 gives the chemical composition and physical properties of
thermal waters obtained from the highest temperature spring vent at the
site. The waters, which are quite similar to the hot springs in the valley
to the north (table 12), are moderately concentrated in sodium and chloride
and have a notably high level of boron.

Reservoir properties

Table 15 summarizes the application of silica and cation geothermo-
meters to Partov hot springs. Although the Na-K-Ca (4/3) temperature is
below 100°C, the silica geothermometers indicate equilibrium took place
at temperatures above 100°C and, therefore, Na-K-Ca (1/3) is taken as the
representative cation reservoir temperature. The quartz conductive and

---

[*]Informally named.

chalcedony temperatures are chosen as the maximum and minimum reservoir estimates respectively:

	Min	Max	Most likely	Mean
Subsurface T (^{o}C)	118	144	134	132
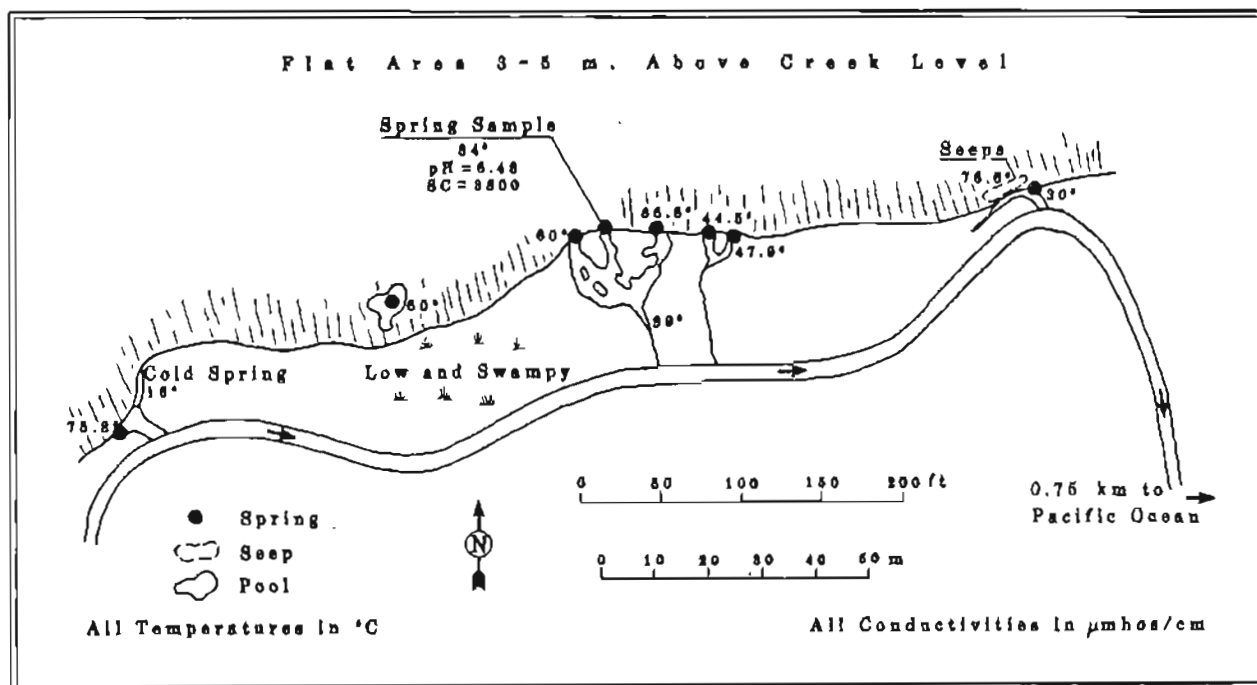
Figure 20.   Detail at Partov spring site.

As in the case with the thermal springs of the Hot Springs Cove area, the thermal waters emerging at the surface at Partov hot springs may have cooled by mixing with ground waters. Assuming a ground-water temperature of 10°C and silica content of 20 ppm and following the quartz mixing model of Truesdell and Fournier (1977), the deep-reservoir temperature may be as high as 202°C. This temperature is similar to the deep-reservoir estimate based on the silica mixing model made for Hot Spring Cove. The similarity in chemistries and estimated deep temperatures suggests the spring systems may originate from a common source.

Comments

As at the Hot Springs Cove site, the thermal springs may result from the circulation of surface waters in deep fractures through volcanically heated rocks. Although the reservoir temperature is conservatively estimated at 132°C, the quartz mixing model suggests deep temperatures may be much higher. Nevertheless, the remoteness of the site, lack of potential users, and lack of protected harbors will probably preclude development of this site.

Table 14. Chemical composition and physical properties of
Partov hot springs
(all chemical analyses in mg/l).

	DGGS determination
SiO_2	113
Al	nd
Fe	0.49
Ca	233
Mg	2.7
Na	456
K	19
Li	3.1
HCO_3	138
SO_4	163
Cl	1050
F	1.0
Br	3.35
I	0.67
B	27.3
H_2S	nd
Sr	2.25
pH, field	6.57
Dissolved solids	2212.9
Hardness (mg/l $CaCO_3$)	596
Sp conductance (μmho/cm at 25°C)	3800
T (^{o}C)	84
Flow rate (lpm)	200[a]
Date sampled	7/31/80

[a] Estimated flow of five springs combined.
nd = not determined.

Table 15. Partov hot springs geothermometry
(all temperatures in ^{o}C).

Surface temperature   84.0

Cation geothermometers

Na-K	152
Na-K-Ca (1/3)	134
Na-K-Ca (4/3)	83

Silica geothermometers

Adiabatic	139
Conductive	144
Chalcedony	118
Christobalite	94
Opal	23

UNALASKA ISLAND

Background

Unalaska Island, second largest in the arcuate chain of Aleutian Islands, is located between latitudes 53°15' and 54° N. and between longitudes 166° and 168° W., 200 km southwest of the Alaska Peninsula (fig. 1). The island is about 140 km long and 60 km wide and follows the trend of this segment of the Aleutian arc, which is about N. 60° E. (Drewes and others, 1961). Most of the island is ruggedly mountainous and, except for the northern bulge, the coastline is deeply indented by fjords (fig. 21). Beaver Inlet, which is more than 30 km long, and Makushin Bay, about 16 km long, split the eastern and western ends of the island, respectively, and separate northern Unalaska from the elongate southern portion.

The western part of northern Unalaska (the northern bulge) is dominated by the still active Makushin Volcano, which is about 2035 m high. The broad dome-shaped summit has a small caldera and is capped by a glacier with tongues that descend the larger valleys to elevations as low as 300 m (1000 ft). Several symmetrical cones and craters occur on the flanks of the volcano.

The terrain immediately around the volcano and extending eastward from it is characteristically rugged with deep glacier-carved valleys, sharp ridges, and peaks. Two broad glacier valleys, Makushin Valley and Glacier Valley, originate on the flanks of Makushin volcano and extend to Unalaska Bay and Makushin Bay, respectively. Unalaska Bay, a deep embayment into the northern coast of the island, with several subsidiary inlets, lies about 20 km east of Makushin Volcano.

Much of the island is discontinuously veneered by a thin mantle of till, volcanic ash, humus, and soil (Drewes and others, 1961). The only trees on the island are several groves of Sitka spruce, planted by Russians in the 19th Century around Unalaska Bay. Willow thickets grow at low elevations in the more protected valleys; blueberry shrubs and salmonberry and crowberry plants are common. The lower elevations and valley bottoms are characterized by tundra vegetation. During the summer the meadows are abloom with a large variety of flowers.

Unalaska village lies on the southern shore of Iliuliuk Bay near the head of Unalaska Bay. The only other permanently inhabited place on the island is a sheep ranch at Chernofski Harbor. The Unalaska community has a permanent resident population of about 600 people, many of whom are Native.

Unalaska village was first visited by Russian fur traders late in the 18th century. During the 19th century, the village became a Russian outpost and a major center for the Aleutian fur trade and Russian Orthodox
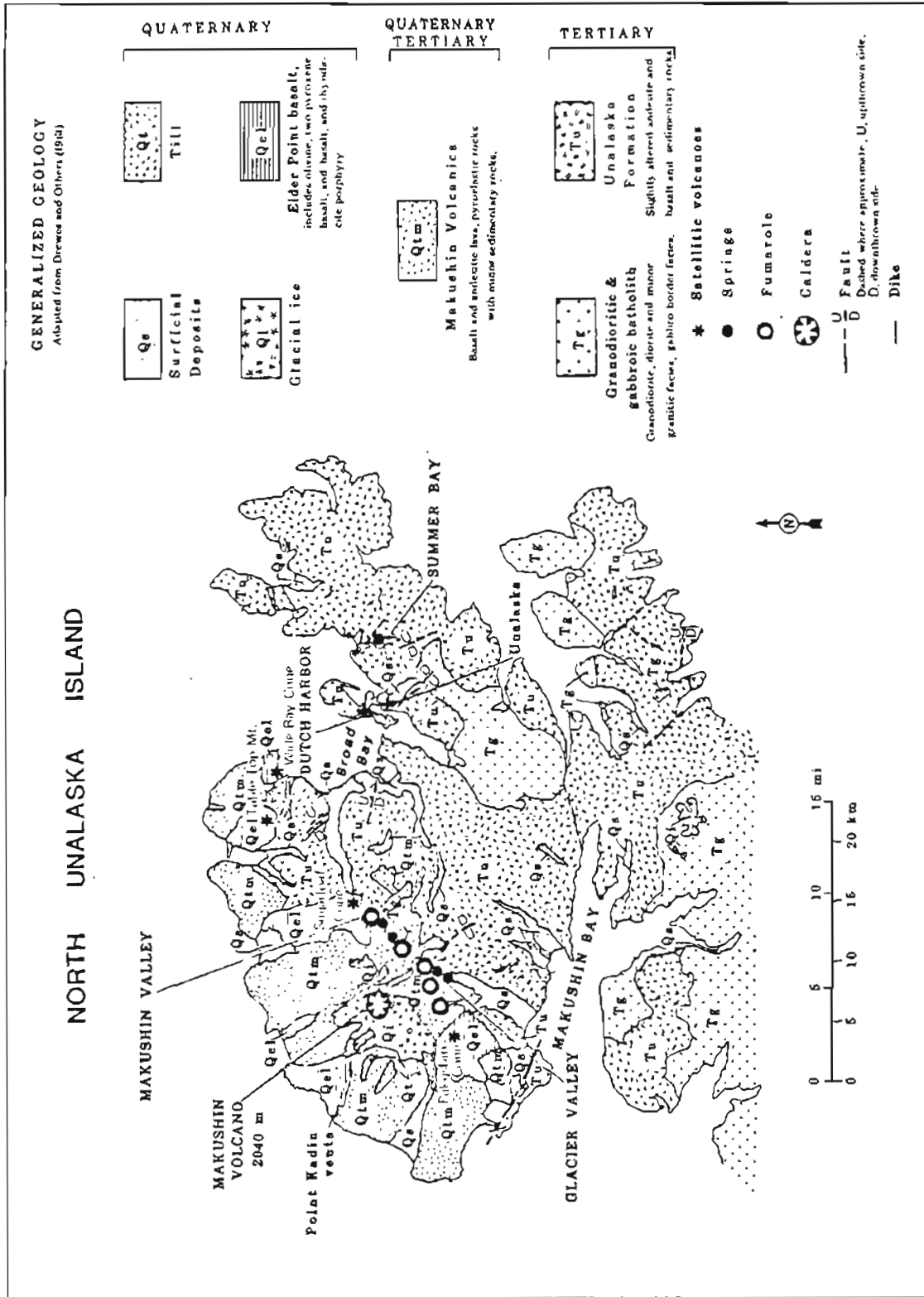
Figure 21. Generalized geology of northern Unalaska Island and locations of thermal fields.

Church. The purchase of Alaska by the United States in 1867 and the rapid
decline of fur-bearing sea-mammal populations later in the century led to
a gradual decrease in White population and influence in Unalaska until 1942.

During World War-II Dutch Harbor, located on Amaknak Island, adjacent
to Unalaska village and now connected to it by a bridge, served as a major
U.S. naval base and staging area for Allied operations. The surrounding
hillsides are still littered with rusting Quonset huts, old tunnels, artil-
lery emplacements, pillboxes, and look-out posts. The Dutch Harbor area
itself contains row upon row of deserted barracks and warehouses, some of
which are now being reclaimed and renovated by the Ounalaska Native Corpora-
tion.

Because of the large and excellent deep-water harbor located in Unalaska
Bay (one of the few protected harbors in the Aleutians), the village has
naturally evolved into the major base of operations for the Bering Sea
fishing industry. Thirteen fish processors operate in the area and bring in
as many as 1,500-2,000 seasonal employees during the height of crab-fishing
season. Unalaska has the distinction of being the crab capital of the world.
With the imminent development of the Alaskan bottom fishery, Unalaska will
undoubtedly continue to expand. The village council is actively seeking an
energy base to support its growing fishing industries.

Geology

The geology of Unalaska Island has been described in Drewes and others
(1961). The Unalaska Formation constitutes the oldest and most extensive
group of rocks in the island and consists of a thick sequence of coarse and
fine sedimentary and pyroclastic rocks intercalated with dacitic, andesitic,
and basaltic flows and sills, cut by numerous dikes and small plutons
(fig. 21). The formation is exposed over two-thirds of the island and is
thought to be early to mid-Tertiary. The formation has been extensively
folded, faulted, and intruded by plutonic rocks, with moderate hydrothermal
alteration occurring near the plutons.

The batholiths and smaller plutons are granodiorite with border phases
as mafic as gabbro. The plutonic rocks are thought to be the products of
crystallization of a granodiorite magma that invaded the rocks of the
Unalaska Formation by assimilation, stoping, and forceful intrusion (Drewes
and others, 1961). The age of the pluton is considered to be younger than
early Miocene and older than middle Pleistocene.

Basalt and andesite flows and pyroclastic rocks of the Makushin Volcanics
unconformably overlie the Unalaska Formation and the plutonic rocks that
intrude it (Drewes and others, 1961). The Makushin Volcanics constitute
most of Makushin Volcano, a broad volcanic dome more than 1,800 m high and
16 km wide. The thickness of the Makushin Volcanics varies greatly but
probably does not exceed 1,500 m. Most of the Makushin Volcanics are believed
to be middle to late Pleistocene. Much of the basalt and andesite is exten-
sively glaciated and must precede at least part of late Pleistocene time.

Late Wisconsin to Recent volcanic cinder cones, composite cones, and lava flows are scattered about the base of Makushin Volcano and have been collectively mapped as Eider Point Basalt (Drewes and others, 1961). These volcanic rocks rest unconformably on glaciated rocks of the Makushin Volcanics and in places on the Unalaska Formation. A series of recent cinder cones and craters lie along a westward-trending fissure extending from the Makushin caldera to Point Kadin. The volcanic vents probably reflect the intrusion of magma into the fissure at shallow depths.

Makushin Volcano is still active and is known to have erupted at least 14 times since 1760, with a report of a minor eruption occurring in 1980 (Coats, 1950; Sean, 1980); Table Top Mountain has probably been active since the last major glaciation (Drewes and others, 1961).

The island has been intensely glaciated and glacial landforms are prominent everywhere. The mountains contain U-shaped valleys, cirques, aretes, and ice-scoured features of every size. An ice field of 40 km^2 caps Manushin Volcano. Till from the latest Wisconsin ice advance occurs in the lowest cirques and valleys. More recent, fresh-looking moraines, located near existing glaciers, indicate small advances and recessionns have taken place, perhaps within the past few hundred years (Drewes and others, 1961).

Faults, joints, and related linear features are abundant, but the length, direction, and amount of displacement have been determined for only a few of them. Most of the faults are nearly vertical. The strong topographic alignment of Beaver Inlet and Makushin Bay, which nearly bisect the island, suggests a major fault. A statistical analysis of linear topographic features from aerial photographs performed by Drewes and others (1961) showed a dominantly northwest trend in the Unalaska Formation in the more altered rocks near and in the batholiths, and a strong pattern of north- and east-trending sets of linear features in the less altered rocks away from the batholiths.

Thermal areas

Several active thermal areas have been identified on northern Unalaska Island, and all but one are associated with Makushin Volcano (figs. 21-23). Fumaroles and hot springs occur within the 2.5-km-dia Makushin caldera and were first investigated by Maddren (1919), who reported the existence of an extensive solfatara field ($\sim$ 30 acres) near the center of the caldera. Fumaroles were audible at distances of over 2 km, and the temperature at the orifice of one of the smaller fumaroles measured 150°C. The continued existence of these high-pressure fumaroles emitting large amounts of vapor was verified during the summer of 1980 (J. Reeder, pers. commun.).

An extensive fumarole field and associated hot springs mentioned in Drewes and others (1961) occur at the head of Glacier Valley in the south-southeast flank of Makushin Volcano (fig. 22). The fumaroles lie at an elevation of about 670 m. A smaller fumarole field, found in 1980, occurs
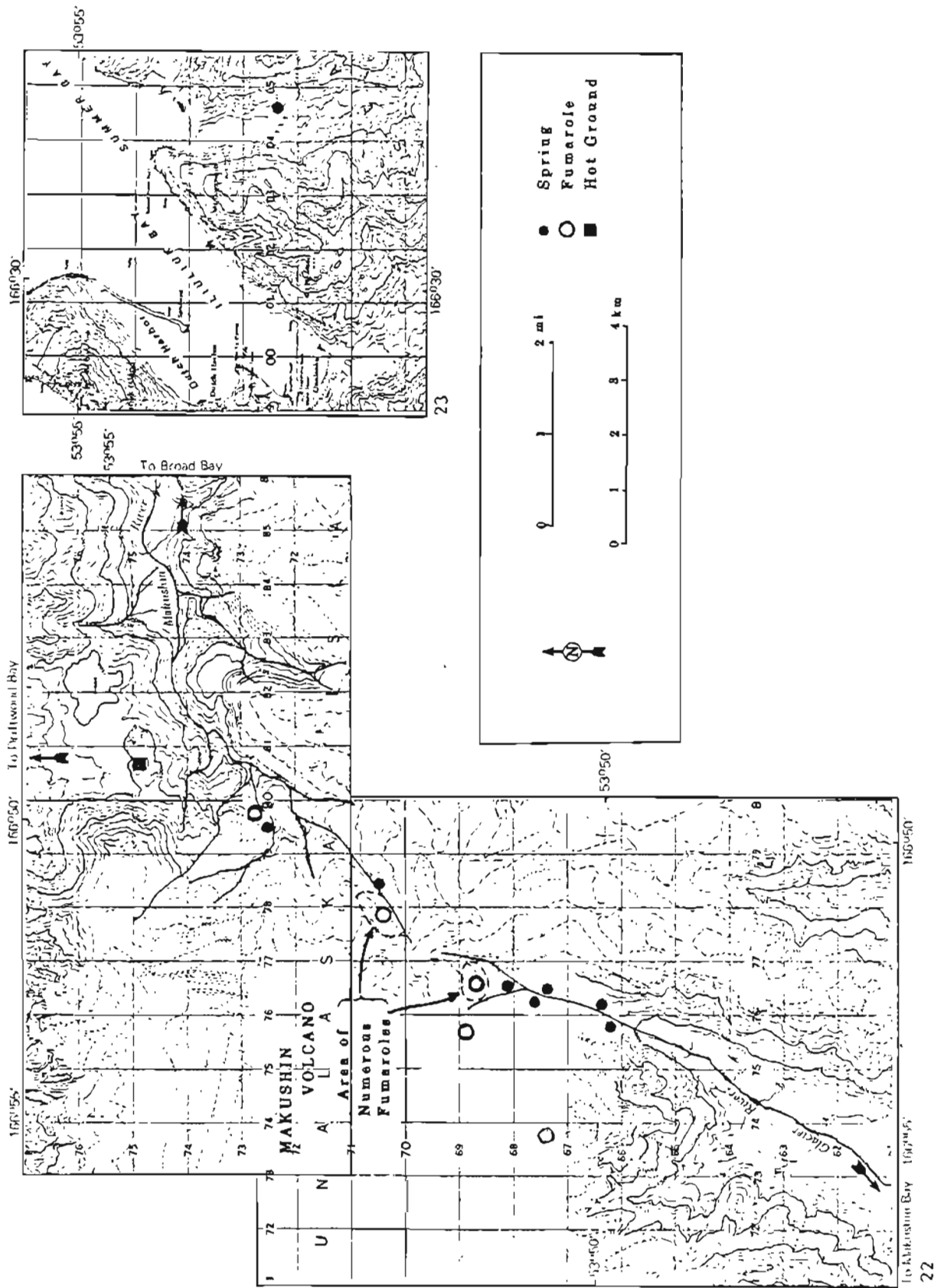
Figure 22. Location of thermal fields on Makushin Volcano. Figure 23. Location of Summer Bay hot springs (at right).

near the toe of a glacier located about 1 km northwest and about 150 m above the previous site. Another fumarole field containing a large, highly pressurized fumarole occurs further west on the south flank of the volcano at an elevation of about 900 m (J. Reeder, pers. commun.).

Two fumarole fields and associated hot springs were found in the upper reaches of Makushin Valley on the northeast flank of Makushin Volcano (fig. 22). The lower and smaller field occurs at an elevation of about 360 m on a small bench located on the steep north valley wall about 25 m above a stream channel. The larger field occurs about 2 km further upstream at the head of one of the tributary valleys on the east flank of the volcano at elevations varying from 600~800 m.

One additional hot-spring site occurs on the island and is located about 2 km south of Summer Bay (fig. 23). This spring is probably the same as that reported by Dall (1870) near Captain's Harbor.

The hot springs near Summer Bay are located within the Unalaska Formation. The hot springs and fumarole fields at the heads of Makushin and Glacier Valleys also occur in that formation and in the plutonic rocks that intrude it. The other fumaroles and hot springs occur in the younger Makushin Volcanics.

During July 1980 the DGGS field party was able to examine briefly the thermal areas at the heads of Makushin and Glacier Valleys and the hot-springs site near Summer Bay.

GLACIER VALLEY THERMAL AREA

Location

Latitude 53°50.8' N., longitude 166°53.0' W.;
Unalaska 1:250,000 Quadrangle, 1951.

General Description

The thermal area is located at the head of Glacier Valley, a 3- to
4-km-wide U-shaped valley that trends north from Makushin Bay for 10 km (fig.
21). The head of the valley terminates in a series of steep ravines in the
south-southeast flank of Makushin Volcano. The active summit caldera of the
volcano lies about 5 km northwest of the thermal site; Pakushin cone, a recent
parasitic pyroclastic cone, is located about 6 km southwest of the site. The
rugged ridges neighboring the thermal area are 600-900 m high and intensively
glaciated.

The thermal sites are located on and above the easternmost branch of the
Glacier Valley river at the very head of the valley (fig. 22). There are three
areas of thermal activity. The first two, a fumarole field and a series of hot
springs, occur on a ridge lying between two ravines in which flow the streams
that comprise the headwaters of the eastern branch of the main valley river.
About 0.5 km downstream from the juncture of these two streams, another series
of hot springs and seeps occur at the base of the eastern valley wall near the
stream bank. In addition to these sites, a small area of fumaroles and boiling
waters was found emanating from a pile of volcanic boulders on the western
margin of a glacier in the adjoining western tributary valley, about 1 km
northwest of the principal site. Still farther west, a highly pressurized
fumarole occurs at an elevation of about 900 m.

The thermal area in Glacier Valley is remote and relatively inaccessible.
The DGGS field party reached the sites by helicopter from the village of
Unalaska, which lies about 22 km east of the thermal area. The sites can also
be reached by taking a boat into Makushin Bay and then walking 10 km up Glacier
Valley.

Geology

The fumaroles, steam vents, and hot-spring waters emanate from an area of
intensely hydrothermally altered rocks belonging to the Unalaska Formation and
the gabbroic plutons that intrude it. The hydrothermal alteration, consisting
mainly of montmorillonite, is the result of interaction of near-surface rocks
with acid waters that are formed by the condensation of hydrogen-sulfide-rich
steam in meteorically derived, shallow ground waters. Fumarolic activity
extends up a ridge to an elevation of about 640 m, where it is capped by a 30-m
sequence of shallow dipping, interbedded basaltic flows that originated from
Makushin Volcano. The exposure of the flows above the fumaroles is nearly
vertical, apparently due to plucking by glacial erosion. These flows do not
appear to be altered, nor does the surface expression of the fumarolic activity
extend beyond the flow-contact boundary.

Several fresh moraines occur adjacent and below the zone of thermal activity at elevations of 300-600 m, and are evidence for recent glacier advances. A glacier still resides in the adjoining western valley and descends to an elevation of about 450 m. Lower portions of the valley are floored with glacial drift, alluvium, and colluvium.

Numerous fossil fumarolic vents and hydrothermally altered ground were found in a small, recent glacial moraine located near the juncture of the streams below the hydrothermally heated ridge. One fossil vent occurs in a cone-shaped, 4-m-dia, 1.5-m-high mound of hydrothermally altered clays. The fossil vents suggest the area was active at least during the waning stages of the last glaciation which, at this elevation, may have occurred as recently as a few hundred years ago.

Drewes and others (1961) mapped a steep normal fault southeast of the thermal sites. The trend of the fault, N. 50° W., is directly in line with the thermal sites and Makushin caldera, and may be providing conduits for thermal fluids to ascend to the surface.

Fumaroles and Hot-springs characteristics

The site consists of three areas of thermal activity that are separate but probably related.

a. The first zone consists of numerous small fumaroles and stream vents, all at boiling point, dispersed over an ara of about 10,000 m^2 and emanating from a series of small knolls and gullies cut into the hydrothermally altered ground. The vents occur between elevation of 550 and 650 m below a steep cliff of volcanic flows and between two forks of the eastern tributary to the main valley river (fig. 22). Orifices are generally a few centimeters or less in diameter with sublimates commonly ringing the vents. Gases are mostly steam. The vents have characteristically low flow rates, although several are moderately pressurized and have vapor plumes several meters high.

    Waterfalls from the lava cliff face above the fumarole field channel a large flux of surface meteoric waters onto and through the fumarole field. Where the waters pass over fumaroles they are heated by condensing steam, in some cases to the boiling point. Much of the water appears to percolate into the ground after passage through the thermal zone.

b. The second area of thermal activity consists of several hot springs and seeps located on a small bench indented into the bluffside at the base of the ridge containing the fumarole field (figs. 22 and 24). The springs occur at an elevation of about 380 m and cover an area of about 1,000 m^2, perched several meters above the juncture of the two streams that drain the thermal area. A recent glacial moraine containing numerous fossil thermal vents occurs immediately southeast of the springs.

    Spring temperatures ranged from 76° to 96°C, and the combined flow from the thermal springs was visually estimated at 200 lpm. The thermal waters
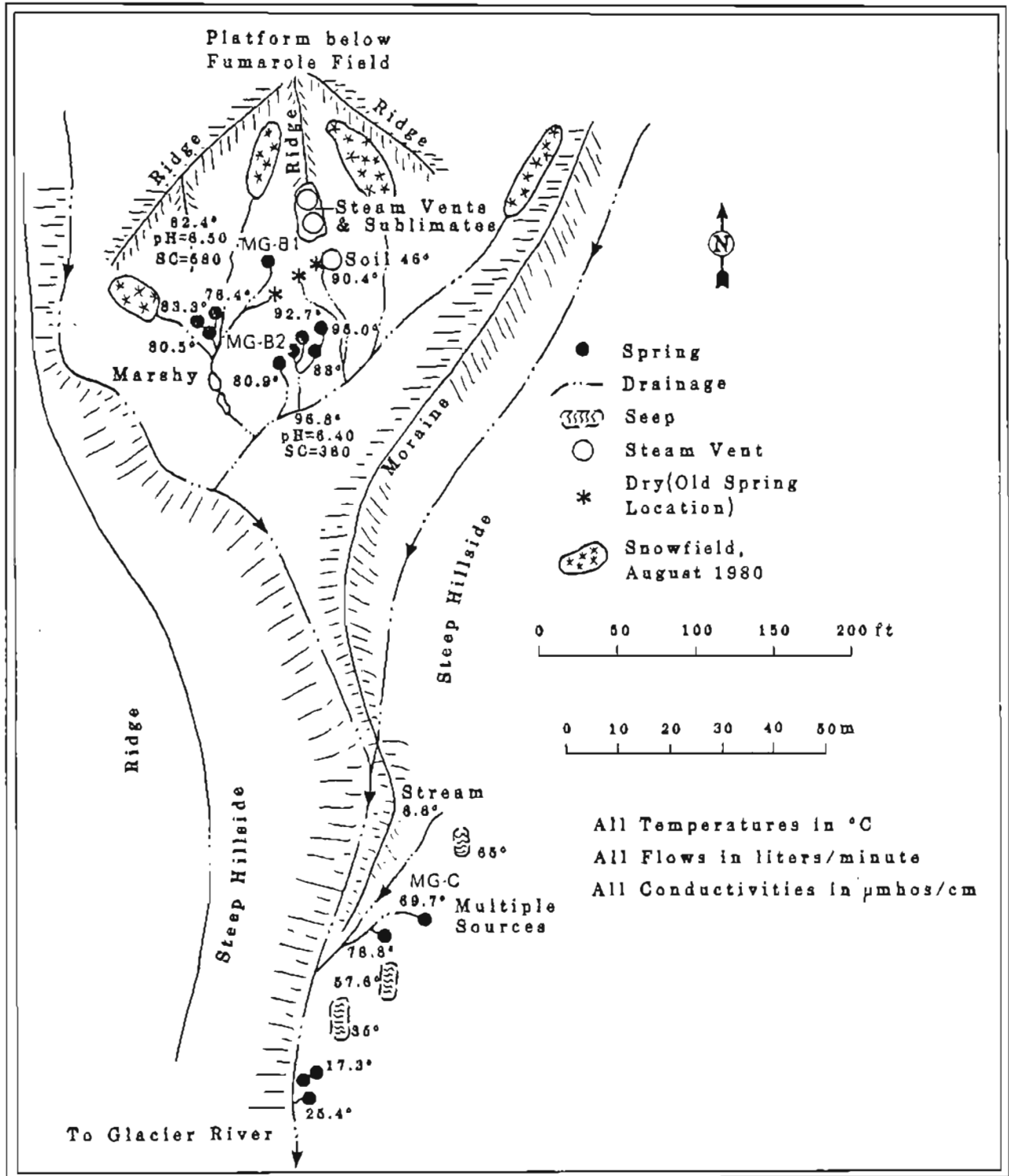
Figure 24. Detail at Glacier Valley thermal area.

typically emerge into shallow pools averaging about 1 m in dia in what appears to be glacial drift. The upper portions of the hot-spring channels were commonly veneered with a 1- to 2-cm-thick layer of calcite. Orange bacterial mats and blue-green algae commonly lined the channels farther down stream. Flow from the hot-spring channels combines with runoff from adjacent snow patches (present on 8/11/80) into a single channel, which then drains along the adjacent moraine and into the cold-water stream below the springs.

A few hot-spring channels were dry, indicating discharge may seasonally fluctuate with the availability of ground water. A small area of steaming ground occurs upslope and adjacent to some of these dry spring basins.

c.   The third area of activity consists of a 50-m linear zone of seeps and a few hot springs located about 0.5 km downstream from the previous hot-springs site (fig. 24). The thermal waters issue from colluvium at the base of the eastern valley wall, several meters above the main stream channel. Water temperatures range from 17° to 78°C, with the combined flow visually estimated at 60 lpm. The waters emerge principally through seeps. Three or four small springs also occur, including one from a small sinter cone and another with an estimated discharge of 30 lpm. The spring channels and much of the surrounding ground are coated with calcite, indicating flow may fluctuate or may have been much greater at one time. Outflow of the thermal waters from the area is diverted by a medial moraine for several meters before it joins the main stream channel.

Table 16 gives data on thermal waters obtained from site B and a partial analysis of a sample from site C.

Key features of the thermal water chemistry are the extremely low levels of chloride present, the nearly neutral pH, the relatively low cation content, and the comparatively high level of magnesium and calcium. The high sulfate content probably arises from the oxidation of H_2S gases associated with the fumarolic activity. The waters are similar to those that have been classified as bicarbonate-sulfate waters by others (White, 1957; Ellis and Mahon, 1964). Such waters typically occur on the flanks (or in wells drilled thereon) of active volcanoes in island-arc settings (Oki and Hirano, 1970; Mahon and others, 1980).

Reservoir Properties

The chemistry of the thermal waters and the occurrence of the fumarole field indicate the presence of at least a shallow vapor-dominated zone underlying the area. The magnesium and calcium contents of the thermal waters emerging at the surface indicates the waters are probably surface meteoric waters infiltrating to relatively shallow depths and being heated by steam rising from a deeper reservoir. The source of steam may ultimately be derived from a deep, boiling, hot-water system overlying a cooling magma body. The high silica content in the spring waters suggests temperatures in the shallow perched reservoir may approach 150°C, if equilibration with quartz is assumed. The large volume of steam escaping from the area and the large area covered by hydrothermal alteration and thermal activity indicate a hot reservoir system exists and that it probably exceeds 150°C.

Table 16. Chemical composition and physical properties of
Makushin Glacier Valley hot springs 1, 2, and 3
(All chemical analyses in mg/l.)

	MG-B1	MG-B2	MG-C
SiO_2	94	125	125
Al	nd	nd	--
Fe	0.10	<.01	--
Ca	11.7	32.1	--
Mg	4.0	10.6	--
Na	52.0	87.2	77.5
K	4.8	5.7	4.5
Li	<0.01	<0.01	--
HCO_3	37	288	--
SO_4	129	95	418
Cl	10	5	10
F	0.14	0.28	--
Br	nd	nd	--
I	nd	nd	--
B	<0.5	<0.5	--
H_2S	nd	<0.5	--
Sr	0.07	0.26	--
pH, field	6.40	6.50	--
Dissolved solids	342.81	649.14	--
Hardness ($mg/CaCO_3$)	45.76	82.4	--
Sp conductance (μmho/cm at 25°C)	360	580	--
T (°C)	96.8	82.4	78.8
Flow rate (lpm)	nd	nd	nd
Date sampled	8/11/80	8/11/80	8/11/80

nd - Not determined.

No geophysical exploration or exploratory drilling has yet been done at the site. The thickness of the perched water reservoir, the underlying vapor-dominated zone, and depth to the hot water or steam reservoir all need to be determined.

Comments

The fault system mapped southeast of this thermal area may provide conduits for the thermal fluids that are ascending from deep within the geothermal system. The trend of this fault and those of a large proportion of linear features on northern Unalaska, including those associated with Makushin Volcano, are approximately N. 50° W. (Drewes and others, 1961). This orientation is about the same as the direction of convergence of the North American and Pacific tectonic plates. Major tensional features are considered to propagate in this direction, the direction of maximum horizontal compressional stress (Nakumura and others, 1977). Such deep-seated fractures can provide avenues for intrusion of volcanic dikes and feeder systems for surface thermal vents.

The setting and chemistry of the Glacier Valley thermal area is similar in many respects to that of other active island-arc volcanic systems (Oki and Hirano, 1970; Mahon and others, 1980). Detailed investigations of such volcanic systems in other areas indicate that the heat driving the secondary hydrothermal reservoirs and producing the surface springs and fumaroles is derived from primary reservoirs of a hot sodium chloride brine that overlie cooling magma bodies. Temperatures in such thermal brine reservoirs are known to exceed 300°C. If such a deep high-temperature brine reservoir exists at Makushin, it may ultimately prove the most productive geothermal reservoir in the system.

The occurrence of a high-temperature geothermal reservoir in the vicinity of a population center seeking to expand its fishing industry makes the detailed investigation of the Makushin geothermal resource attractive. One potential deterrent to the development of this resource is the volcanic hazards associated with the still-active Makushin Volcano.

MAKUSHIN VALLEY THERMAL AREAS

Location

Latitude 53° 55' N., longitude 166° 50' W.;
Unalaska 1:250,000 Quadrangle (1951)

General Description

The Makushin Valley thermal areas are located at the head of Makushin Valley on the east-northeast flank of Makushin Volcano, about 5 km east of the summit caldera (fig. 21 and 22). Makushin Valley trends westward for 13 km from Broad Bay before terminating on Makushin Volcano. The lower part of the valley is a 3-km-wide U-shaped glacier valley, whereas the upper reaches of the valley consist of several small canyons incised into the flanks of Makushin Volcano. The canyons are flanked by steep valley walls rising 300 to 600 m above stream level. Ridge tops are commonly rounded plateaus and range from 300 to 900 m high.

The region has been intensely glaciated. A glacier still resides on the upper flanks of the volcano above the thermal area, and in places descends to elevations of 700 m. The upper part of the volcano, however, still retains the shape of a shield volcano.

There are three areas of thermal activity that occur along the upper reaches of the Makushin River (fig. 22). The highest of these consists of a broad field of mild fumarolic activity, located between 640 and 820 m in elevation on the east flank of the volcano. The second area consists of a cluster of hot springs at an elevation of 570 m, located at the base of the ridge containing the fumarole field. The third area occurs about 2.5 km farther downstream and consists of a few steam vents and mild fumaroles with associated thermal waters.

The thermal areas are relatively inaccessible and were reached by helicopter from the village of Unalaska, which lies about 20 km east of the sites. Although remote, the sites could be reached by following an old military jeep trail starting either from Broad Bay and going up Makushin Valley or from an abandoned airstrip near Driftwood bay and ascending to a basalt plateau at an elevation of 300 m, located north of the thermal areas. From there the sites can be reached by a 5-km cross-country trek.

Geology

Bedrock in the vicinity of the thermal field consists of a complex mixture of the Unalaska Formation and the plutons and dikes that intrude it. Recent lava flows and pyroclastic rocks, collectively termed the Eider Point Basalt, occur immediately north of the thermal area (Drewes and others, 1961).

Outcrops on the ridge above the thermal field are altered porphyritic gabbros containing subhedral to euhedral phenocrysts of plagioclase, labradorite to bytownite in composition, up to 8 mm long, contained in a fine-grained groundmass of feldspars, pyroxenes, and sulfides. The gabbroic rocks are cut by basaltic dikes of similar composition. The fumaroles them-

selves emanate mainly from highly chloritized rocks of the Unalaska Formation. The ground surrounding the fumaroles has been intensely hydrothermally altered to varicolored clays, predominately kaolinite.

The slope above the fumarole field is capped by a 20-m-thick series of five or six basaltic flows that probably originated from the summit of Makushin Volcano. These flows terminate in a vertical cliff face, formed by glacial erosion. The lava flows do not appear altered; the fumarolic activity does not extend beyond the cliff face.

Fresh glacial debris is scattered over much of the thermal field, indicating the area was probably covered with ice during neoglacial advances. The stream bed below the fumaroles lies in a steep ravine floored with boulder-sized angular volcanic rocks.

Fumaroles and hot-springs characteristics

The thermal activity occurs in three different areas; two of the sites are probably related and occur in a cirquelike feature.

a. Mild fumarolic activity covers an area of about 0.25 km^2 and lies between elevations of 640 and 820 m on the steep northwest slope of the southeast fork of the upper Makushin River valley. The thermal field occurs near the headwaters of the stream and consists of numerous fumaroles and steam vents dispersed over a series of rounded knolls and terraces that form the valley slopes. Three broad terraces of fumaroles, each about 20 m wide, lead in steps to the vertical cliff of volcanic flows above the thermal field.

    The vents are mildly to moderately pressurized, with vapor plumes of several meters rising from the more active vents. Boiling water can be heard just below the surface at several of the orifices, which indicates surface runoff is being heated by condensing steam. Fumaroles were at or slightly below the boiling point; associated pools ranged from 80° to 95°C. The orifices were commonly surrounded by sublimates and multihued alteration clays. Several of the vents occurred in small bowl-shaped depressions; others emanated from small mounds of debris probably carried to the surface by the upflow of steam and gases.

b. This site consists of a semicircular cluster of hot springs perched a couple of meters above stream level at the base of the cirque containing fumarole field A. The springs are located at an elevation of about 560 m in a small bowl indented into what appears to be glacial drift. The thermal waters issue from four principal vents, spaced about 1 m apart, each having an estimated discharge of 10 lpm; thermal water also arises from several additional seeps in the marshy basin of the bowl. Outflow from the springs and seeps merge into a single channel before entering the main cold stream. Spring temperatures ranged from 80° to 87.5°C. Reddish oxide-stained rocks occur near the thermal waters; siliceous orange sinter deposits and blue-green algal mats line the spring channels.

    Another series of thermal springs measuring up to 80°C occur about 50 m farther downstream along the banks of the main cold-water channel and at the base of a waterfall on the steep northern valley slope. The valley narrows beyond this point to form a small canyon several kilometers long.

c. The third site occurs at an elevation of about 360 m on a small 30-m-wide bench located about 75 m above stream level on the steep northern wall of the valley, about 2.5 km downstream from the previous sites. Thermal activity consists of a 2,500-m^2 area of mild boiling-point fumarolic activity, mudpots, and hydrothermally altered ground, and a thermal spring and some seeps about 100 m west and 4 m below the fumaroles. The fumaroles and spring emanate from colluvium accumulated on the bench. The hot spring has a temperature of 67°C and a low rate of discharge, visually estimated at less than 10 lpm.

Table 17 gives the chemical and physical properties of thermal spring waters obtained from sites B and C. These waters are similar in most respects to those found at the Glacier Valley site, namely, very low chloride, high silica, high proportion of calcium and magnesium, and relatively high bicarbonate and sulfate. The Makushin Valley springs are slightly more acidic. As in the Glacier Valley case, the comparatively high Ca and Mg content of the waters relative to the other cations indicates the waters are derived from a low-temperature reservoir or perhaps result from the admixture of heated surface waters with deeper, hotter thermal waters. The sulfate and bicarbonate probably result from the oxidation of H_2S and CO_2 gases rising from deeper in the volcanic system.

Table 17. Chemical composition and physical properties of
Makushin Valley hot springs sites B and C
(all chemical analyses in mg/l).

Characteristics	DGGS Site B	DGGS Site C
SiO_2	140	88
Al	nd	nd
Fe	0.09	0.03
Ca	69.3	23.1
Mg	12.2	8.0
Na	28	13.9
K	5.6	3.4
Li	<0.01	<0.01
HCO_3	191	116
SO_4	155.3	21.4
Cl	5	5
F	0.12	0.11
Br	nd	nd
I	nd	nd
B	<0.5	<0.5
H_2S	nd	nd
Sr	0.28	0.10
pH, field	5.48	5.32
Dissolved solids	606.9	279.04
Hardness (mg/$CaCO_3$)	218.87	90.74
Sp conductance (μmho/cm at 25°C)	600	255
T (°C)	87.4	67.0
Flow rate (lpm)	nd	nd
Date sampled	8/13/80	8/13/80

nd - Not determined.

Table 18 gives the chemical composition of fumarolic gas samples obtained from sites A and C. The dominant gas in both fields is carbon dioxide. Gases emerging from the upper fumarole field (site A) contain proportionately higher percentages of hydrogen sulfide and hydrogen gas than those emerging from the lower thermal field (site C), perhaps because fumarolic gases at site C have had more interaction with ground waters. The nitrogen and argon are probably of atmospheric origin, and are probably dissolved in infiltrating surface waters (Mazor and Wasserberg, 1965). The low concentration of oxygen in both cases is probably due to oxidation of H_2S and H_2.

Reservoir Properties

The occurrence of the thermal springs at the base of fumarole fields in Makushin Valley suggests that at least part of the spring waters may originate as condensation of steam in surface waters, which then percolate into the porous colluvium and country rock to eventually emerge as springs. The high silica content of the thermal waters, however, indicates that a large portion of the waters must have originated from a subsurface reservoir where temperatures exceed 150°C, assuming the silica is in equilibrium with quartz. Surface waters infiltrating this reservoir may become heated on descent, causing dissolution of cations in the wall rock, a process aided in part by the slight acidity of the waters. The levels of calcium, and particularly magnesium, relative to sodium and potassium indicate the residence time of waters in the reservoir is too short for these constituents to equilibrate to the estimated reservoir temperature. Silica can equilibrate rather rapidly, within several days to a few weeks. This suggests the reservoir supplying the thermal-spring waters lies at fairly shallow depths. The low chloride content and the slightly acid-sulfate chemistry of the thermal waters, together with their association with fumarolic activity, are evidence for a perched reservoir supplied by meteoric waters that are heated by steam and volcanic gases rising through a vapor-dominated zone from a much deeper reservoir.

Table 18. Chemical composition of fumarolic gases from
Makushin Valley thermal field
(analysis in volume percent).

	Site A	Site C
He	0.009	0.003
H_2	0.49	0.025
Ar	0.083	0.0072
O_2	<0.0001	<0.0001
N_2	7.93	0.56
CH_4	0.0018	0.0031
CO_2[b]	89.14	99.05
H_2S[b]	2.38	0.30

[a] J. Welham and R. Poreda, analysts, Scripps
Institution of Oceanography, La Jolla, Calif.
[b] M. Moorman, analyst, DGGS.

The hydrogen sulfide and helium probably have magmatic origins, as does as least part of the carbon dioxide (Craig, 1963; White, 1968). An analysis of

the ratio of ^{3}He:^{4}He in the fumarolic gases obtained in cooperation with R. Poreda at the Scripps Institute of Oceanography is given below:

	MV-A	MV-C
$\dfrac{(^3\text{He}/^4\text{He})}{(^3\text{He}/^4\text{He})\text{AIR}}$	4.9	6.6

An enrichment in ^{3}He in fumarolic gases has been correlated with magmatic activity on a worldwide basis, the source of ^{3}He thought to be derived from primordial mantle material (Lupton and Craig, 1975; Craig and others, 1978; R. Poreda, pers. commun.). The values for the Makushin fumaroles are within the range of other volcanic island-arc geothermal systems.

The hydrogen content of the gases is probably produced by high-temperature reaction of water with ferous oxides and silicates contained in the deep reservoir rocks (Seward, 1974).

Table 19 gives the results of applying the D'Amore and Panichi (1980) gas geothermometer to the Makushin fumarole samples. From the proportions of gases present, B is chosen as 0 and the respective reservoir temperature estimates are 278°C and 168°C for sites A and C. These estimates must be used with caution. The accuracy of this geothermometer has not yet been generally accepted. Furthermore, the gases have probably undergone reaction with a shallow reservoir which may have affected their H_2S and H_2 contents.

Despite the uncertainties in the gas geothermometers, the large flux of steam and the probable magmatic origin of some of the fumarolic gases indicate the existence of a high-temperature, deep geothermal reservoir.

Table 19. Gas geothermometry,[1] Makushin Valley fumaroles (temperatures °C).

B*	Site A	Site C
-7	380	231
0	278	168
7	204	119

*for explanation of B, see table 3b.

Comments

The Makushin Valley hydrothermal system is similar in most respects to the Glacier Valley system. Both are characterized by extensive fields of mild fumarolic activity and thermal springs low in chloride and rich in sulfate and bicarbonate. The proximity of these fields to each other and to the active summit caldera indicate a common source of heat underlies the volcano. Comparison with similar volcanic systems elsewhere in the world suggests the origin of the hydrothermal system is a high-temperature sodium-chloride brine overlying a cooling body of magma. Gases and steam escaping from this deep reservoir give rise to reservoirs rich in secondary bicarbonate-sulfate at shallower levels and to the fumarolic fields on the flanks and summit of the volcano.

The postulated deep brine reservoir should be the ultimate target of any exploratory energy-development program. The Makushin Valley site lies near the village of Unalaska, the capital of the Bering Sea fishing industry. An old military road exists along the lower part of Makushin Valley, affording potential access to the site. However, caution must be exercised before proceeding with any development plans. The volcanic hazards and potential impact from eruptions must be evaluated.

SUMMER BAY HOT SPRINGS

Location

Latitude 53°53.1' N., longitude 166°26.9' W.
Unalaska Quadrangle 1:250,000 (1951) T. 73 S., R. 117 W., Seward Meridian

General description

The Summer Bay hot-springs site is located near the base of the east slope of a north-south trending glacial valley about 2 km south of Summer Bay and 5.5 km west of the village of Unalaska (figs. 21 and 23). The springs occur at the edge of a marsh located about 0.5 km southeast of a shallow 1.5-km-long lake that occupies the northern part of the valley. Glaciated ridges surrounding the valley rise up to 550 m in elevation.

The site can be reached from the village of Unalaska via a jeep trail up the Unalaska River Valley, over a 460 m pass and then north into the unnamed valley containing the springs; the 12-km trip requires about 2 hr. A road from Unalaska village to Summer Bay along the coast of Iliuliuk Bay is under repair and should be open by the summer of 1981. Both roads date from WW-II. The springs are also accessible by small boat, although caution should be used.

The lake and associated streams in the valley are spawning grounds for salmon, making the area popular with local sport fisherman. The springs are reported to be used occasionally for recreation by local townspeople.

Vegetation in the valley is predominantly marsh grass. The adjacent valley to the north is drier and sometimes used as grazing pasture for livestock. There are numerous old military buildings in the area which are now by the local native corporation.

Geology

The valley is covered with alluvial deposits; beach deposits occur near the coast. Bedrock consists of the Unalaska Formation, a thick sequence of coarse- and fine-grained sedimentary and pyroclastic rocks intercalated with dacitic, andesitic, and basaltic flows and sills, cut by numerous dikes (Drewes and others, 1961). Dikes near the springs site generally trend west-northwest and were found to be feldspathic basalt porphyries.

Several northwest-trending normal faults occur in the area. A fault immediately north of the springs site has a strike of N. 50° W. Another normal fault located south of the valley has a similar trend and is thought to be Recent (Drewes and others, 1961).

Spring characteristics

The thermal springs emerge from the alluvium into shallow pools located at the base of the eastern valley slopes. The main pool is about 1 m in diameter and has a maximum temperature of 36°C. Discharge from this pool, measured at 64 lpm, joins a small warm stream with a temperature of 15° to 20°C and a flow rate of about 40 lpm. The combined waters in turn flow into a second 1 m-dia

warm pool measuring 20°C. The warm waters eventually flow into a marsh that
drains towards the valley lake. Both pools are floored with organic muck and
exhibit slight gas bubbling.

During the fall of 1980, two shallow test wells were drilled into iron-
stained sediments on the southeast shore of the valley lake. The work was done
by Dames and Moore Associates under supervision of a DGGS geologist (J. Reeder,
pers. commun.). The wells were spaced about 200 m apart and were located about
500 m northwest of the springs site. Both tests found a warm-water aquifer
system in black sandy soils at a depth of about 13 m. Bedrock was encountered
at a depth of about 17 m. Water flowed from well 1 under artesian pressures at
180 lpm and a temperature of 50°C; well 2 showed 30 lpm and 44°C.

Table 20 gives the chemical and physical properties of thermal waters
sampled from the two wells during artesian flow and from the main pool at the
springs site. All three waters have chloride and sulfate as their major anions
and sodium and calcium as the major cations. Compared to hot springs sampled
elsewhere in the Aleutians, the thermal waters at Summer Bay are notably low in
silica. However, the systematic variations of water chemistry vs measured
temperatures at Summer Bay indicate that cold waters are mixing with thermal
waters (table 21). Except for Ca/Mg, the three waters are nearly identical in
each of the various ratios, indicating that the waters have a common-parent
thermal water and that it undergoes varying degrees of mixing with cold waters.
The colder samples are generally more dilute than the warmer samples, which
suggests that the cold-water fraction itself is very dilute with respect to the
major constituents and that the chemical constituents present in the sampled
waters are mainly derived from the parent thermal water. The variation in
magnesium content could be attributed to varying degrees of reequilibration of
waters in the shallow warm-water aquifer or perhaps to the derivation of
magnesium from the cold-water fraction.

Although the above evidence indicates most of the constituents present in
the waters originated from a deeper parent water, the wells showed marine sedi-
ments at shallow depths. The possibility that some or most of the constituents
present in the waters originated from interaction of warm waters with these
shallow sediments cannot be discounted.

Reservoir properties

The test wells drilled at Summer Bay documented the existence of a shallow
warm-water aquifer ranging up to 50°C and located south of the valley lake.
From the well log, the cap for the system appears to be a lightly cemented
layer of "chalky clay" that occurs at a depth of about 10.5 m (Dames and Moore,
1980). Artesian pressure was probably provided in part by the surrounding
cold-water hydrostatic head and by the bouyancy of the heated waters. Bedrock
was encountered after passing through about a 17-m-thick sedimentary sequence
of coarse- and fine-grained sands and chalky clays, some of which contained
shell fragments. Bottom cuttings of bedrock from the wells were basaltic
chips.

Table 20. Chemical composition and physical properties of
Summer Bay hot spring and wells 1 and 2
(all chemical analyses in mg/l).

	Hot spring	Well 1	Well 2
SiO_2	18	35	25
Al	nd	nd	nd
Fe	0.09	0.10	0.14
Ca	202	460	372
Mg	1.0	6.34	10.3
Na	150	332	276
K	3.0	6.49	5.45
Li	0.03	0.16	0.12
HCO_3	73	nd	nd
SO_4	245	528	423
Cl	404	923	741
F	0.22	0.44	0.40
Br	1.25	3.02	2.65
I	0.00	0.19	0.00
B	0.5	0.5	0.5
H_2S	nd	nd	nd
Sr	0.94	2.0	1.52
pH, field	6.98	nd	nd
Dissolved solids	1099.1	2297.2	1858.1
Hardness ($mg/CaCO_3$)	509.68	1177.3	970.5
Sp conductance ($\mu mho/cm$ at 25°C)	1810	3850	3000
T (°C)	35	50	44
Flow rate (lpm)	64	180	30
Date sampled	7/18/80	9/26/80	9/27/80

nd - Not determined.

Table 21. Ratios of chemical constituents in
Summer Bay thermal waters.

Ratio	Thermal spring	Well 1	Well 2
Na:Cl	0.37	0.36	0.37
K:Cl	0.007	0.007	0.007
Ca:Cl	0.50	0.50	0.50
SO_4:Cl	0.61	0.57	0.57
Ca:Mg	202	73	36
Na:K	50	51	51
Ca:Na	1.35	1.39	1.35

Table 22 summarizes the application of silica and cation geothermometry to
Summer Bay thermal waters. Even with the assumption of equilibration with
quartz, the silica geothermometer predicts a relatively cool, deep-reservoir
temperature of 60° to 86°C. Although the low silica contents of these waters
may be due in part to reequilibrium in the shallow warm-water aquifer, the
linear trend with temperature of silica and several other constituents indi-
cates that the low silica is probably due to extensive mixing of cold surface
waters with ascending thermal waters. Such mixing could also partially explain
the ambiguous results of the cation geothermometer.

If mixing is assumed and the linear trend of the silica vs enthalpy line is extended to its intersection with the quartz solubility curve (eg. Truesdell and Fournier, 1977), the deep-reservoir silica-content and temperature may be as high as 150 ppm and 160°C. Extrapolation of the linear chloride trend of the surface and shallow aquifer thermal waters to 160°C suggests deep-reservoir chloride concentrations may be as high as 5,000 ppm.

Comments

The chemistry of the waters and the location of the thermal site at the floor of a drainage basin indicate mixing of cold surface waters and deep ascending thermal waters occurs in the shallow subsurface warm-water aquifer. Steep normal faults are located near the site, suggesting deep-seated fractures are conduits for the circulation of meteoric waters. The waters become heated at depth and eventually emerge at the floor of the valley. The trend of the faults is in the direction of convergence of the North American and Pacific tectonic plates in this section of the Aleutian arc.

Table 22. Summer Bay thermal-water geothermometry
(all temperatures in °C).

	Thermal spring	Well 1	Well 2
Surface temperature	35	50	44
Cation geothermometers			
Na-K	109	108	109
Na-K-Ca (1/3)	92	95	95
Na-K-Ca (4/3)	24	35	33
Silica geothermometers			
Adiabatic	60	86	72
Conductive	60	86	72
Chalcedony	27	55	40
Cristobalite	11	36	23
Opal	-49	-28	-39

Silica mixing models indicate deep reservoir temperatures may be as high as 160°C. Chloride-enthalpy analyses suggest that the thermal waters are briny with a chloride content as high as 5,000 ppm. Future exploration programs at Summer Bay should be designed to locate the fracture system(s) that are supplying the hot geothermal brine to the shallow warm-water aquifer.

AKUTAN ISLAND

Background

Akutan Island is located in the eastern Aleutian Islands at approximately 54°05' latitude and 165°55' longitude, about 45 km northeast of Unalaska Island and 80 km southwest of Unimak Island (fig. 1). The island is about 20 km wide and 30 km long, with its long axis aligned with the trend of this segment of the Aleutian arc. Vertical aerial photography is lacking for most of the island and, except for the coastline and areas immediately adjacent to it, topographic coverage on U.S. Geological Survey and U.S. Coast and Geodetic Survey maps is nonexistent or unreliable.

The island is mountainous and rugged with shorelines dominated by steep cliffs and rocky headlands. Akutan volcano (1,300 m), a composite shield volcano, and its satellitic vents dominate the western part of the island. The volcano has erupted numerous times in recorded history and remains active, with several eruptions occurring during the past decade. Portions of the island not covered by recent volcanic flows show signs of intense glaciation: serrated ridges, cirques, hanging valleys, and broad U-shaped valleys. The east end of the island is split by Akutan Harbor, a deep 8-km-long fjord. The lower elevations of the island are covered by a thin mantle of soil and recent volcanic ash commonly blanketed by lush and verdant tundra vegetation.

Akutan village, the only habitation on the island, is located on the east coast of the island at the base of a steep 460 to 520 m ridge that borders the north shore of Akutan Harbor. The village was established in 1879 as a fur storage and trading post; in 1912 a whale-processing station was built across the bay from Akutan and operated until 1939 (Morgan, 1980). The present population of about 120 inhabitants depends on subsistence, commercial fishing, and fish processing for their economy. Several floating fish processors now operate in the protected waters of Akutan Harbor, which bring in a seasonal influx of 200-700 nonresident workers.

Boats and amphibious aircraft are the only means of transportation into Akutan, which has no airstrip. Reeve Aleutian Airways maintains scheduled commercial air service from Cold Bay and Dutch Harbor to Akutan by float plane. Charter Air Services are also available from both villages.

Geology

Reconnaissance geologic mapping of the island was undertaken by F. Byers and T. Barth in 1948. Copies of Byers' field notes and field map were made available to DGGS courtesy of Beyers and the U.S. Geological Survey Archieves. A brief description of the island's volcanic geology is also contained in Byers and Barth (1953). A generalized geologic map based on their work appears in figure 25.

Akutan Island consists of an older sequence of volcanics deeply eroded by glaciation and a younger volcanic pile at the western end. The older volcanic complex consists of a lower member of mainly pyroclastic deposits (chiefly volcanic and tuff breccias, with intercalated basaltic andesitic flows and sills) overlain by a series of shallow-dipping basaltic and andesitic flows
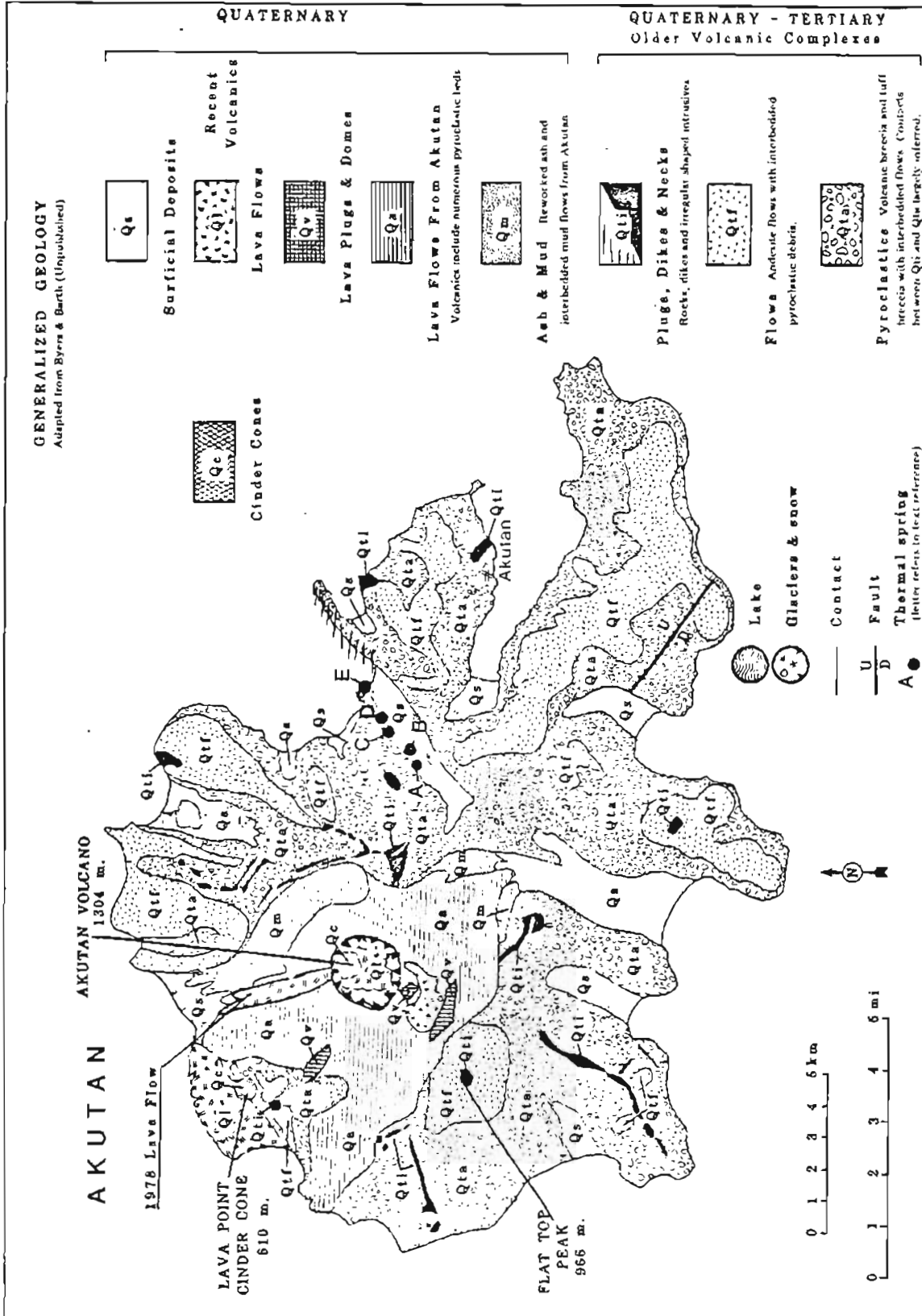
Figure 25.   Generalized geology of Akutan Island.

with some interbedded pyroclastic deposits. This sequence, which is exten-
sively exposed over much of the island and in places exceeds 700 m thick, has
been intruded by numerous volcanic necks, plugs, and dikes. A series of ring-
dike intrusions exposed on the northern part of the island suggest the
existence of an ancestral collapse caldera near the present site of Akutan
volcano.

Recent volcanic activity has concentrated at Akutan volcano with fresh
lava flows, lahars, and pyroclastic debris mantling the glacially eroded sur-
face of the older volcanic complex. The volcano is capped by a small 2-km-dia
collapse caldera thought to have formed as recently as 500 years ago
(Byers and Barth, 1953). Recent prehistoric eruptive activity also occurred
northwest of Akutan volcano at Lava Point, where over 5 km^2 of rough, jagged
aa lava extends seaward from a volcanic cone at the south edge of the flow.
The flow is over 20 m thick and composed of a vesicular porphyritic olivine
clinopyroxene basalt, with trachytic texture in the groundmass.

Akutan volcano is one of the most active volcanoes in the Aleutian chain,
having erupted more than 25 times since 1700 (Byers and Barth, 1953; Coats,
1950; Sean, 1980). The most recent eruptions include a lava flow that breached
the northern caldera rim in February 1974, a series of incandescent ash erup-
tions in 1976 and 1977, a lava eruption in September 1978 in which flows
traveled 2 to 3 km down the north flank of the volcano, and a brief ash erup-
tion in late July 1980. The 1978 flow was examined by the DGGS in August 1980
and found to be still warm and degassing. One of the lava flows entered a
large stream channel. The flow rate of water draining from beneath the distal
end of this lava flow was estimated at several thousand liters per second and
measured 22°C.

The 1978 lava flows were found to be composed of a slightly vesicular,
porphyritic, olivine-bearing, two-pyroxene basalt. Phenocrysts consisted of 20
percent euhedral plagioclase laths, 0.4-2.4 mm long, 5 percent subhedral
clinopyroxene, 0.2-1.0 mm in size, 2 percent euhedral hypersthene up to 0.5 mm,
and less than 1 percent unaltered subhedral olivine, 0.2 mm in size. The black
groundmass consisted mainly of glass with some scattered crystals of plagio-
clase, clinopyroxene, and magnetite.

Byers and Barth (1953) reported the existence of an acid lake, fumarolic
activity, and fresh lava flows within the Akutan caldera. Recent eruptive
activity, however, has probably obliterated much of what was present in 1948.

In addition to the active caldera and fresh lava flows of Akutan volcano,
other geothermal activity that occurs on the island includes an extensive
series of hot springs located in a valley at the head of Hot Springs Cove.

AKUTAN HOT SPRINGS

Location

Latitude 54°09' N., longitude 165°55' W.
Unimak 1:250,000 Quadrangle (1951), T. 69 S., R. 112 W.

General description

Akutan hot springs are located in the eastern valley* at the head
of Hot Springs Bay on the northern side of Akutan Island (figs. 25 and
26). Numerous hot springs lie along the western margin of the valley
bottom in a 1.5-km linear zone extending southward from the intertidal
area on Hot Springs Bay. The valley is glacial, 1 km wide, and flanked
by steep parallel ridges rising up to 460 m high. The valley trends
S. 55° W. for 4.5 km from Hot Springs Bay before taking a sharp dogleg
to the west and terminating on steep serrated ridges extending from
Akutan volcano.

The relatively flat-bottomed marshy floor of the valley is drained
by two streams, one on either side of the valley. The eastern fork joins
the western branch, which is the larger channel, about 1 km from the
beach to form a single flow to the bay in the northwest corner of the
valley. Vegetation on the valley floor consists of moist tundra and tall
meadow grasses.

The Akutan hot springs are located about 4 km northwest of Akutan
Harbor and 10 km northeast of the active Akutan volcano. Although the
springs are relatively close to the volcano, an intervening valley and
ridge forms a barrier to lava flows or debris flows associated with
eruptions. The springs are easily accessible from the village of Akutan
via a 6-km-long trail from the head of Akutan Harbor over a 150-m pass and
down a steep slope. The springs can also be reached by boat, but caution
should be exercised.

The springs were well known to early Aleuts and to white fur traders
and are reported in Waring (1917). Previous investigations of the springs
include Byers and Barth (1953) and Baker and others (1977). Land surround-
ing the springs site was selected by Akutan Village Corporation under terms
of ANCSA.

Geology

The glacial valley containing the hot springs has been carved from a
massive volcanic breccia that in places exceeds 400 m in thickness. Rock
exposures on valley walls and ridge tops extending up valley from the springs

---

*The location of the hot springs on U.S. Coast and Geodetic Survey maps has
been mistakenly placed in the adjacent western valley.

site consist of a thick sequence of mostly autobrecciated lava flows and some tuff breccias, with intercalated lenses and small sills of cognate lava. The flow and tuff breccias tend to grade into one another without clear-cut boundaries. Some exposures of the tuff breccias are palagonitic. The volcanics composing the breccias consist of porphyritic andesitic basalts containing 30 percent subhedral phenocrysts of plagioclase, 0.4 to 3 mm long, and 4 percent subhedral to euhedral phenocrysts of augite, 4 mm in size, in a dark-gray aphanitic groundmass composed chiefly of plagioclase.
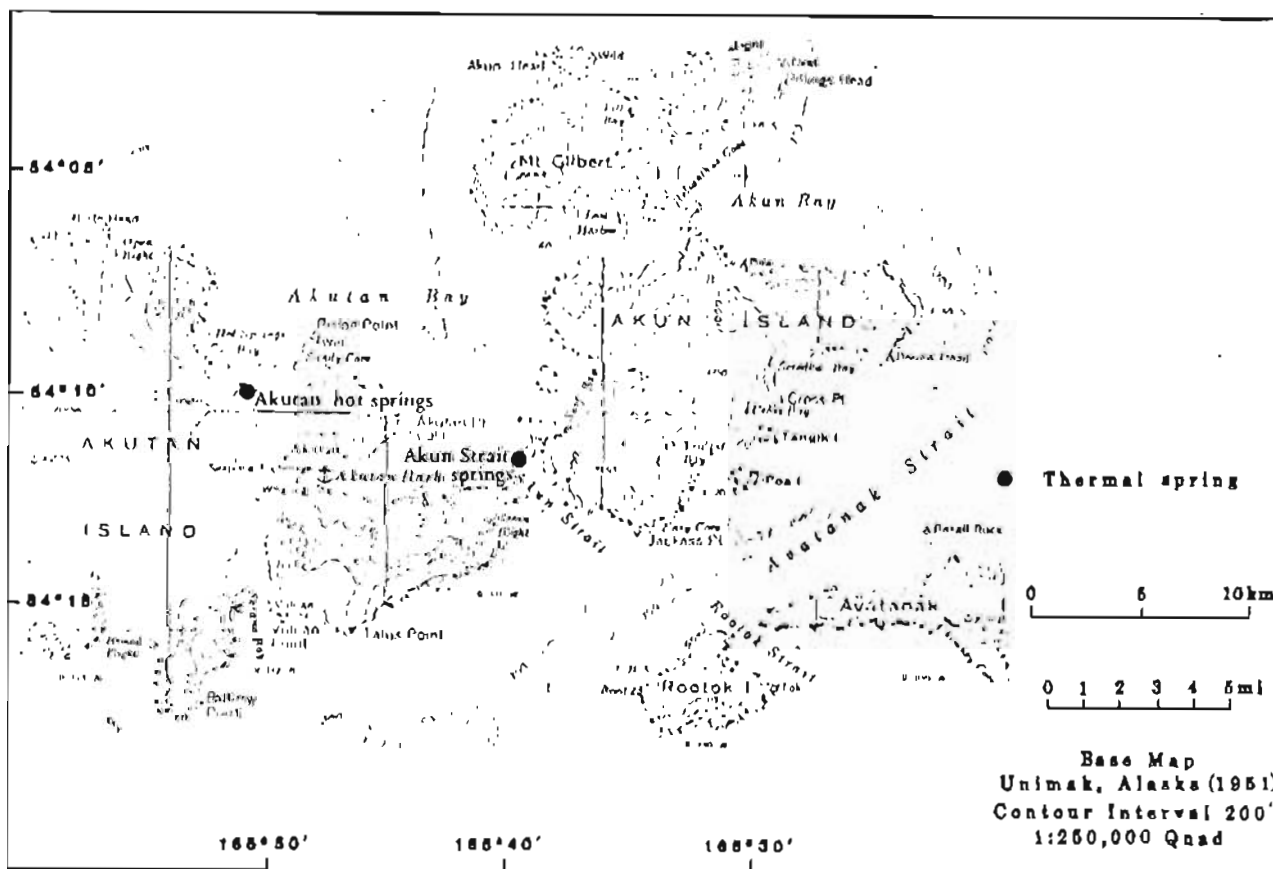
Figure 26. Location of Akutan and Akun Strait hot springs.

Outcrops occurring downvalley at the Hot Springs Bay coastlines are laharlike with large 1- to 2-m-dia angular blocks of andesitic basalts contained in a poorly sorted matrix of ash(?), scoria, and pebble- and cobble-size volcanic-rock fragments. The lahar unit is intruded by numerous vertical dikes, some of which are up to 5 m wide, with most having a general E-W trend. The dikes are trachytic basalts consisting of a dark glassy matrix containing from 10 to 30 percent phenocrysts of labradoritic plagioclase.

The valley itself is floored with an unknown thickness of alluvial sediments mantled by soil. There are two parallel dunes near the mouth of the valley, the older of which is about 12 m high and lies about 1 km from the coast behind an abandoned lagoon. The second dune is about 7 m high and borders the present shoreline.
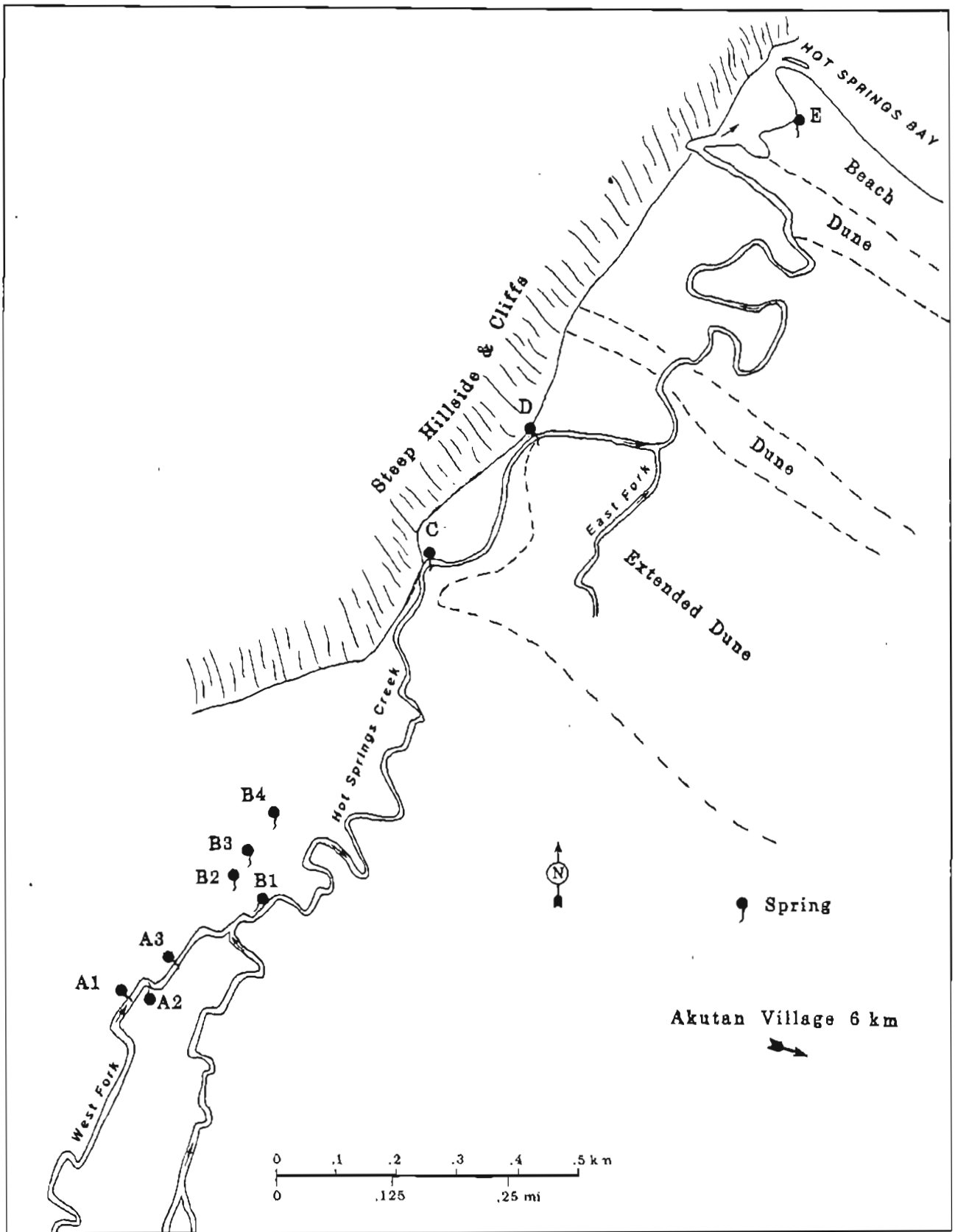
Figure 27. Locations of springs at Hot Springs Bay on Akutan Island.
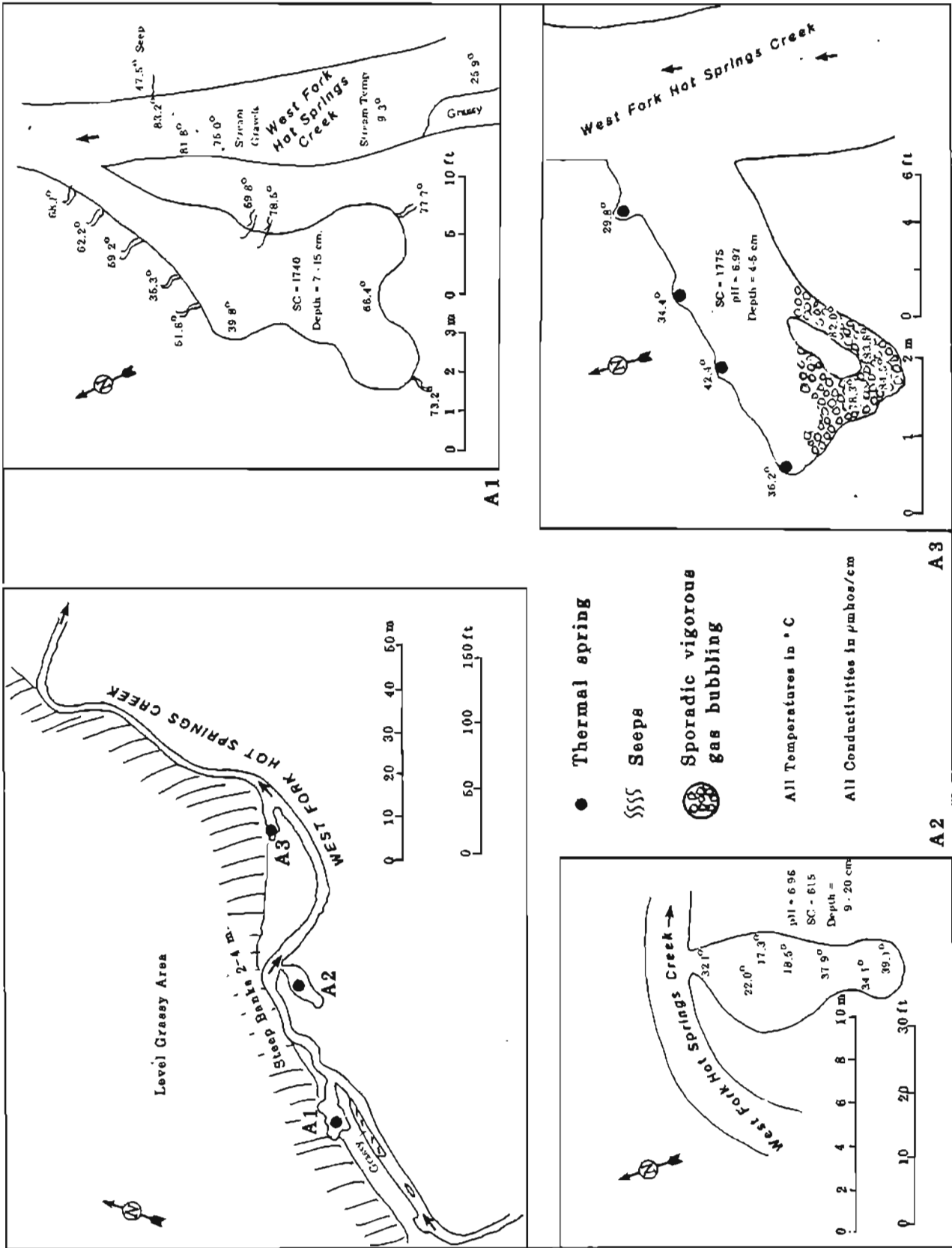
Figure 28. Detail at site A, Akutan hot springs.

Spring Characteristics

The hot springs occur along and at the base of the west valley wall in a 3 km long zone that extends southwest from Hot Springs Bay (fig. 27). The thermal waters issue from fissures in hydrothermally cemented stream bank sediments, from pools in valley alluvium, and through beach sands in the intertidal zone near the mouth of the Hot Springs Creek. Spring locations, temperatures, and additional characteristics are provided in figures 28 through 31. The springs have been grouped according to their geographic location. Table 23 gives the chemical and physical properties of thermal waters obtained from springs A3 and D2. Silica and chloride analyses of strea, waters above and below site A and of a cold spring near site A are given in table 24.
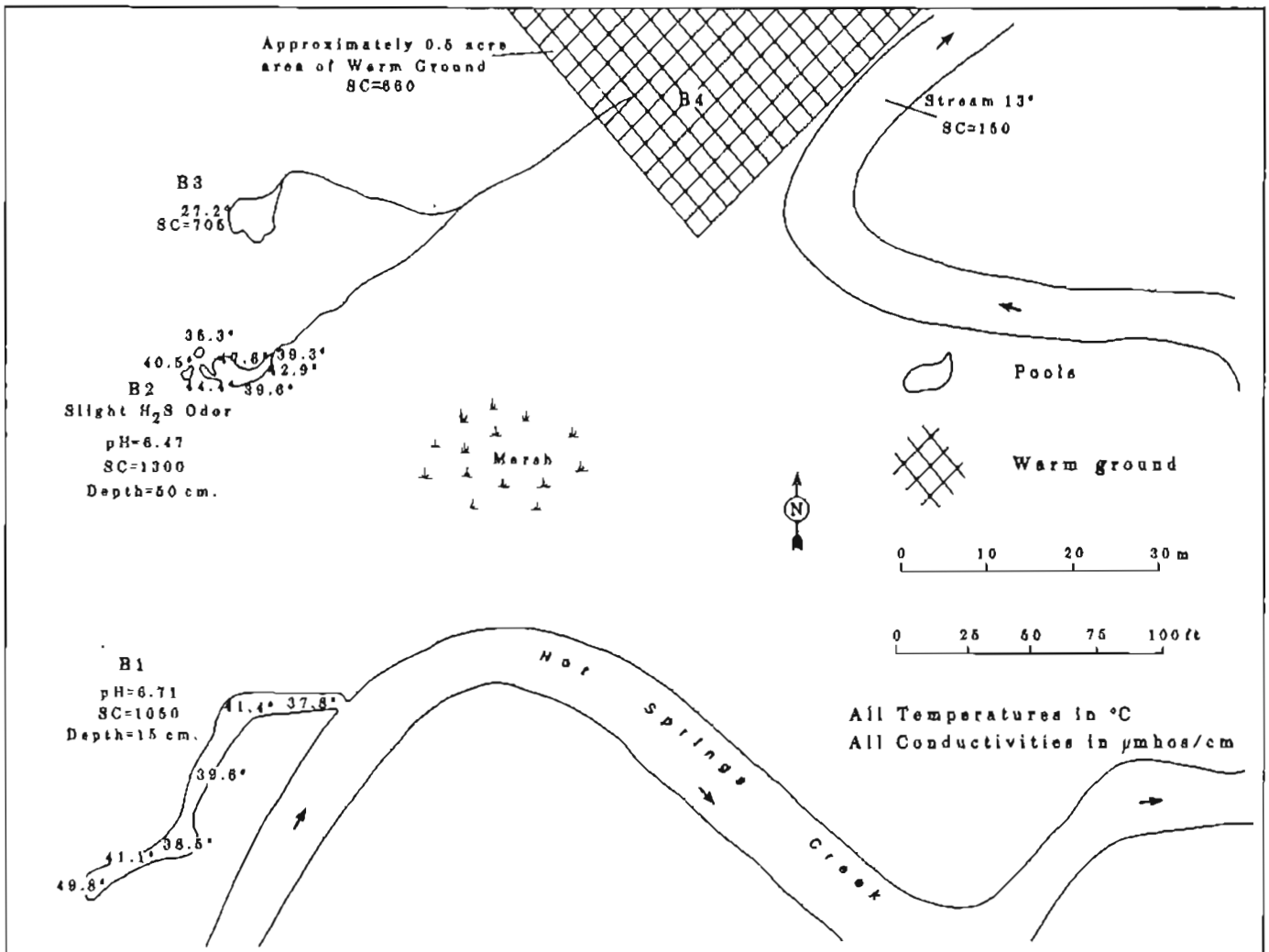
Figure 29. Detail at Akutan spring site B.

Site A is located on the west fork of the main channel of Hot Springs Creek and contains the southernmost and hottest springs in the valley. The thermal waters issue from numerous small fissures in hydrothermally cemented alluvial sediments and from the bottom of pools into three small, elongate shallow basins (fig. 28). Spring-vent temperatures in basins A1 and A3, both located near the west bank of the cold-stream channel, ranged from 40° to 78.5°C and 30° to 84.5°C, respectively. Sinter deposits line the outflow channels from these basins and appear to be cementing the surface sediments. Basin A2, located on the east bank, contains a warm-water (17° to 39°C) pool floored with muck and algae.

Thermal waters from all three basins flow directly into the west fork channel. Thermal waters from A1, A2, and A3 flowed at 40, 51, 118 lpm, respectively. The stream bed of the west fork above the outflow basin A1 measured 75.0° to 83.2°C just a few cm below the ground surface, which indicates thermal waters are discharging directly into the cold stream channel. The silica and chloride content of stream waters above and below site A and in the sampled thermal waters provide a means of estimating the cold- and hot-water mixing fractions in the stream from the equation: $C_m = (1-X)C_h + XC_c$ where X is the cold-water fraction and C is the concentration of either silica or chloride in the mixed (m), hot (h), and cold (c) fractions. The values from table 24 give a cold-water mixing fraction of 0.922 for Cl and 0.928 for SiO_2. Total water flow in the west fork channel below site A measured 4,280 lpm $\pm$ 5 percent. The average of the SiO_2- and Cl-determined mixing fractions gives an estimated total hot-water discharge from site A of 320 lpm. Stream temperatures above and below site A measured 9.8° and 15.4°C, respectively. Substituting these values into the equation $T_m = (1-X)T_h + XT_c$ gives an estimated temperature at 84.5°C for the hot-water fraction, a temperature consistent with the hottest spring vent temperature measured at the site. The heat flux loss represented by this hot-water discharge relative to the stream temperature of 9.8°C is about 1.6 MW.

Site B consists of four shallow, warm pools located about 300 m down-stream from site A in a marshy area near the junction of the west fork and the main channel of Hot Springs Creek (fig. 29). No obvious vents were perceived in any of the pools and the thermal waters appear to be seeping directly through valley alluvium. The warmest temperatures, 38.5° to 49.8°C, occur in B1, a 20-m-long pool that drains into Hot Springs Creek. Temperatures at the other pools ranged from 20°C at B4 to 47.8° at B2. No flow measurements were made at the site, but the discharge from the pools appears to be considerable.

Site C is located about 1 km farther downstream from B and consists of numerous seeps and small springs issuing from a series of fissures in hydrothermally cemented sediments in the west bank of Hot Springs Creek (fig. 30). Vent temperatures ranged from 40° to 74.8°C. Anamolously warm temperatures measured a few cm below the surface of a gravel bar in the creek indicate that thermal waters are discharging directly into the cold stream channel. No thermal anomalies were detected on the opposite bank of the creek.
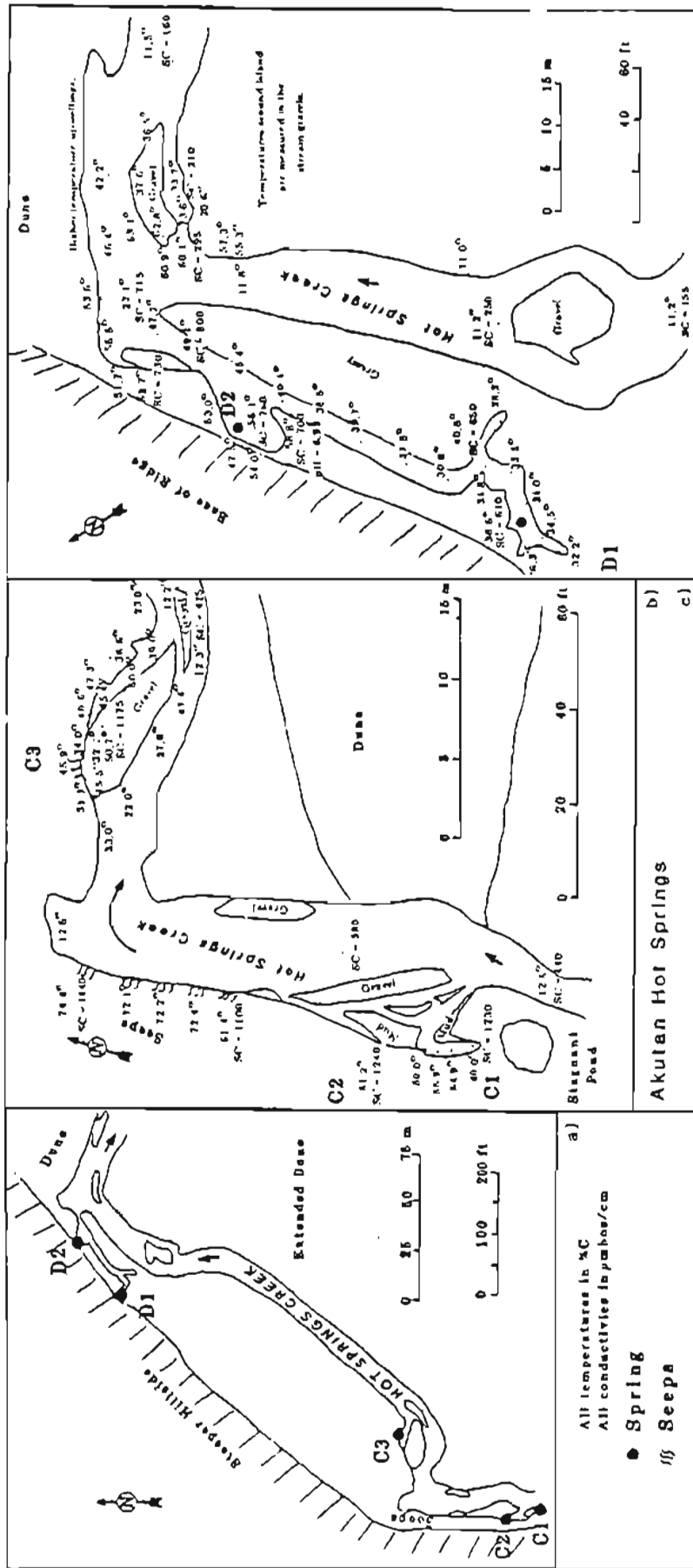
Figure 30a. Relations of springs C and D. 30b. Detail at Akutan site C.
30c. Detail at Akutan spring site D.
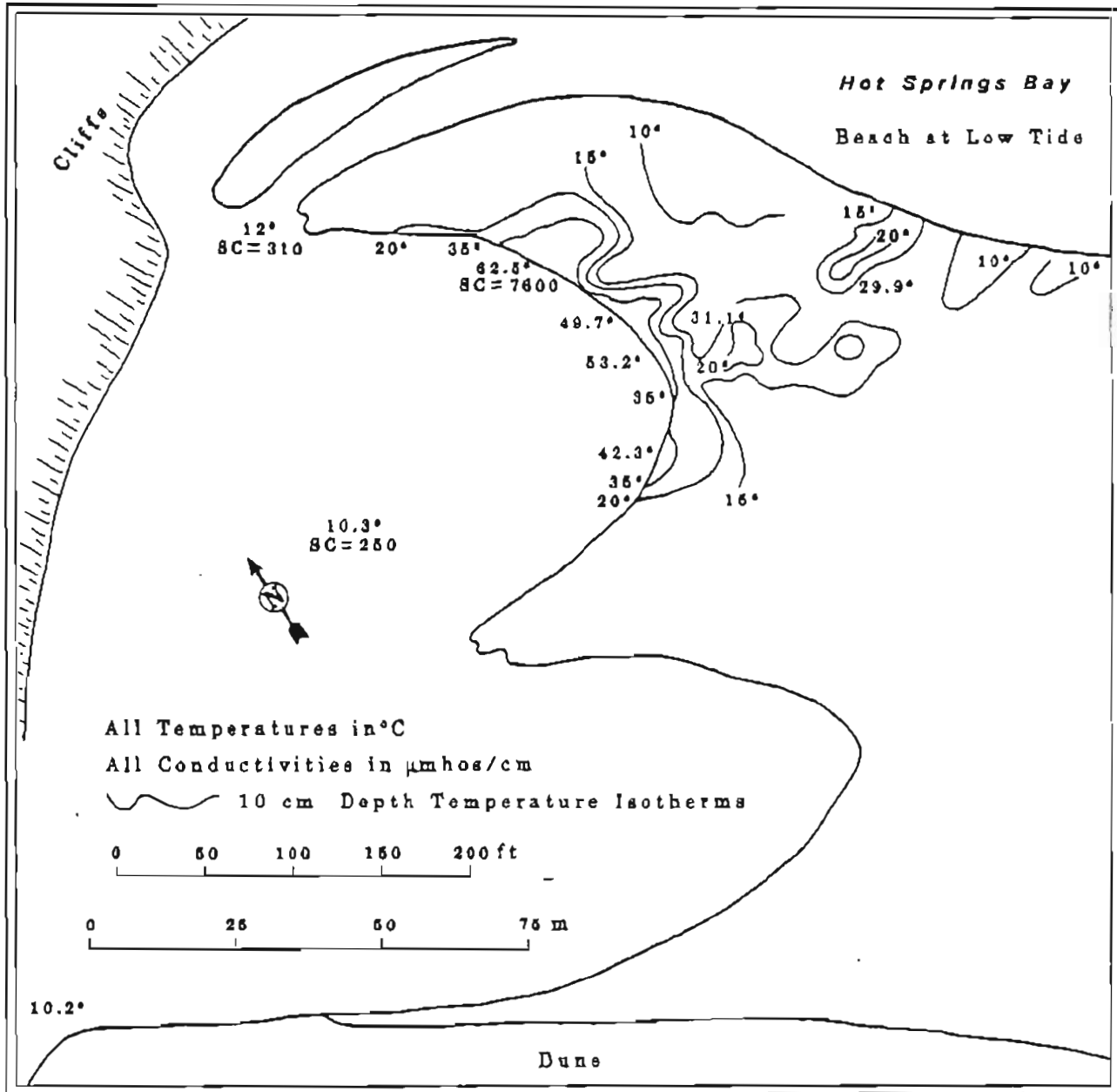
Figure 31.   Detail at Akutan spring site E.

Table 23. Chemical composition and physical properties of
Akutan hot springs A2 and D2
(all chemical analyses in mg/l).

	DGGS spring A2	DGGS spring D2
SiO_2	145	91
Al	nd	nd
Fe	0.05	0.03
Ca	11.3	11
Mg	2.5	11.8
Na	323	128
K	24.8	9.3
Li	1.28	0.34
HCO_3	172	128
SO_4	42.7	26.4
Cl	424	136
F	1.1	0.88
Br	1.31	nd
I	0.42	nd
B	11.4	3.4
H_2S	0.5	nd
Sr	0.11	0.09
pH, field	6.98	6.82
Dissolved solids	1161	546.24
Hardness (mg/l $CaCO_3$)	33.8	76.15
Sp conductance (μmhos/cm at 25°C)	1775	700
T (°C)	84	58.8
Flow rate (lpm)	118	20
Date sampled	8/7/80	8/8/80

nd = Not determined.

Table 23. Chemical composition and physical properties of
Akutan hot springs A2 and D2
(all chemical analyses in mg/l).

	DGGS spring A2	DGGS spring D2
SiO_2	145	91
Al	nd	nd
Fe	0.05	0.03
Ca	11.3	11
Mg	2.5	11.8
Na	323	128
K	24.8	9.3
Li	1.28	0.34
HCO_3	172	128
SO_4	42.7	26.4
Cl	424	136
F	1.1	0.88
Br	1.31	nd
I	0.42	nd
B	11.4	3.4
H_2S	0.5	nd
Sr	0.11	0.09
pH, field	6.98	6.82
Dissolved solids	1161	546.24
Hardness (mg/l $CaCO_3$)	33.8	76.15
Sp conductance (μmhos/cm at 25°C)	1775	700
T (°C)	84	58.8
Flow rate (lpm)	118	20
Date sampled	8/7/80	8/8/80

nd = Not determined.

Site D consists of two primary hot-spring basins. The associated outflow channels also contain numerous fissures in cemented alluvium through which the thermal waters issue. The site is located a short distance downstream from site C on the west bank of Hot Springs Creek at the base and upvalley side of an old beach dune, 1 km inland from the coast. Vent temperatures at the site varied considerably--- from 26.3° to 54.0°C. No flow measurements were made; the combined discharge from the basins probably does not exceed 50 lpm. High temperatures measured in the stream bed and gravel bar at the bend of Hot Springs Creek indicates that thermal waters flow into the river here also.

The most northerly site, E, occurs on the shores of Hot Springs Bay in the intertidal zone east of the mouth of Hot Springs Creek (fig. 31). Temperatures higher than those of local surface waters were found at 10 cm depth over an area of about 2,500 m^2 of intertidal beach. The highest measured temperatures (62.5°C) occur adjacent to the outflow channel of Hot Springs Creek. Thermal waters emerging from the beach sand have a high specific conductivity, reflecting mixing with tidal waters.

Although flow measurements are available only for site A, the combined discharge from all the springs, including thermal waters that issue directly into Hot Springs Creek, is conservatively estimated at greater than 600 lpm.

The thermal waters from spring A3 and D2 are moderately concentrated sodium chloride waters with a relatively high level of bicarbonate. The more dilute waters of spring D2 may be the result of mixing with colder surface waters, which may also account for the magnesium present in the waters. The similarity in the ratios of the conservative elements boron to chloride in the two waters suggests the springs are derived from a common parent thermal reservoir.

Reservoir properties

Table 25 summarizes the application of silica and cation geothermometry applied to Akutan hot spring waters. In addition, an analysis of the oxygen-isotope compositions of dissolved sulfate and water from hot-spring A3 was obtained through the cooperation of N. Nehring (USGS, Menlo Park, Calif.). The results of the analysis and the application of the sulfate oxygen isotope geothermometer is given in table 25. No boiling occurs at the surface and therefore $T_1 = 186$°C, the conductive cooling temperature, is chosen as the sulfate geothermometer applicable to the subsurface reservoir (McKenzie and Truesdall, 1977). This temperature is in good agreement with the Na-K temperatures for both springs and with the Na-K-Ca '1/3' temperature for spring A3. For waters equilibrating above 150°C, the Na-K geothermometer is considered a more accurate geothermometer than the Na-K-Ca (1/3) (Fournier, pers. comm.). The lower Na-K-Ca 1/3 temperature for spring D2 may have been partly caused by dilution of ascending thermal waters with surface waters. Mixing

may also account for the comparatively low silica temperatures, although this may have also resulted from reequilibration of silica either on ascent from the deep reservoir or during residence in a shallow reservoir.

The rate of equilibration in oxygen-isotope exchange between dissolved sulfate and water is substantially slower than that for the chemical geothermometers (SiO_2, Na/K, Na-K-Ca) (McKenzie and Truesdell, 1977). Thus, unless the cold waters infiltrating into the deep reservoir have a relatively short residence time within the reservoir (<18 yr) the sulfate oxygen-isotope geothermometer is probably the most representative temperature of the deep reservoir. If so, spring-A3 Na-K and quartz conductive temperatures are the maximum and minimum, respectively:

	Min	Max	Most likely	Mean
Subsurface T (°C)	159	195	186	180

Table 25. Akutan Hot Springs geothermometry (all temperatures in °C).

	Spring A3	Spring D2
Surface temperature	84.5	58.8
Cation geothermometers		
Na-K	195	191
Na-K-Ca (1/3)	183	164
Na-K-Ca (4/3)	173	115
Silica geothermometers		
Adiabatic	151	128
Conductive	159	132
Chalcedony	135	105
Cristobalite	109	81
Opal	37	12

Sulfate-water oxygen isotope geothermometer[a]

$^{18}O-SO_4$ °/oo	$^{18}O-H_2O$ °/oo	T_1	T_2	T_3
+0.32	-9.17	186	171	174

[a]N. Nehring, USGS, Menlo Park, Calif., analyst.
Temperature estimates are based on three different end-member cases of water cooling discussed on page 26.

The difference in chloride and silica contents of springs A3 and D2, the similarity in their B:Cl ratios, and the large combined flow of the springs indicate that the deep thermal waters may be diluting in a shallow subsurface aquifer. If so, all three geothermometers would tend to underestimate the deep-reservoir temperature estimates. Following the method of Truesdell and Fournier (1977), application of the quartz mixing model suggests deep-reservoir temperatures as high as 235°C.

Comments

No geophysical exploration or exploratory drilling has yet been done near the Akutan hot springs. Thickness of the alluvial fill in the valley is unknown but is probably on the order of 100 m. Bedrock underlying the valley may be an extension of the volcanic breccia sequence exposed along the valley walls. If capped by hydrothermal cementation, such a

The estimated deep-reservoir temperature of 180°C is sufficient for a variety of applications, including the generation of a modest amount of electrical power, e.g., a 1-MW- well-head-driven Rankine binary system. The nearness of this hot-water system to a well-protected deep-water harbor with a population center and potential industrial users (e.g., fishing processors) make the Akutan hot spring site a particularly attractive one for future development. The ridge that lies between the site and Akutan volcano should help provide a protective barrier from eruptions from the active volcano.

AKUN STRAIT HOT SPRINGS

Location

Latitude: 54°8.4'N., longitude: 165°38.4'W.;
Unimak 1:250,000 (1951); T. 70 S., R 111 W.

General description

Akun Strait hot springs are located on the east shore of a small 0.5-km-long unnamed islet adjacent to the southwest coast of Akun Island, south of Surf Bay (fig. 26). The springs are 9 km east of the village of Akutan. Maximum elevation of the islet is about 35 m. At low tide the islet is connected to Akun.

The existence of these springs was reported to the DGGS field party by Luke Shelikoff of Akutan village. The hot springs may be those mentioned by Grewingk (1850) as located on a little island on the northwest side of Akun Island (see also Waring, 1917, p. 3). The inhabitants of Akutan village have no knowledge of any hot springs other than those on the islet.

One major spring and several seeps issue at half-tide level from the north side of a prominent NE-SW trending basaltic dike. The dike extends to the 20-m-high cliffs that tower above the beach. Local flora is mainly tundra. Sea mammals and birds frequent the coastal waters. The beaches are littered with gastropod shells.

The springs are accessible by boat from the village of Akutan but requires crossing of Akun Strait, which is relatively shallow (3 fathoms) and has a 12-knot tidal current with heavy riptides, standing waves, and overfalls.

The islet and adjacent Akun Island have been selected by the Akutan Native Corporation under the provisions of ANCSA. A dwelling was observed on Akun Island across from the springs.

Geology

The islet consists of consolidated, poorly sorted basaltic-andesitic volcanic rocks and clasts cut by a 1.5-m-wide vertical basaltic dike that trends N. 55° E. Volcanic rock fragments exposed in the 20-m-high beach cliff ranged from rounded and angular pebbles and cobbles to large angular boulders. A sill-like feature exposed in the cliff is a lapilli tuff with augite and plagioclase phenocrysts dispersed in a glassy matrix.

The basaltic dike contains 0.5-3 mm anhedral phenocrysts of plagioclase in a dark-gray groundmass. Other phenocrysts present included iddingsite, augite, and trace amounts of olivine.

The southern part of Akun Island adjacent to the islet consists of Late Tertiary and Quaternary basaltic and andesitic flows and pyroclastic debris (F.M. Byers, unpub. data, 1948). Mt. Gilbert, a Recent andesitic stratovolcano, lies 8 km north of the islet.

Spring characteristics

The spring emerges into a shallow pool alongside a basaltic dike. The pool is 1.5 m in diameter and 0.5 m deep. Discharge from the pool is small and estimated to be 15 lpm. Spring temperature is 42.8°C. Considerable gas bubbling occurs in the pool. Four seeps were found at lower tide levels about 10 m seaward of the main spring. Temperatures of the seeps ranged from 31.9° to 43.5°C. Additional thermal springs and seeps may occur below sea level.

Table 26 gives the physical and chemical properties of waters obtained from the principal spring. The high dissolved solids, salinity, and bromide content of the waters reflect the probable influence of seawater. The springs are probably diluted by ocean water before they emerge at the surface. Some of the waters charging the hydrothermal system may also have originally been seawater.

The thermal springs are probably a result of deep circulation of surface waters along fractures associated with the adjacent dike.

Reservoir properties

Table 27 summarizes the application of silica and cation geothermometry applied to Akun Strait hot springs. Cation geothermometry indicates subsurface equilibration took place at temperatures above 100°C. Therefore Na-K-Ca (1/3) is chosen as the cation temperature representative of the reservoir temperature. The quartz conductive temperature is 102°C. However, in basaltic terrain chalcedony could also be the controlling silica phase (Fournier, pers. comm.). In estimating reservoir temperature the chalcedony temperature is taken as minimum, the quartz conductive as most likely, and the Na-K-Ca (1/3) as maximum.

	Min	Max	Most likely	Mean
Subsurface T (°C)	72	118	102	97

The low rate of discharge of the springs suggests the thermal waters cooled conductively on ascent. The high salinity of the waters and the location of the springs in the tidal zone indicate that seawater infiltration may also be causing cooling of the thermal waters. Seawater has a chloride content of about 19,000 ppm and a sodium-to-chloride ratio of 0.55:1. A ratio of 0.48:1 is found in the thermal waters, which have a chloride content of 3,440 ppm. If the undiluted ascending thermal

Table 26. Chemical composition and physical properties of
Akun Straits hot springs
(all chemical analyses in mg/l).

	Akun Straits hot spring
SiO_2	50
Al	nd
Fe	0.19
Ca	475
Mg	45.5
Na	1660
K	34.9
Li	0.55
HCO_3	82
SO_4	222
Cl	3440
F	0.67
Br	11.25
I	0.86
B	5.7
H_2S	2.6
Sr	6.0
pH, field	7.47
Dissolved solids	6037.3
Hardness (mg/l $CaCO_3$)	1380
Sp conductance (μmho/cm at 25°C)	9800
T (°C)	42.8
Flow rate (lpm)	15
Date sampled	8/10/80

nd = Not determined.

Table 27. Akun Straits hot springs geothermometry
(all temperatures in °C).

Surface temperature	42.8
Cation geothermometers	
Na-K	112
Na-K-Ca (1/3)	118
Na-K-Ca (4/3)	102
Silica geothermometers	
Adiabatic	102
Conductive	102
Chalcedony	72
Cristobalite	51
Opal	-14

waters are assumed to have a chloride content of 400 ppm (a level similar to other thermal springs in the Aleutians not obviously affected by seawater), the mixing fraction of seawater required to attain the chloride level in the spring would be 16 percent. This mixing fraction is nearly identical to the ratio of bromide in the spring waters to bromide in seawater. If mixing were taking place near the surface, the temperature of the thermal waters before mixing would be 50°C for a seawater temperature of 5°C. Because seawater contains less than 3 ppm silica, the premixed thermal waters would have had a silica content of 60 ppm. This value would increase the quartz conductive temperature estimate to 111°C.

No geophysical exploration has been done at Akun Strait hot springs, and the extent of the subsurface reservoir is not known.

Comments

The hot springs probably result from deep circulation of surface waters along fractures. The high salinity and bromide content of the thermal waters indicate that the waters become diluted with seawater on ascent or that seawater may be a major component of the deep circulating system or both. Thermal waters may be discharging offshore and going undetected. The remoteness, low temperature, and low flow rate make these springs impractical for most geothermal applications.

ALASKA PENINSULA
FALSE PASS

Location

Latitude 54°55.8' N., longitude 163°14.4' W.,
False Pass 1:250,000 quadrangle (1949); T. 61 S., R. 93 W., Seward
Meridian.

General description

False Pass hot springs are located on the southwest side of a broad
glaciated valley that trends southeasterly from Hot Springs Bay, an
extension of Bechevin Bay (figs. 32 and 33). The springs lie about 1 km
inland from the head of the bay at the base of a steep ridge that rises
over 300 m. Existing aerial photographic coverage of the site is poor
because of cloud cover, and the topography of the immediate area is still
unmapped.

The springs emerge in two shallow pools in gently sloping alluvial
cover about 10 m above the main valley floor. Outflow from the two pools
converge into a single channel that joins a small unnamed stream about
150 m northeast of the pools.

The valley floor is relatively flat as a result of alluvial infilling
and at one time may have formed an extension of Hot Springs Bay. The
slope and shape of the valley and ridge topography indicates the major
erosional features are of glacial origin. Vegetation consists mainly of
muskeg, grasses, and low bushes.

The nearest settlement to the springs is False Pass, a village of
about 60 inhabitants located on Unimak Island, about 16 km southwest of
the hot springs. The springs are accessible from False Pass by boat
across Isanotski Strait into either Traders Cove or Hot Springs Bay
and then overland to the springs. The heads of these inlets are very
shallow and negotiable only by small boat at high tide. In optimum
weather and water conditions a float plane can be landed on either Hot
Springs Bay or Traders Cove.

The False Pass area supports a fishery that is primarily dependent
on salmon. Village economy is based on this fishery and the local cannery.
The village maintains an airstrip and is accessible from Cold Bay by
light twin-engine aircraft.

The Bureau of Land Management is currently transferring lands
surrounding the springs to the False Pass Village Native Corporation
under provisions of ANCSA. An easement for a 25-ft-wide trail from
Hot Springs Bay to the springs site has been established to accomodate
recreational use and scientific study. Additional easements have also
been made at the site itself.
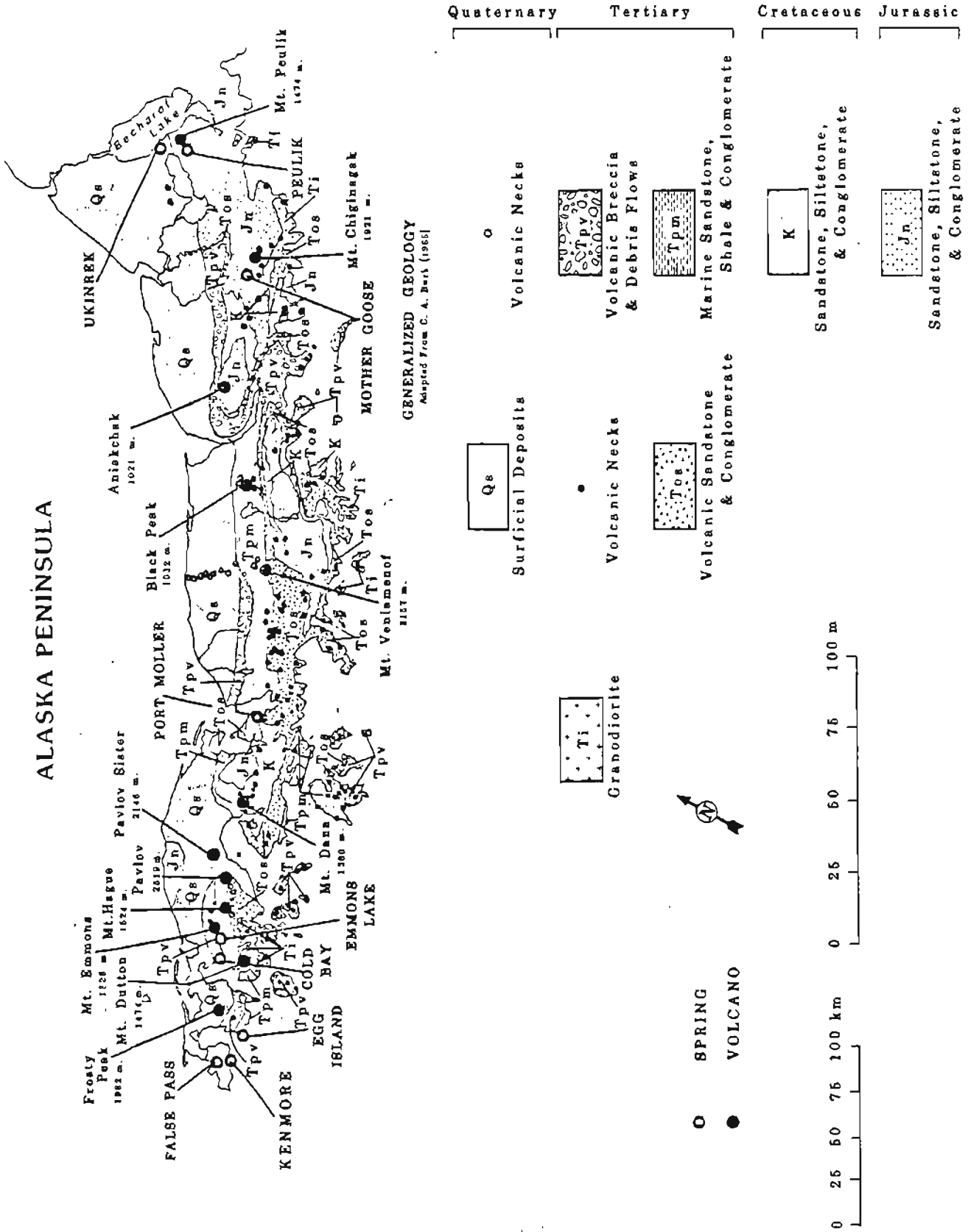
Figure 32. Generalized geology of western Alaska Peninsula.
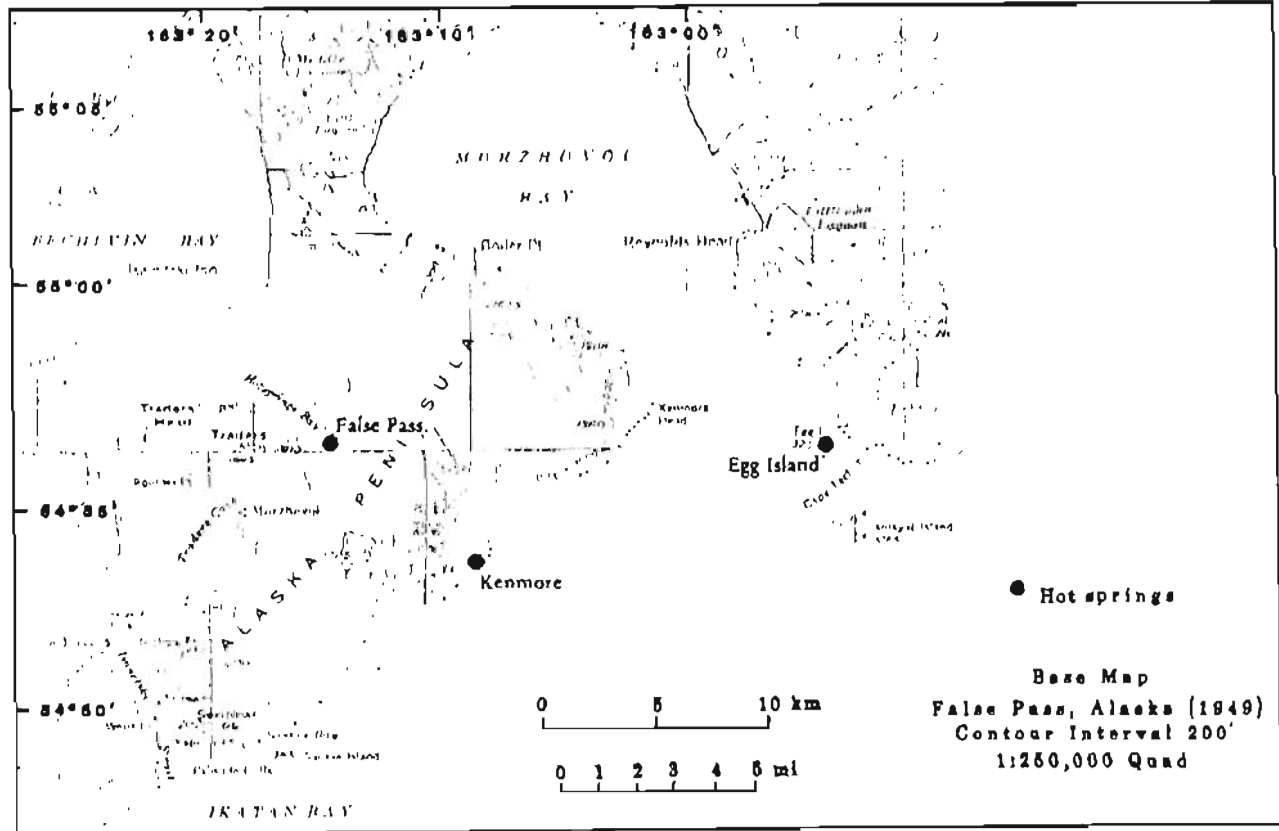
Figure 33. Location map for False Pass, Kenmore, and Egg Island hot
springs.

Ruins of the abandoned Native village of Morzhovoi can be found
5 km from the springs on the southwest shore of Traders Cove (fig. 33).
An old trail leading from Morzhovoi to the springs, rotting lumber, and
an old building site at the springs indicate that the former inhabitants
of this village used the springs for bathing.

Geology

The geology of the area has not been mapped. Extrapolating
from Burk's (1965) geologic map of the Alaska Peninsula northeast of this
site, the bedrock in the vicinity of the springs probably consists of
Quaternary volcanic rocks, including basaltic and andesitic flows and
pyroclastic flows (fig. 32). Outcrops on the ridge above the springs were
found to consist of weathered and slightly chloritized interbedded andesitic
flows. One of the flows examined was an olivine-bearing hypersthene
andesite. Bedrock outcrops are absent on the valley floor.

No active volcanoes are present in the immediate vicinity of the
site.

-112-

Spring characteristics

The hot springs emerge in two shallow pools surrounded by ferns and set about 2 m apart in the alluvium. The larger of the two pools is 2 m in diameter and is 0.5 m deep; the smaller pool is 1 m in diameter and 0.3 m deep. The pools are floored with small boulders and cobbles covered with thick mats of orange bacteria.

The temperatures of both pools measured 62.2°C. The larger pool has the greater discharge. Outflow from the two pools coalesce about 3 m downslope from the pools. The combined flow was measured to be 225 lpm. A similar rate of discharge was measured by Baker and others (1977) in 1977. Both pools exhibited continuous gas bubbling. The predominant component is probably CO_2, but a faint odor of H_2S was also detected.

Table 28 gives the chemical composition and physical properties of waters obtained from the larger of the two pools. The waters are notably low in dissolved solids, with the three major anions present in about equal proportion.

Table 28. Chemical composition and physical properties of
False Pass hot springs
(all chemical analyses in mg/l).

	DGGS
SiO_2	63
Al	0.15
Fe	0.02
Ca	20.4
Mg	0.01
Na	50.6
K	2.6
Li	0.08
HCO_3	45
SO_4	46.9
Cl	53
F	0.3
Br	nd
I	nd
B	1.5
H_2S	0.6
Sr	0.1
pH, field	8.44
Dissolved solids	261
Hardness (mg/l $CaCO_3$)	51.1
Sp conductance (µmho/cm at 25°C)	375
T (°C)	62.2
Flow rate (lpm)	225
Date sampled	7/2/81

nd = Not determined.

The thermal waters probably originate from circulation of meteoric
waters along a deep fracture zone. The surface expression of such a
zone would be masked by the alluvial cover. The valley in which the
springs lie is roughly colinear with a valley on the Pacific side of
the peninsula (fig. 33). The linear trend of the valleys, N. 50° W.,
is similar to the direction of convergence of the North American and
Pacific tectonic plates (N. 40° W.) in this sector of the Aleutian Range.

Nakamura and others (1977) have found evidence based on faults
and volcanic formations that, in the Aleutians, the maximum horizontal
compression is parallel to the maximum principal tectonic stress, i.e.,
the direction of convergence. Fractures and faults tend to propagate
perpendicular to the minimum stress direction, providing avenues for
circulation of meteoric waters through deep-seated hot rocks. Another
hot-spring system occurs on the Pacific Coast roughly in line with False
Pass hot springs and the valley trend.

Reservoir properties

Table 29 summarizes the application of silica and cation geothermo-
metry to False Pass hot springs. Cation geothermometry suggests sub-
surface equilibrium took place at temperatures below 100°C. The tempera-
ture given by the Na-K-Ca (4/3) geothermometer, however, is lower than
that measured at the surface and is therefore discounted. Therefore, the
silica temperatures are relied on in estimating reservoir temperature. In
basaltic terrain at temperatures below 150°C., the reservoir waters
could be equilibrating with either chalcedony or quartz (Fournier, pers.
comm.). In estimating reservoir temperature, the chalcedony temperature
is taken as minimum and quartz conductive as both most likely and as maximum:

	Min	Max	Most likely	Mean
Subsurface T (°C)	84	113	113	103

Table 29. False Pass hot springs geothermometry
(all temperatures in °C).

Surface temperature	62.2

Cation geothermometers

Na-K	166
Na-K-Ca (1/3)	129
Na-K-Ca (4/3)	49

Silica geothermometers

Adiabatic	112
Conductive	113
Chalcedony	84
Christobalite	62
Opal	-4.5

The hot springs issue from the surface at temperatures below boiling
and have a large combined flow rate, factors which suggest mixing of
colder waters (Fournier and Truesdell, 1974). In addition, their location
in valley alluvium increases the potential of dilution by infiltration
of surface and ground waters. Cold springs in similar locations else-
where on the Alaska Peninsula and in the Aleutians had an average tempera-
ture of about $10^{\circ}C$ and a silica content of 20 ppm. By using these para-
meters to characterize the cold-water fraction and following the method
of Truesdell and Fournier (1977), application of quartz mixing models
give the following results:

| | Parent hot water | | |
Mixing model	Max T $(^{\circ}C)$	SiO_2 (ppm)	Fraction (%)
Maxiumum steam loss	132	93	59
No steam loss	161	148	35

Temperatures from the quartz mixing models must be used with caution.
No corroborative evidence for mixing such as from chloride-temperature
analysis or water oxygen-isotope analysis is available. Further, the
parameters used for the cold waters may not be representative of waters
actually mixing with the thermal water.

Some of the ascending thermal water may go undetected, discharging
beneath the surface into the alluvium overlying the bedrock. A shallow
reservoir may have formed in the alluvium over the point of emergence
of hot waters from the subsurface bedrock. If the residence time of
the waters in such a reservoir is long enough, the chemical constituents
present in the waters could reequilibrate to the lower temperatures.
Such a situtation could account for the anomalously low cation-equili-
bration temperature.

No geophysical exploration has yet been done at False Pass hot springs,
and the extent of any subsurface thermal reservoirs is unknown.

Comments

Surface temperatures and flow rates at False Pass hot springs are
sufficient for a variety of small-scale direct-heat applications, including
aquaculture and space heating. The estimated reservoir temperature is
well below that presently required for generation of electrical power. If
subsurface mixing of colder waters is occurring, however, mixing models
suggest reservoir temperatures of over $150^{\circ}C$, which could be enough to
generate electricity.

Hot waters may be discharging below the surface directly into the alluvium. If a shallow reservoir is present in the alluvium, drilling of shallow wells into the reservoir could add substantially to the resource presently emerging at the surface at a relatively low cost.

The hot springs probably result from deep circulation of meteoric waters along fractures. Such fractures could be generated by the large compressive stress caused by the convergence of two major tectonic plates.

KENMORE HOT SPRINGS

Location

Latitude 54°54.2' N., longitude 163°08.6' W.; False Pass 1:250,000 Quadrangle (1949); T. 61 S., R. 92 W., Seward Meridian.

General description

Kenmore* hot springs are located on the Pacific shore of the Alaska Peninsula near its southwesternmost end, halfway between Morzovoi and Ikutan Bays (fig. 33). The springs occur at half tide level about 0.5 km southwest of a stream draining a prominent glacial valley located opposite "Hot Springs Valley." Topographic coverage for much of this portion of the Alaska Peninsula is lacking. The area has been intensely glaciated with ridge tops rising to 460-560 m. Steep beach cliffs rise abruptly from the shoreline along much of this part of the coast.

The springs are reached from the False Pass hot springs by traversing a 300-m-high pass separating the Hot springs Bay valley on the northwest side and the glacial valley on the southeast side. The overland trek is about 8 km long. The site can be alternatively reached by landing a small aircraft on a broad sand beach at the mouth of the glacial valley, near a fishing shack. The existence of these springs was reported to DGGS by a local fisherman, who had explored much of the surrounding area.

Vegetation in the area consists mainly of tundra, willows, and alders. Local fauna include caribou, brown bear, fox, and abundant bird life. Local land status is not known.

Geology

The geology of the area is still unmapped. On the basis of geologic mapping of the peninsula northeast of Morzhovoi Bay (Burk, 1965) and a brief reconnaisance of the hot spring area by DGGS in 1980, the region is inferred to consist of late Tertiary and Quaternary volcanic flows, sills, and dikes and associated sedimentary rocks (fig. 32). The springs are near a 2-m-wide vertical basaltic-andesitic dike with a strike of 111°. The dike rock consists of about 30 percent euhedral phenocrysts of plagioclase averaging 3 mm in length and andesine in composition, about 10 percent 3-mm phenocrysts of iddingsite in a matrix of about 35 percent fine-grained plagioclase, and 20 percent fine-grained iddingsite with traces of augite and opaques. The dike cuts a series of volcanic flows and sedimentary rocks exposed in the beach

---

*Informal name.

cliff. Additional dikes, pillow lavas, and columnar jointing in some
of the flows was also observed in the beach cliff. The mineralogy
of the pillow lavas was similar to that of the dike by the spring.

Spring characteristics

The springs, which emerge in three small pools from amongst
beach boulders near a basaltic dike, are found at half-tide level about
30 m seaward of a steep beach cliff that rises 150 m above the shoreline.
Upwelling and gas bubbling cover an area of about 4 m^2. Temperatures
ranged from 40° to 43.3°C, with the highest temperatures occurring
in the largest pool. The discharge for all sources combined was visually
estimated at 80 lpm. No odor of H_2S was detected.

Table 30 gives the chemical and physical properties of thermal
waters obtained from the largest and warmest pool. The waters are
notably high in dissolved solids. The large amounts of sodium, chloride,
and particularly magnesium and bromide suggest either a seawater origin
for the thermal waters or perhaps contamination by surface seawater
influx. If the Mg and Br in the thermal waters are assumed to be
derived solely from seawater contamination, the average seawater values
of 1,272 and 65 ppm for Mg and Br, respectively, yield a maximum cold
seawater mixing fraction of 5 to 8 percent. This amount of mixing could
account for a large part of the other constituents present in the
thermal water.

Reservoir properties

Table 31 summarizes cation and silica geothermometry applied to
Kenmore hot springs. The magnesium in the waters is assumed to
be mainly of surface seawater origin and no magnesium correction has
been applied to the cation geothermometer. The Na-K-Ca (4/3) geothermo-
meter indicates subsurface equilibrium takes place at temperatures
below 100°C. In estimating the subsurface reservoir temperatures,
the Na-K-Ca (4/3) temperature is taken as most likely, the chalcedony
as minimum, and the quartz as maximum:

	Min	Max	Most likely	Mean
Subsurface T (°C)	62	93	73	76

These estimates may be slightly higher if seawater contamination
is occurring. Alternatively, the deep circulating thermal waters may
themselves be of a seawater origin. The flow rates of the springs are
low and cooling probably occurs by conduction during ascent of the
thermal waters.

-118-

Table 30. Chemical composition and physical properties of
Kenmore hot springs
(all chemical analyses in mg/l).

	DGGS
SiO_2	41
Al	nd
Fe	0.11
Ca	275
Mg	66
Na	783
K	13.2
Li	0.20
HCO_3	102
SO_4	359
Cl	1570
F	0.25
Br	5.19
I	0.09
B	3.0
H_2S	nd
Sr	1.8
pH, field	7.39
Dissolved solids	3220
Hardness (mg/l $CaCO_3$)	961
Sp conductance (μmho/cm at 25°C)	5600
T ($^{\circ}$C)	43.3
Flow rate (lpm)	20 (est)
Date sampled	7/3/80

nd = Not determined.

Table 31. Kenmore hot springs geothermometry
(all temperatures in $^{\circ}$C).

Surface temperature	43.3

Cation geothermometers

Na-K	101
Na-K-Ca (1/3)	104
Na-K-Ca (4/3)	73

Silica geothermometers

Adiabatic	93
Conductive	93
Chalcedony	62
Cristobalite	43
Opal	-22

-119-

Comments

The thermal waters probably result from the deep circulation of surface waters (including possibly seawater) along fractures associated with the dike intrusions in the area. Depth of circulation would reach 1.5 to 2.5 km if thermal gradients of 30 to 50°C/km are assumed. The remoteness, low discharge, and low temperature of the springs make them impractical for most geothermal applications.

Location

Latitude 54°56.1' N., longitude 162°54.6' W.; False Pass D-3
1:63,360 Quadrangle, T. 60 S., R. 90 W.

General description

Egg Island is a verdant, elongate, wedge-shaped island located
about 1 km offshore at the eastern edge of the mouth of Morzhovoi Bay
on the Pacific side of the Alaska Peninsula (fig. 33). Egg Island is
only 600 m long, aligned northeast-southwest, with sea cliffs rising
sharply to a central peak about 400 m high. The island's steep slopes
are covered to varying degrees with coarse grasses and serve as rookeries
for multitudes of gulls, puffins, and murres.

Several hot springs and hot-water seeps are found on the southeast
shore of the island at low-tide level. The springs emanate from several
small fractures on a wave-cut platform of volcanic rocks that runs the
length of the island and extends seaward to the southeast for 50 m. A
narrow boulder beach borders the northwest side of the island. The
southwest side is incised by several tidal channels at least 5 m deep
and wide and up to 30 m long. The regularity of the parallel sheer walls
of the channels suggests some structural control in their formation.
These vertical walls are roughly aligned with the steep outer edge of
the above wave-cut platform.

Cold Bay is the nearest population center to Egg Island and lies
30 km to the NNE. The fishing village of King Cove is 40 km east of
the island. Although the island can be reached by boat or float plane
from Cold Bay, the boulder beaches and dense kelp beds that surround the
island make landings hazardous. Egg Island itself is part of the
Aleutian Wildlife Refuge System.

Geology

Waldron (1961) mapped Egg Island as a Tertiary hornblende-andesite
plug and correlated it with Amagat Island 3 km to the south, although
he viewed Egg Island only from a boat. Both islands are characterized
by exceedingly steep relief, but much of Egg Island was found to be
composed of a coarse-grained holocrystalline diorite containing euhedral
to subeuhedral complexly zoned plagioclase, biotite, and clinopyroxene.
A dioritic stock similar in lithology to Egg Island was mapped by Waldron
(1961) west of Thinpoint Lagoon, which is east of Egg Island; it intrudes
middle and upper Tertiary volcanics of basaltic composition. Egg Island
is separated from the peninsula mainland by a shallow, kelp-infested strait.

On the other side of the strait is a broad U-shaped valley formed
on the flanks of the old Morzhovoi stratovolcano. Farther north
is Frosty Peak, a spectacular composite volcano of late Pleistocene
or Recent age that is the dominant topographic and geologic feature
of the area.

Spring characteristics

Several springs occur at low-tide level and emanate from small
fractures in a wave-cut platform on the southeast side of the island.
The springs are located midway down the length of the island and about
4 m from the outer edge of the platform. The main spring that was
sampled flows from the bottom of a small, 0.75-m-deep depression in
the horizontal bench of volcanic rock. The pool is only 0.5 m in
diameter, but is connected by channels to a network of similar pools
covering an area 2 m^2. Three seeps with steady streams of gas bubbles
originate from fractures in the bottom of this pool, which has a tempera-
ture of 50.6°C. There was no strong odor of H_2S. Numerous tiny patches
of bubbling activity are found along fractures several meters inland on
the marine bench. A complete survey made of the periphery of the island
confirmed that geothermal activity is confined to the immediate vicinity
of the pool sampled.

Table 32 gives the chemical and physical properties of the thermal
spring sampled. Flow from the main spring area was impossible to measure
because of the interconnecting pools, but is probably considerable.
Although the sampling was performed at lowest tide, a time when the
ledge is essentially supratidal, waves breaking against the wall of rock
at the outside edge of the shelf splashed large amounts of seawater onto
that area of the shelf. However, the low magnesium and sulfate present
in the thermal waters indicate little contamination of the water sample
with fresh seawater. This suggests that outflow from the spring must be
great enough to rapidly flush out most incoming seawater. The high
levels of sodium, chloride, calcium, bromide, iodide, and strontium
indicate seawater is the parent fluid that is being circulated at depth
and heated, with magnesium and sulfate being selectively removed by
subsurface water-rock interactions.

Although the intertidal volcanic shelf hosts a luxuriant growth
of algae, the hot-spring area is barren. There are no conspicuous
mineral deposits surrounding the spring vents.

Reservoir characteristics

Table 33 summarizes the silica and cation geothermometry of Egg
Island hot springs. The cation geothermometers indicate subsurface
equilibration takes place at temperatures below 100°C. The Na-K-Ca (4/3)

-122-

temperature is close to the chalcedony temperature of 69°C. Alternatively, the waters may be equilibrating with quartz and reservoir temperatures may be as high as 99°C:

	Min	Max	Most likely	Mean
Subsurface T (°C)	69	99	70	79

Table 32. Chemical composition and physical properties of
Egg Island hot spring
(all chemical analyses in mg/l).

	DGGS
SiO_2	47
Al	nd
Fe	0.29
Ca	869
Mg	6.2
Na	2,030
K	18.3
Li	0.85
HCO_3	67
SO_4	26.5
Cl	4,505
F	0.37
Br	14.79
I	2.94
B	32.5
H_2S	0.15
Sr	5.02
pH, field	7.66
Dissolved solids	7,626
Hardness (mg/l $CaCO_3$)	2,201
Sp conductance (μmho/cm at 25°C)	12,300
T (°C)	50.6
Flow rate (lpm) (est)	200
Date sampled	8/21/80

nd = Not determined.

The combined flow of the hot-springs system is estimated at about 200 lpm. Water chemistry indicates that contamination with seawater near the surface is minimal. If mixing of colder waters is taking place it occurs at deeper levels and may not involve seawater.

Comments

The hot springs probably result from circulation of surface waters along deep-seated fractures in the country bedrock. Chemical analysis indicates that the parent thermal waters may have a seawater

-123-

origin. If the waters are conductively cooling on ascent, the circulation depths must be about 1.5 to 2.5 km, assuming geothermal gradients of 30 to 50°C/km.

Table 33. Egg Island hot springs geothermometry
(all temperatures in °C).

Surface temperature	51
Cation geothermometers	
Na-K	72
Na-K-Ca (1/3)	86
Na-K-Ca (4/3)	70
Silica geothermometers	
Adiabatic	99
Conductive	99
Chalcedony	69
Cristobalite	49
Opal	-16

Egg Island hot springs are thought to be the hot springs reported by Waring (1917), from second-hand information, as occurring on an island at the mouth of Morzhovaoi Bay. Waring assumed the island to be Amagat Island, and the notion of hot springs occurring on Amagat has persisted in the literature. However, residents of the Cold Bay area could not confirm the presence of any springs on Amagat.

The small size, remote location, and poor accessibility of Egg Island and the inclusion of Egg Island in the Aleutian Wildlife refuge make this geothermal site a poor candidate for any development or use.

Location

Latitude 55°13.3' N., longitude 162°24.7' W., Cold Bay 1:250,000
Quadrangle (1943); T. 57 S., R. 87 W.

General description

. Cold Bay hot springs are located about 6 km east of Cold Bay, a
large embayment near the southwest end of the Alaska Peninsula (fig. 34).
The hot-springs site is near the southwestern edge of a broad lowland
formed by the merging of several valleys that drain northward from the
slopes of Mt. Dutton (1,475 m) and other mountains south and west of the
lowlands. These mountains have been deeply incised by glacier erosion.
Eskers and moraines form prominent local topographic features on the
lowlands, but the dominant surface expression of the lowlands is a pitted
outwash plain with numerous low hills and depressions that commonly
contain lakes, ponds, or mud playas (Waldron, 1961). The outwash surface
in turn is blanketed with a thick cover of tundra, grasses, ferns, shrubs,
and thickets of alders and willows.
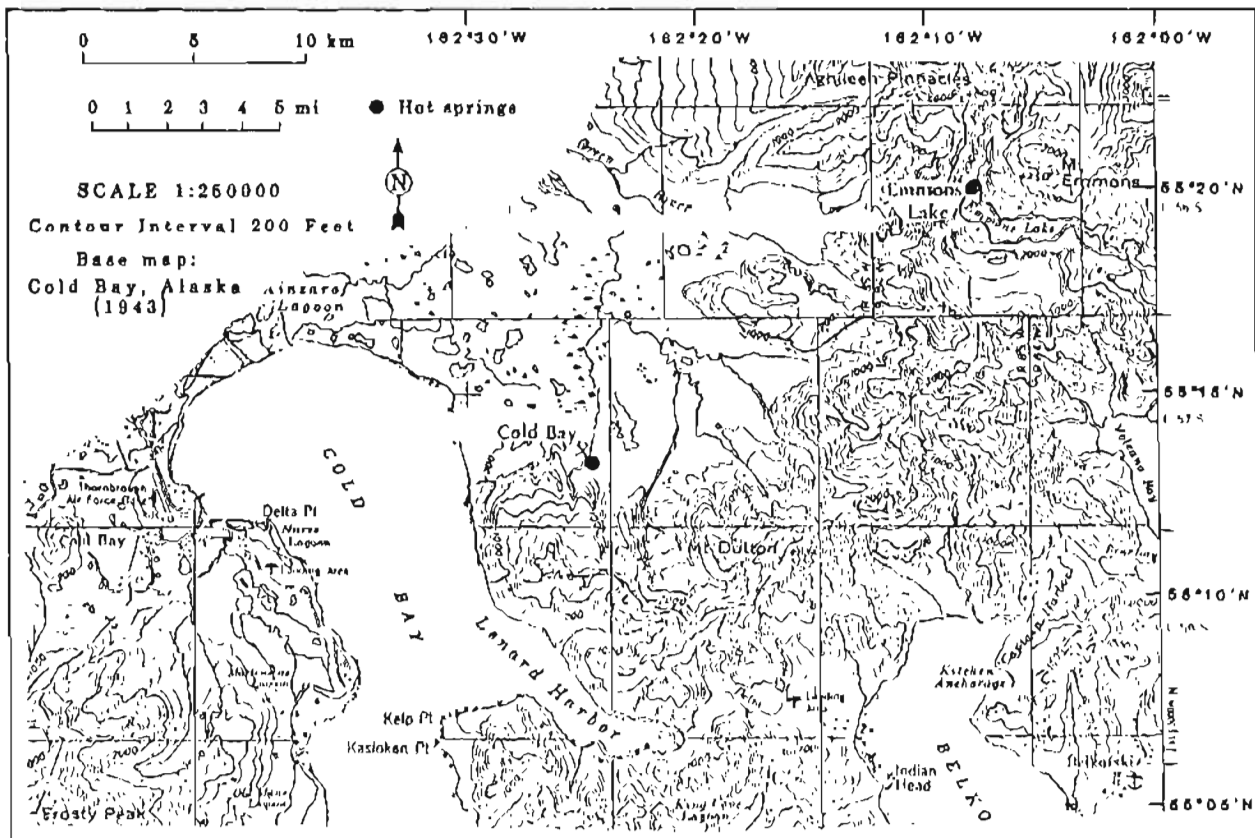
Figure 34. Location map for Cold Bay and Emmons Lake hot springs.

The springs site consists of a series of hot springs, seeps, and bubbling warm pools issuing from the soil on the south slope of a 15-m-high, elongated hillock that is probably of glacial origin. The thermal waters drain into a small cold-water creek that flows ENE. Numerous brown-bear trails radiate from the springs site.

The nearest settlements are the village of Cold Bay, located about 18 km west of the springs site and King Cove, an Aleut fishing village about 20 km SSE. The springs are accessible from Cold Bay by small boat to the eastern shore of the bay. An old trapper's cabin near the beach and at the mouth of a prominent ravine serves as a landmark for the beginning of a 6-km overland trek to the springs; no trail exists.

The village of Cold Bay has a population of about 100 and serves as the gateway to the Aleutians. It was a major staging area for Allied Forces in the Aleutians during World War II. Abandoned, rusting military buildings still dot much of the surrounding countryside. Today the Cold Bay airport is a major crossroads for traffic servicing villages and the fishing industry throughout the Aleutian and Pribilof Islands and for aircargo flights to and from the Orient. The village is also the headquarters for the Izembek National Wildlife Range and for the regional office of Alaska Department of Fish and Game, which operates a salmon hatchery near the village.

The village of King Cove is located on a protected bay affording excellent anchorage for the local fishing fleet. The village population of about 80 is primarily of Aleut and Scandinavian background. Most of the fishing vessels in King Cove are locally owned and support a local salmon and crab cannery.

The springs are presently located within the boundaries of the Izembek National Wildlife Range. The land surrounding the springs, however, has been tentatively selected by the King Cove Village Corporation under terms of ANCSA.

Geology

Bedrock exposed south and east of the lowlands consists of tan late Tertiary sandstones and conglomerates that are more than 900 m thick in places (Burk, 1965) (fig. 32). These strata, which probably underlie the lowlands, resemble the Miocene Bear Lake Formation of Port Moller, but they may be equivalent to the Pliocene Tachilni Formation southwest of Cold Bay. East and south of the lowlands and particularly in the area of the Aghileen Pinnacles, this sandstone-conglomerate unit is overlain by a thick sequence of Pliocene to early Pleistocene volcanic breccias with a few interbedded lava flows. Farther east is the Emmons Lake volcanic complex, which consists of Pleistocene and recent volcanic flows and breccias and several active volcanic vents.

The ridges and volcanic slopes bordering the lowlands have been extensively modified by glacier erosion. Bedrock in the lowland area is mantled by an unknown thickness of glacier drift and alluvial deposits, probably late Pleistocene and derived from these mountains (Waldron, 1961). The low-land surface is in turn mantled by ashy and silty soil. A semiconsolidated layer of tephra was found exposed in a stream bank near the springs site about 0.35 m below the surface. The layer is a least 0.5 m thick and consists of lapilli-size pumice and andesitic rock fragments in a gray ash matrix of glass and crystal shards. Crystals found in the layer include zoned euhedral plagioclase, hornblende, and augite.

Spring characteristics

Over 14 hot springs, seeps, and warm pools issue from the soil in an area of about 300 m by 200 m on the south slope of a small morainal hillock (fig. 35). Table 34 lists the individual springs and their temperatures. Spring A had the highest measured temperature, 62.3°C, and spring L was estimated visually to have the greatest discharge. Blue-green algae line most of the outflow channels and orange bacterial mats occur in some of the hotter pools.

Table 34. Temperatures of Cold Bay hot springs (flows visually estimated).

Spring	T (°C)	Comments
A	62.3	Actively bubbling pool with moderate flow (30 lpm); pH = 5.55
B	51	Small bubbling spring (10 lpm)
C	15	Low flow (10 lpm)
D	15	Low flow (10 lpm)
E	51-54	3-m-dia hot pool with continuous bubbling; moderate flow (30 lpm)
F	42.5	Low flow (10 lpm)
G	60	Bubbling spring with moderate flow (50 lpm)
H	44	Seep (1 lpm)
I	50	Low flow (10 lpm)
J	42.5	Gassy spring, very low flow (5 lpm)
K	22-25	Several shallow warm bubbling pools averaging about 1 m in dia
L	53.6	Large pool and large flow (100 lpm); pH = 6.70
M	22	Seep (1 lpm)
N	40	Moderate flow (50 lpm)
O	41	Low flow (10 lpm)
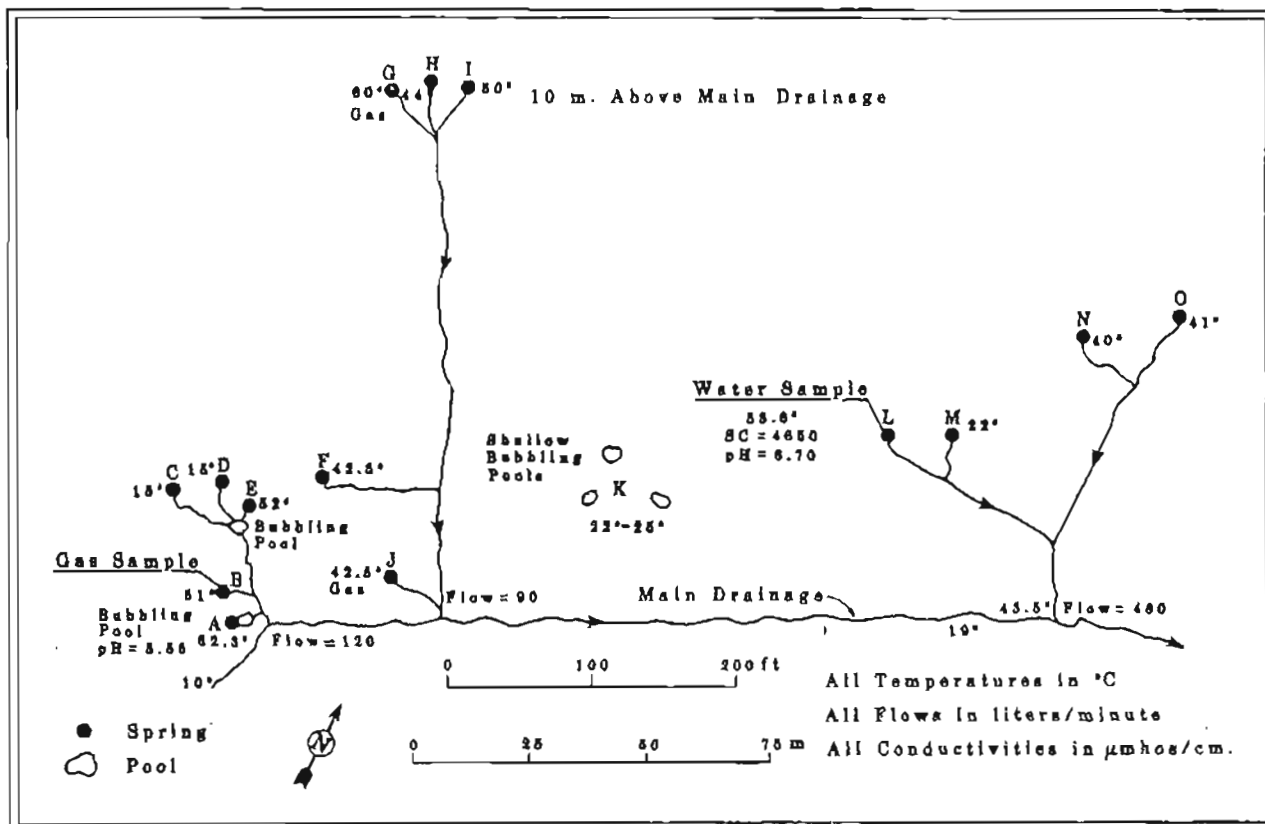
Figure 35. Detail at Cold Bay hot springs.

Table 35. Flow rates in major hot spring channels

Springs	Flow (1pm)
A, B, C, D, and E	118
F, G, H, I, and J	89
L, M, N, and O	478
	Total 685

The springs tend to occur in groups. The highest group, springs G, H, and I, lies about 10 m in elevation above the lowest springs. Outflow from springs in individual groups merge into three channels, which eventually drain into a cold-water stream at the base of the hillock. The combined measured discharge for all three channels is 685 1pm (table 35).

The large measured flow rate constrasted with the lower visual estimates made at the spring sources suggests that thermal waters may be infil-trating through the channel beds and contributing to the outflow. Some thermal waters may also be discharging below the surface and go undetected.

Considerable bubbling was noticed in several of the pools and springs. An analysis of a gas sample obtained from spring A is given in table 36.

The values for nitrogen and oxygen probably represent air contamination because the proportions are almost those of air. In addition, during analysis, gas pressure in the sampling tube was found to be very low, possibly due to equipment malfunction while acquiring the sample (W. Evans, pers. comm.). Despite these problems, the analysis shows clearly that methane is the major gas discharging with the thermal springs. The late Tertiary sedimentary beds thought to underlie the area may be the source of this methane-rich gas.

Table 36. Analysis of gases obtained from
Cold Bay hot springs, spring A.*

	Volume percent
He	0.2
H_2	0.1
Ar $\}$	
O_2	6.03
N_2	27.14
CH_4	66.04
CO_2	2.85
C_2H_6	0.06
H_2S	----

*W.C. Evans, analyst, USGS, Menlo Park, Calif.

Table 37 gives the chemical composition and physical properties of thermal waters obtained from spring L. Although no odor of H_2S was detected at the site, chemical analysis in the field showed a trace amount of H_2S in the waters. The thermal waters are notably concentrated in sodium and chloride with the chloride content much greater than the combined content of bicarbonate and sulfate.

Because Mg becomes increasingly less soluble with increasing temperature, a high Mg content is sometimes thought to indicate a low equilibration temperature (Potter and Fournier, pers. comm.). The Mg level at Cold Bay hot springs, however, is consistent with the level of Mg found in other thermal waters in the Aleutians and Alaska Peninsula examined in this study. An alternative source of the Mg could be the mixing of a colder water.

Reservoir properties

Table 38 summarizes silica and cation geothermometry applied to spring L at Cold Bay hot springs. The silica geothermometers and the closeness of the Na-K-Ca (4/3) temperature to $100^{\circ}C$ indicate that subsurface

Table 37. Chemical composition and physical properties of
Cold Bay hot spring L
(all chemical analyses in mg/l).

	Site L
SiO_2	125
Al	0.05
Fe	1.32
Ca	162
Mg	5.7
Na	751
K	16.4
Li	0.95
HCO_3	248
SO_4	14
Cl	1370
F	0.67
Br	4.11
I	1.0
B	25
H_2S	0.44
Sr	0.86
pH, field	6.70
Dissolved solids	2726
Hardness (mg/l $CaCO_3$)	429
Sp conductance (μmho/cm at 25°C)	4650
T (°C)	53.6
Flow rate (lpm)	100
Date sampled	7/6/81

equilibration took place at temperatures above 100°C. The Na-K-Ca (1/3) temperature is chosen as the minimum reservoir temperature, the quartz conductive as the maximum, and chalcedony as the most likely:

	Min	Max	Most likely	Mean
Subsurface T (°C)	116	150	125	130

The Mg correction suggested by Fournier and Potter (1978) for cation geothermometry is too low to affect the above estimates.

The springs all emanate at temperatures below boiling and have a large combined discharge, which suggest that subsurface mixing of colder waters is occurring (Fournier and Truesdell, 1974). In addition, the location of the springs in glacial debris and near the foot of a mountain range increases the potential of dilution by infiltration of surface and ground waters. A silica content of 132 ppm was found in thermal waters discharging from spring A, which has a temperature of 62.3°C.

Table 38. Cold Bay geothermometry, hot-spring L
(all temperatures in °C).

Surface temperature	53.6

Cation geothermometers

Na-K	114
Na-K-Ca (1/3)	116
Na-K-Ca (4/3)	92

Silica geothermometers

Adiabatic	143
Conductive	150
Chalcedony	125
Cristobalite	100
Opal	29

Although the difference in silica contents between springs A and L is within the variance normally expected from lab analyses, the correlation of higher spring temperature and silica content suggests mixing.

No geophysical exploration has yet been done at Cold Bay hot springs and the extent of any subsurface thermal reservoirs is unknown. A shallow reservoir may have formed in the glacial debris over the point of emergence of hot waters from the subsurface bedrock. The magnesium in the waters emerging at the surface could have resulted from the reequilibration of ascending thermal waters in such a low-temperature shallow reservoir or from mixing with cold ground-waters.

Comments

Surface temperatures and flow rates at Cold Bay hot springs can support a variety of small-scale direct heat applications such as aquaculture and space heating. The estimated reservoir temperature is below that now required for generating electrical power. However, if subsurface mixing of colder waters is occurring, mixing models suggest reservoir temperatures may exceed 150°C, which may be high enough to generate electricity.

EMMONS LAKE HOT SPRINGS

Location

Latitude 55°20.0' N., longitude 162°08.4' W.; Cold Bay 1:250,000 Quadrangle (1943); T. 56 S., R. 84 W.

General description

Emmons Lake hot springs are located near the northern shore of an 8-km-long alpine lake that occupies the bottom of a steep-sided nearly enclosed crescent-shaped basin 14-km north of Volcano Bay (fig. 34). The lake lies at an elevation of about 300 m at the southwest end of a 20-km-long arc of active volcanism that extends from the glacier-clad Pavlof Volcano (2,710 m) and Pavlof sister (2,135 m). Recent basaltic flows from Mt. Emmons (1,325 m), the volcanic vent closest to Emmons Lake, impinge on the lake's northern shore. The milky-blue lake is fed in part by glacier meltwaters and drains into Volcano Bay through a narrow gorge formed beside a fresh lava flow originating from Mount Hague (1,400 m).

The landscape near the springs is a blend of heavily glaciated older volcanic terrain overlain on the east by recent volcanic flows, vents, and cinder cones. Steep glaciated valley walls tower 600 m above the southern and western shores of the lake. A small glacier flows northwest from the summit of Mount Emmons, and a somewhat larger glacier occupies much of the upland south of Emmons Lake. The spectacular Aghileen Pinnacles (1,200 m) and the scenic Cathedral Valley lie immediately north of the springs site.

The nearest communities are King Cove, located 35 km southwest of the springs, and Belkofski, a small native village located 32 km due south. The nearest commercial airport is at Cold Bay, 40 km west of the springs. An airstrip long enough for twin-engined aircraft is located just north of King Cove. The springs site lies in rugged alpine terrain and is quite remote and difficult to reach. The DGGS field team used a helicopter from Cold Bay.

Exact land status is unknown. Lands surrounding the spring site may have been selected by the Tanadguisix Village Corporation under the terms of the ANCSA. Otherwise the lands are under the jurisdiction of the Bureau of Land Management.

The hot-springs site was first reported by Kennedy and Waldron (1955), who estimated the spring temperatures at 60°C. They also reported that six large fumaroles and numerous smaller ones occupied a steep gully on the southwest side of Mount Hague, at altitudes ranging from 1,050 to 1,250 m.

Geology

The regions east and south of Emmons Lake were mapped in 1946 by Kennedy and Waldron (1955). The oldest exposed rocks in the area are thought to be Tertiary and consist of arkosic rocks conformably overlain by a thick sequence of fragmented volcanic deposits, principally well-bedded tuffs south of Emmons Lake and agglomerate north of the lake. The bedded rocks are intruded by quartz diorite stocks, basalt plugs, andesite sills, and numerous basaltic dikes.

After a long interval of erosion, during which deep canyons were carved in the tuff and agglomerate beds and in the intrusive rocks, a series of basalt flows issued from vents along or near a great curving rift of northeast trend and filled topographic depressions in the old erosional surface. The most widespread of these older lavas is the Dushkin Basalt, thought to be Pliestocene. The unit consists of a thick series of interbedded flows and is well exposed in the cliffs south of Emmons Lake, where it exceeds 650 m in thickness. Kennedy and Waldron (1955) speculated that the crescent-shaped basin containing the lake may be part of a collapse caldera formed when lavas of the Dushkin Basalt were being erupted.

Recent volcanism is represented by six large stratovolcanoes---Pavlof, Pavlof Sister, Little Pavlof, Double Crater, Mount Hague, and Mount Emmons---that lie along an arc about 20 km long and appear to be built over a major rift of northeast trend. This chain of stratovolcanoes is made up of interbedded lava flows and pyroclastic material, numerous satellitic cinder cones and associated lava flows, and minor glacial and alluvial deposits. With the possible exception of Little Pavlof, the volcanoes have been active in Holocene times; Pavlof has erupted several times in the past decade.

Spring characteristics

The springs emerge from colluvium near the northwest corner of Emmons Lake at the base of a steep valley wall composed of Dushkin Basalt and occur near the aggrading outwash delta at the head of the lake (fig. 36). There are several orifices dispersed over an area of about 1,000 m^2, which is marked by lush, verdant vegetation.

The hottest vent, which measured 65.1°C, occurs by itself, issuing from a small pool about 0.6 m in diameter and 0.5 m deep. This spring is located about 5 m above lake level and has a discharge rate of 38 lpm; calcite coats the upper part of the channel where it flows into the lake. The spring exhibited vigorous bubbling.

Several meters to the southeast, a small basin, about 20 m in diameter, contains several more spring orifices with temperatures ranging from 42.1° to 63.6°C. Numerous minor warm seeps also occur around the periphery of the major spring vents. The combined flow rate of the thermal waters measured in the basin outflow channel was 560 lpm. The spring channels were lined with orange-bacterial and blue-green algae mats.

-133-
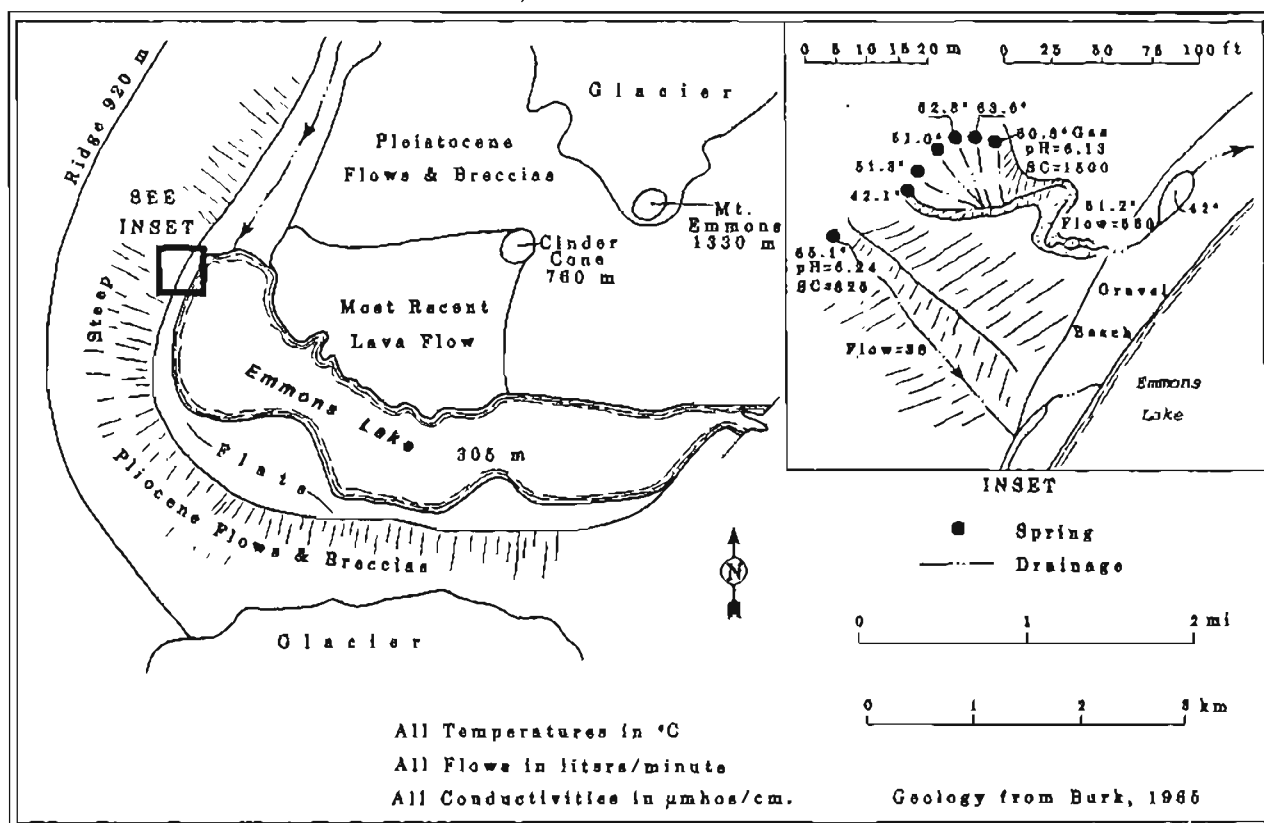
Figure 36. Detail at Emmons Lake hot springs.

Table 39 gives the chemical and physical properties of the thermal waters obtained from the hottest spring vent. The waters are notably high in silica and in carbonate and mildly concentrated in sodium and chloride. An analysis of gases emerging with the thermal waters is given in table 40. The principal active gases present in the system are CO_2 and CH_4. The nitrogen is probably of atmospheric origin with oxygen selectively removed in oxidizing reactions.

Reservoir properties

Table 41 summarizes the application of silica and cation geothermometry to Emmons Lake hot springs. An analysis of the $^{18}O_2:^{16}O_2$ ratios in the thermal waters and in the sulfates present in the spring waters was obtained through the cooperation of N. Nehring (USGS, Menlo Park, CA). The results of the anlysis and the application of the sulfate-oxygen isotope geothermometer appear in table 40.

Because the springs are well below boiling and no obvious manifestations of subsurface boiling occurs elsewhere in the area, $T_1 = 184^\circ C$ is chosen as the representative sulfate-oxygen isotope reservoir temperature

(MacKenzie and Truesdell, 1977). This temperature is nearly identical to the Na-K temperature but considerably higher than either the quartz-conductive or Na-K-Ca (1/3) temperatures. For thermal waters originating from a high temperature environment (180°C) the Na-K geothermometer is generally considered to give excellent results, mainly because it is less affected by dilution (Fournier, pers. comm.). In estimating the deep reservoir temperature, the sulfate temperature is taken as most likely, the Na-K as the maximum, and the quartz conductive as minimum:

	Min	Max	Most likely	Mean
Subsurface T ($^{\circ}$C)	160	184	189	178

Table 39. Chemical composition and physical properties of Emmons Lake hot spring (all chemical analyses in mg/l).

	Result
SiO_2	148
Al	nd
Fe	0.55
Ca	30
Mg	0.97
Na	139
K	9.8
Li	0.6
HCO_3	292
SO_4	51.5
Cl	102
F	1.7
Br	nd
I	nd
B	4.6
H_2S	0.5
Sr	0.11
pH, field	6.24
Dissolved solids	780.8
Hardness (mg/l $CaCO_3$)	82.6
Sp conductance (μmho/cm at 25°C)	825
T ($^{\circ}$C)	65.0
Flow rate (lpm)	560
Date sampled	8/21/80

nd = Not determined.

The high combined flow rate of the springs and the orifice temperatures, which are considerably below geothermometer temperatures, suggest the thermal springs are of a mixed origin. However, application of the silica mixing model of Fournier and Truesdell (1977) results in a line that does not intercept the quartz solubility curve (pg. 38). Because no obvious fumarole vents occur in the general area, steam separating from an adiabatically cooling liquid seems unlikely and use of the maximum steam-loss line in the silica mixing model appears unwarranted. Either the thermal waters emerging at the surface may have cooled after mixing or the reservoir waters may have cooled partly by conduction on ascent and partly by mixing with colder waters. Any combination of the preceding would invalidate the use of the silica mixing model. The lower quartz temperature could also be due to precipitation of silica on ascent of the thermal waters or because of reequilibration in a shallow lower-temperature reservoir.

Table 40. Analysis of gases obtained from Emmons Lake hot springs.[a]

	Volume percent
He	0.01
H_2	0.005
Ar	0.66
O_2	0.22
N_2	47.6
CH_4	4.36
CO_2	47.4
C_2H_6	0.01
H_2S	-----

[a]W.C. Evans, USGS, Menlo Park, California.

Comments

The Belkofski Tuff appears to underlie the Dushkim Basalts exposed near the springs. The tuffs, which are probably porous and highly permeable, are capped by relatively impermeable basalt flows, providing the potential for an excellent deep reservoir for geothermal fluids. The source of heat driving the hydrothermal system may be a shallow body of magma suggested by the high level of volcanic activity that occurs east of the springs.

The estimated reservoir temperature of 178°C places the hydrothermal system in the high-temperature category---one that is potentially useful for electrical power generation and a variety of other applications. Because of the remoteness of the site, however, development of the resource appears unlikely.

Table 41. Emmons Lake hot springs geothermometry
(all temperatures are in °C).

Surface temperature   65.1

Cation geothermometers

Na-K	189
Na-K-Ca (1/3)	156
Na-K-Ca (4/3)	93

Silica geothermometers

Adiabatic	152
Conductive	160
Chalcedony	136
Cristobalite	110
Opal	38

Sulfate-oxygen isotope geothermometer[a]

$(\delta^{18}O\text{-}SO_4)$ °/oo	$(\delta^{18}O\text{-}H_2O)$ o/oo	T_1	T_2	T_3
-0.61	-10.21	184	165	170

[a] N. Nehring, analyst, U.S.G.S., Menlo Park, Calif.
Temperature estimates are based on three different end member cases of water cooling as discussed on page 26.

PORT MOLLER HOT SPRINGS

Location

Latitude 55°51.7' N., longitude 160°29.5' W.; Port Moller D-2
1:63,360 Quadrangle (1963); T. 50 S., R. 73 W.; sec. 13, SE1/4 of
SW1/4 of Seward Meridian.

General description

Port Moller hot springs are situated on the south side of Port
Moller Bay, southeast of Moller Spit and north of Mud Bay (fig. 37).
The nearest habitation is the Port Moller cannery which lies 16 km
north of the springs; the native village of Nelson Lagoon is located
near the Bering seacoast about 40 km northwest of the springs.

The principal thermal springs occur near the head of a shallow
0.5-km-long, N-S trending trough located adjacent to a 10-to 20-m-high
bedrock ridge that juts out slightly into Port Moller Bay (fig. 37).
Minor seeps of warm waters were also found at half-tide level emerging
from fractures on the wave-cut platform east of the ridge. The area
west of the trough consists of an undulating coastal lowland containing
small marshes and ponds and lushly vegetated with muskeg, willows, and
alders. South of the springs site the terrain is ruggedly mountainous,
rising to the 825-m summit of Staniukovich Mountain. The bottoms of
valleys and gullies on the flanks of the ridges and mountains are vege-
tated with willow and alder thickets. Seaward of the springs site lies
a huge clam-rich mud flat that extends several kilometers into the bay
at low tide.

The springs site is surrounded by numerous middens, some up to
2 m high, consisting of seashells and sea-mammal bones. The middens
and associated relict dwellings have been unearthed and examined by
a team of archeologists from Hokkaido University, Sapporo, Japan
(Okada and Okada, 1980, and pers. comm.). The site has been intermit-
tently occupied for at least 3,000 yr. Other archeological sites occur
in the area, but the Port Moller hot-springs site was by far the most
densely used.

The springs site can be reached by small boat or aircraft from
Port Moller. The beach north of the spring site is well packed,
allowing landing of bush airplanes. Port Moller can be reached by
charter air or boat from Cold Bay, 170 km to the southwest. The lands
surrounding the site have been selected by the local native corporation
under terms of ANCSA.

A summary of an early visit to the springs site is contained in
Waring (1917). More recently, Port Moller hot springs were included in
a study of potential fish-hatchery sites (Baker and others, 1977).
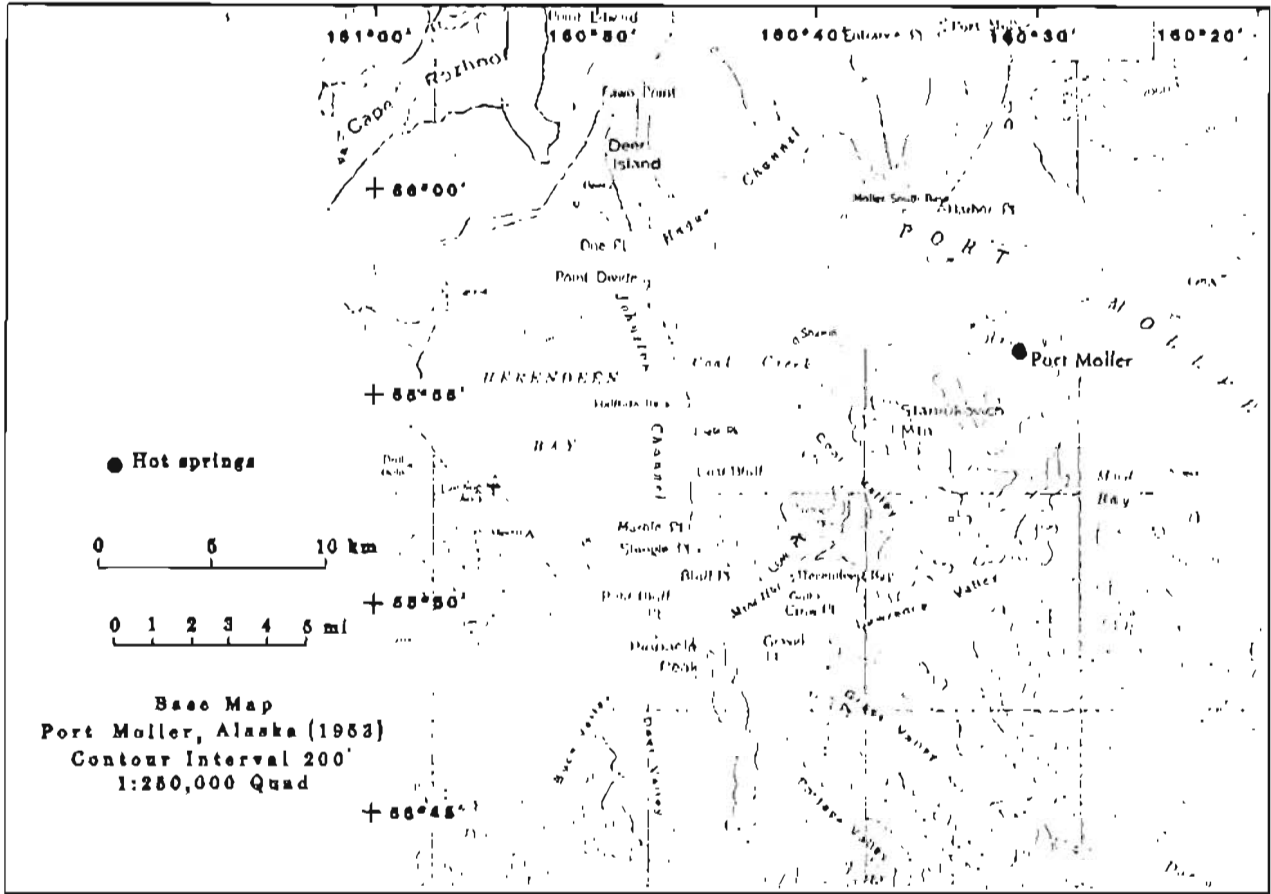
Figure 37. Location map for Port Moller hot springs.

Geology

Bedrock in the area includes Upper Jurassic and Cretaceous sedimentary rocks and Tertiary volcanic and sedimentary rocks that form the mountains and beach cliffs south and west of the site (Burk, 1965). The small bedrock ridge exposed east of the springs consists of fossiliferous feldspathic sandstones and shales of the Staniukovich Formation, which dip 15° to 20° to the west. The formation, which is Upper Jurassic to Lower Cretaceous, is also exposed on the north flank and summit of Staniukovich Mountain, where it is up to 600 m thick. Small outcrops of Upper Cretaceous Herendeen Limestone, consisting of calcareous feldspathic sandstones, occur at the base and flanks of Staniukovich Mountain and conformably overlie the Staniukovich Formation. The shoreline west of the springs site consists of the upper Cretaceous Chignik Formation, a series of coal-bearing sandstones and conglomerates that unconformably overlies the rocks of the Herendeen Limestone.

Early Tertiary volcanic sandstones, flows, conglomerates, and black siltstones of the Tolstoi Formation crop out along the beach south of the springs. These rocks are unconformably overlain by shallow-dipping Pliocene volcanic rocks, flows, and breccia and associated vents that comprise the east flank of Stanuikovich Mountain, south of the springs.

The nearest active volcanoes, Pavlof and Veniaminof, lie about 110 and 80 km from the site, respectively. Mt. Dana, a Quaternary volcano located 45 km southwest of the site, has had no recorded activity in recent history.

Spring characteristics

The hot springs occur about midway up a shallow gully floored with sandy soil. The 0.5-km-long, 20-m-wide depression slopes southward towards a small bight off Port Moller Bay. The thermal waters emerge into a shallow muck-floored oval pool, 4.5 m long and 1.5 m wide oriented E-W and set into the sandy soil. Waters from the pool drain southward alongside a bedrock ridge in a channel lined with orange bacteria and blue-green algae mats. The waters pass through a series of terraced bathing pools past a small cabin before entering the small bight south of the gully. Sea shells and rocks in the channel were coated with a veneer of yellowish flaky material for several meters downstream from the spring source. Vigorous and continuous bubbling occurs throughout the pool. Maximum temperature was 71.3°C; the flow rate measured in the outflow channel was 52 lpm, slightly lower than that measured by Baker and others (1977).

Several additional small warm seeps, about 20°C and accompanied by virgorous bubbling, occur on the opposite side of the bedrock ridge, directly east of the principal hot spring. The waters issue at midtide level from a small vertical fracture.

Table 42 gives the chemical composition and physical properties of thermal waters obtained from the principal hot pool. The waters are notably high in sodium, calcium, and chloride and low in bicarbonate and sulfate, though a measurable quantity of H_2S was found dissolved in the waters. The relatively high salinity of the waters and the high bromide and strontium levels suggest that a portion of the thermal waters has a seawater origin. The very low level of magnesium indicates little or no near-surface contamination with cold seawater.

Table 42. Chemical composition and physical properties of
Port Moller hot springs
(all chemical analyses in mg/l).

	Result
SiO_2	63
Al	0.05
Fe	0.03
Ca	228
Mg	0.16
Na	792
K	12.3
Li	0.34
HCO_3	71
SO_4	16.5
Cl	1615
F	2.7
Br	5.34
I	0.85
B	13
H_2S	1.47
Sr	2.92
pH, field	8.24
Dissolved solids	2825
Hardness (mg/l $CaCO_3$)	573
Sp conductance (μmho/cm at 25°C)	5300
T (°C)	71
Flow rate (lpm)	251.5
Date sampled	8/18/80

Table 43 gives the chemical composition of gases emerging from the hot-springs pool. The gases are notably rich in methane, which probably originates from organic matter in the Staniukovich Formation.

Table 43. Analysis of gases obtained from
Port Moller hot springs.[a]

Volume percent

He	0.01
H_2	0.01
Ar	0.25
O_2	0.02
N_2	11.61
CH_4	87.89
CO_2	0.02
C_2H_6	0.66
H_2S	----

[a]W.C. Evans, USGS, Menlo Park, Calif.

Reservoir properties

Table 44 summarizes the application of silica and cation geo-thermometry to Port Moller hot springs. The Na-K-Ca (4/3) geothermo-meter temperature indicates that subsurface equilibration took place at temperatures below $100^{\circ}C$. For temperatures below $150^{\circ}C$, dissolved silica may be equilibrating with either quartz or chalcedony (Fournier, 1973). In estimating the reservoir temperature, the quartz-conductive temperature is taken as maximum, the chalcedony temperature as most likely, and the Na-K-Ca (4/3) as minimum:

	Min	Max	Most likely	Mean
Subsurface T ($^{\circ}C$)	75	113	84	91

Although the springs emerge at a high rate of discharge, the geo-thermometers are not much above surface temperature, which indicates the thermal waters probably cooled conductively on ascent. Although some mixing with cooler surface groundwaters cannot be dismissed because of the low Mg content of the thermal waters, surface seawater is unlikely to have contributed to such mixing.

Comments

Port Moller hot springs probably result from the circulation of surface waters along deep-seated fractures in the host sedimentary rocks. Spring geochemistry suggests that part of the deep thermal waters may have had a seawater origin. If the waters are being heated solely by conduction from wall rocks, circulation depths must be about 2 to 3 km, assuming geothermal gradients of 30 to $50^{\circ}C/km$.

Table 44. Port Moller hot springs geothermometry
(all temperatures in $^{\circ}C$).

Surface temperature	71.3
Cation geothermometers	
Na-K	97
Na-K-Ca (1/3)	102
Na-K-Ca (4/3)	75
Silica geothermometers	
Adiabatic	112
Conductive	113
Chalcedony	84
Cristobalite	62
Opal	4.5

The low reservoir temperature and the remoteness of the site make the resource impractical for most geothermal applications except perhaps local space heating and recreation.

MOTHER GOOSE HOT SPRINGS

Latitude 57°10.8' N., longitude 157°01.1' W.; Ugashik A-4 1:63,360
Quadrangle (1963); T. 35 S., R. 48 W.

General description

Mother Goose hot springs are found at the northern base of Mount
Chiginagak (2,225 m), a large stratovolcano located on the Alaska
Peninsula, southwest of Ugashik Lakes and 25 km north of the Pacific
Ocean (fig. 32). The upper slopes of the volcano are mantled with
glaciers with tongues descending to elevations as low as 760 m. The
springs occur along the southwest side of a narrow flat-bottomed valley
formed by a tributary of Volcano Creek near its head (fig. 38). Volcano
Creek is fed primarily by snow and glacial meltwaters originating on
Mount Chiginagak and flows westward 15 km into Mother Goose Lake. The
floor of the valley of Volcano Creek has a flat flood-plain relief and
widens considerable as it nears Mother Goose Lake. The entire area lies
between the drainages of the King Salmon and Dog Salmon Rivers on the
Alaska Peninsula, southwest of Ugashik Lakes.

Villages nearest the springs are Ugashik, 44 km to the north, and
Pilot Point, 54 km to the northwest. The major transportation center of
King Salmon is 175 km north-northeast; Dillingham is 225 km due north.
The springs are remote but can be reached by float plane from King Salmon
to any of several nearby lakes and thence overland to the site. Muskeg,
grasses, and patches of alders constitute the dominant vegetation of the
valleys.

Mother Goose hot springs were investigated as a possible salmon
hatchery site (Baker and others, 1977), but was rejected because of its
remote location, poor surficial-water quality, and geologic hazards
associated with volcanic eruptions and possible periodic flooding. Koniag
Inc., of Kodiak, Alaska has selected lands adjacent to the spring under
provisions of ANCSA. The regions surrounding the spring site are part of
the newly formed Alaska Peninsula National Wildlife Range.

Geology

Mount Chiginagak is part of the Aleutian arc of active volcanism.
The stratovolcano is composed mainly of Quaternary interbedded basaltic
and andesitic flows with associated pyroclastic material (Burk, 1965).
Tertiary volcanics are exposed on ridges and mountains east and west of
the volcano and may underlie the Quaternary sequence of Mt. Chiginagak.
Outcrops of volcanic rocks exposed in the vicinity of the thermal springs

Figure 38. Location map for Mother Goose hot springs.

at the base of the volcano are slightly altered porphyritic andesitic basalts containing phenocrysts of hornblende, clinopyroxene, and labradorite. The age of these volcanics is not clear but they may be related to the older Tertiary volcanics in the area.

The Mother Goose thermal springs occur near the contact between the volcanics of Mount Chiginagak and the underlying fossiliferous feldspathic sandstones of the lower Cretaceous Staniukovich Formation. Colluvial sediments from which the springs emerge cover the exact location of the contact in this vicinity. The Upper Jurassic Naknek Formation, which conformably underlies the Staniukovich Formation, is exposed in the valley wall across Volcano Creek from the springs site. The Naknek Formation consists of arkosic and feldspathic sandstones and siltstones and locally abundant conglomerates.

There have been at least two reported eruptions of Mount Chiginagak since 1760 (Coats, 1950). An area of fumarolic activity persists on the east flank of the volcano near the summit (Baker and others, 1977).

The upper reaches of Volcano Creek are incised into the flanks of Mount Chiginagak and its valley is floored with fluvial and colluvial deposits. A whitish deposit coats the boulders in the channels of upper Volcano Creek and may be due to mineralized waters issuing from the base of the volcano.

Spring characteristics

Two areas of thermal-spring activity, about 1 km apart, occur at the northwest base of Mount Chiginagak south of upper Volcano Creek (fig. 39). The larger and more westerly of the two areas consists of a series of thermal springs that emerge from colluvial debris cemented by travertine, located at and just above the base of the south valley slope. Most of the hot springs at the site issue from fissures and seeps along the south bank of a small tributary stream that flows for 300 to 400 m at the base of the slope before entering Volcano Creek (fig. 39). The most conspicuous of these springs discharges from a 30-cm-dia hole in the cemented stream-bank sediments located just above stream level. Thermal waters pour from the vent in a torrent of 66°C water at a visually estimated rate of over 400 lpm. Numerous other but much smaller orifices occur along the entire length of this small stream, and range from 37° to 63°C.

Temperature at the eastern head of the tributary measured 15°C. Stream temperature above the main series of thermal springs was 36°C and total flow was measured at 676 lpm. Just below the main spring MG1, the stream had a measured flow of 2,570 lpm and a temperature of 50°C. At the point where the small stream joins Volcano Creek its temperature is 45°C with a measured flow of 6,100 lpm. This tremendous flux of thermal water discharging into Volcano Creek is much too high to be accounted
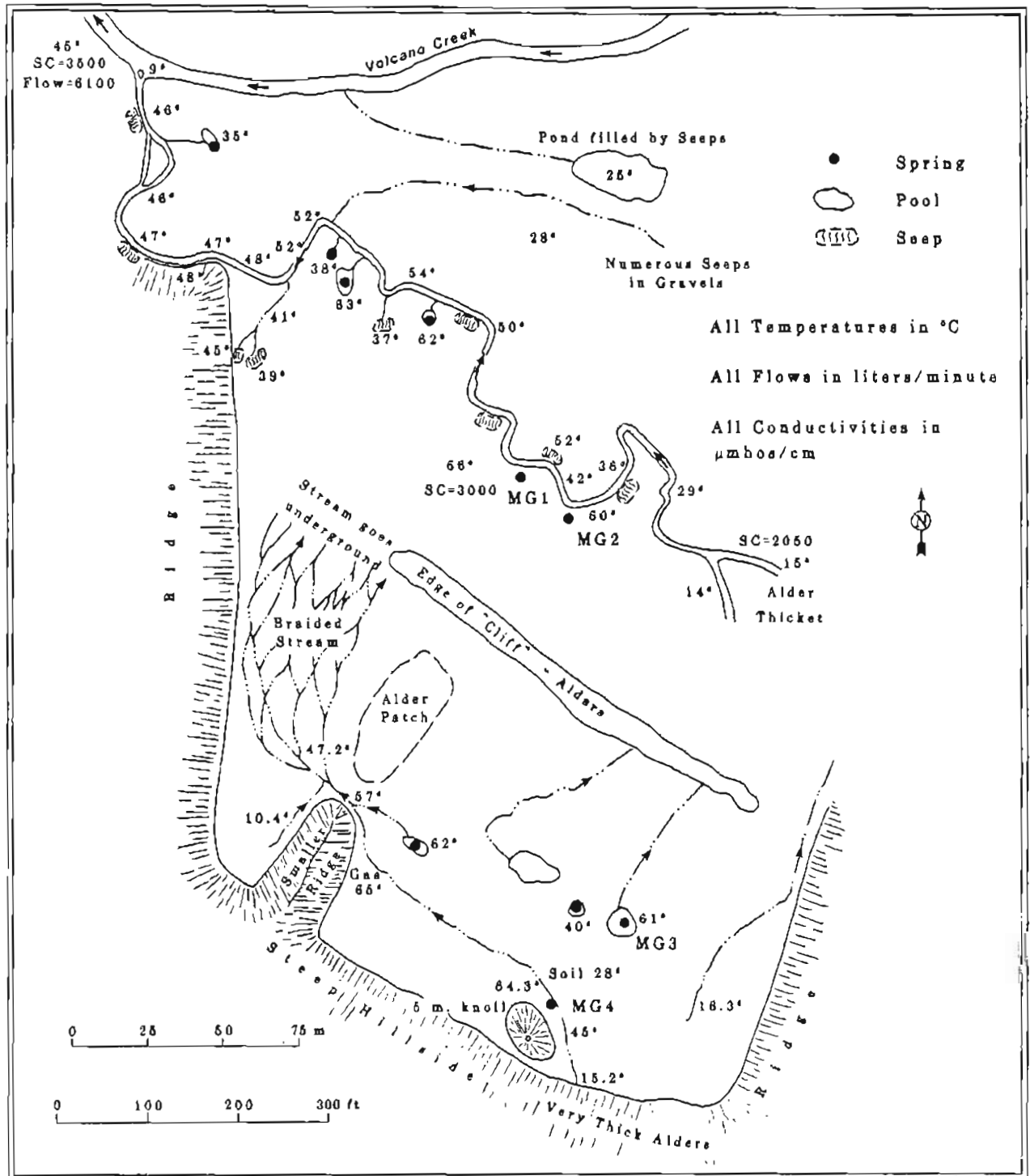
Figure 39. Detail at Mother Goose hot springs.

for simply by flow from the visible thermal spring orifices; a considerable addition of thermal water must occur below stream level along the course of the tributary stream. The heat flux represented by this discharge of thermal waters referenced to Volcano Creek water temperature of 9°C is approximately 4 MW.

Two additional thermal-spring areas occur on a small knoll that rises 15 to 20 m above the tributary stream (fig. 39). MG3 consists of a series of small springs that emerge at a temperature of 60°C from the upper part of an extensive travertine terrace. Spring discharge is quite low, visually estimated at about 30 lpm. The large terrace suggests that flow may have been much greater in the past.

Thermal spring MG4 discharges at a temperature of 64°C directly into a 15°C cold-spring channel at a small waterfall that marks an abrupt break in slope. The hot waters were observed to emanate from the contact zone between a 1-m-thick surficial soil cover and underlying cemented debris. Thermal waters at temperatures of 60° to 65°C continue to discharge into the spring channel for 50 to 60 m downslope before the stream fans out onto a broad apron of travertine deposits that is intermittently covered with vegetation. A flow measurement of 980 lpm was obtained in the single drainage channel above the apron. Below the apron the waters reenter the ground and drain through porous soils into the tributary stream.

The other area of thermal-spring activity occurs 1-km farther east along Volcano Creek and was only briefly examined. The site consists of several pools and springs that range from 20° to 55°C. The thermal waters emerge from lushly vegetated soil that overlies what appears to be an old gravel bar of Volcano Creek located at the base of the valley slopes. A few of the spring vents have associated travertine deposits.

Table 45 gives the chemical composition and physical properties of thermal waters obtained from spring MG1. The DGGS analysis of these waters is similar in all respects to a previous USGS analysis of Mother Goose thermal waters. The spring temperature reported by USGS, however, was several degrees lower than that measured by DGGS for spring MG1, indicating that either the USGS sampled a different, more dilute spring or that MG1 itself may have been more dilute in 1973.

The Mother Goose thermal waters are characterized by two seemingly contradictory subsurface chemical indicators. The very high level of silica and the comparatively low Na:K ratio suggests that at least part of the spring waters originate from a high-temperature reservoir. In contrast, the presence of magnesium and the comparatively high level of magnesium and calcium indicate that much of the spring water must originate from a relatively low-temperature environment.

Table 45. Chemical composition and physical properties of
Mother Goose hot spring, MG1
(all chemical analyses in mg/1).

	Spring MG1
SiO_2	245
Al	0.05
Fe	0.12
Ca	227
Mg	131
Na	198
K	47.4
Li	0.22
HCO_3	560
SO_4	491
Cl	528
F	0.41
Br	0.81
I	0.21
B	0.8
H_2S	0.5
Sr	0.42
pH, field	6.35
Dissolved solids	2430
Hardness (mg/1 $CaCO_3$)	1107
Sp conductance (µmho/cm at 25^oC)	3000
T (^oC)	66
Flow rate (lpm)	2567
Date sampled	8/13/80

The fumaroles on the east flank of the mountain are evidence for
the passage of steam through the interior of the volcano, at least at
its upper levels. Condensation of volcanic steam and oxidation of H_2S
and CO_2 in infiltrating cold surface waters would result in the forma-
tion of bicarbonate-sulfate-rich waters at shallow subsurface levels.
The resulting relatively cool waters might then drain through volcanic
flows, dissolving Mg and Ca along the way. As these Mg-rich bicarbonate-
sulfate waters migrate to the base of the volcanic sequence they may have
intercepted a high-temperature stream of chloride- and silica-
rich deep geothermal waters. The resulting mixture of such waters
draining through the relatively permeable underlying sandstone formations
and would then emerge from beneath the volcanic flows as thermal springs
at the base of the volcano. A situation similar to the forgoing hypothesis
has been demonstrated to exist at Hakone volcano in Japan (Oki and Hirano,
1970).

Reservoir properties

Table 46 summarizes the application of silica and cation geother-
mometry to spring MG1 of Mother Goose hot springs. A sulfate-water
oxygen-isotope geothermometer is also available from an earlier USGS
analysis. Because of the puzzling chemistry of the thermal spring
waters, interpretation of the various geothermometers is problematic.
The level of magnesium in the waters renders the use of cation geother-
mometers uncertain and ambiguous. Although the high-silica content of
the waters indicates the presence of a high-temperature source near 175°
to $195^\circ C$, the silica concentration is nearly the equilibrium level
for amorphous silica at the spring orifice temperature. This suggests
that silica could have been equilibrated by the passage of relatively
cool waters through highly silicified strata. The sulfate geothermometer
also suggests a relatively low reservoir temperature. However, the
derived sulfate temperatures may merely reflect the temperature of
sulfate formation at shallow levels rather than be representative of deep
reservoir temperatures.

Table 46. Mother Goose hot springs geothermometry
(all temperatures in $^\circ C$).

Surface temperature	66.0

Cation geothermometers

Na-K	292
Na-K-Ca (1/3)	203
Na-K-Ca (4/3)	100
Na-K-Ca (1/3) Mg-corrected	20

Silica geothermometers

Adiabatic	180
Conductive	194
Chalcedony	175
Cristobalite	145
Opal	70

Sulfate-water oxygen-isotope geothermometer[a]

($\delta^{18}O$-SO_4) $^o/oo$	($\delta^{18}O$-H_2O) $^o/oo$	T1	T2	T3
5.87	-12.32	86	83	84

[a]From Nehring and others, 1980, erroneously listed as
"Indecision Creek." Temperature estimates are based
on three different end-member cases of water cooling
as discussed on page 26.

The high chloride content of the waters argues for the existence of a deeper high-temperature reservoir. On the basis of the chloride level and silica content of the waters, the deep-reservoir temperature is estimated to exceed 150°C. Even if the thermal spring waters are exclusively derived from shallow warm-water reservoirs, the reservoir probably exists because of heat derived from condensation of steam rising from a high-temperature reservoir deeper in the volcanic system.

Comments

Mother Goose hot springs are distinguished from other thermal spring systems in the Aleutian arc by their enormous rate of discharge and by their puzzling thermal-water chemistry. These waters are simultaneously rich in both magnesium and silica, constituents that are indicative of cold- wnd hot-water environments, respectively. The geologic setting and chemistry of the Mother Goose hot springs are analogous to spring systems that occur at the base of Hakone Volcano in Japan (Oki and Hirano, 1970). The Hakone spring systems have been shown to be derived from the mixing of relatively cool waters from shallow reservoirs with high-temperature silica- and chlorite-rich waters ascending from a deep thermal reservoir.

Despite the ambiguity in applying the Mother Goose geothermometers, the occurrence of fumarolic activity near the summit of the volcano indicates the existence of a deep thermal reservoir in excess of 150°C. The Mother Goose hot springs are remote and probably are not practical to develop for the foreseeable future. However, the spring system remains one of the more interesting ones in Alaska.

OTHER THERMAL SPRING SITES

The 1980 DGGS investigation of thermal-spring sites in the study
area extending from Atka Island to Becherof Lake was by no means
exhaustive. Several other thermal areas have been reported in this
region in addition to those described herein (fig. 1). These addi-
tional sites fall into three categories: a) sites visited by DGGS
at which thermal activity either could not be found or the activity had
substantially diminished (Bogoslof Island, Mount Peulik, and Ukinrek
maars), b) sites not visited by DGGS because of time constraints
or remoteness but within which, based on the accuracy of previous
reports, thermal activity is considered certain or at least probable
(Atka north, Sequam, Chuginadak, Kagamil, Okmok, Unimak, Pavlof,
Surprise Lake, and Gas Rocks), c) sites not visited by DGGS about which
no corroborative information could be found and the existence of any
thermal-spring activity in the area is questioned (Atka west, Akun,
Amagat Island, Frosty Peak, Balboa Bay, and Stepovak Bay).

Sites Visited, Thermal Activity Not Found or Diminished

Bogoslof Island

The listing of this site in the compilations of Miller (1973) and
Markle (1980) is based on Waring's 1917 account, which described the
occurrence of small thermal springs at the base of the volcanic island.
Bogoslof is a recently constructed volcanic island that lies in the
Bering Sea about 50 km north of Umnak Island and the main axis of
Aleutian volcanism (fig. 1). The island owes its existence to a
series of volcanic eruptions commencing in 1796. Details of the
geology and volcanic evolution of the island are given in Byers (1959).
Much of the island was blanketed by a series of tephra layers deposited
during eruptions in 1926 and 1927. A 0.5-km-dia basaltic dome emplaced
in 1927 now occupies the northwest end of the island. Byers did not
report any thermal activity on the island and the volcanic dome must
have cooled rapidly. A brief reconnaissance of the island by DGGS in
1980 found no signs of surface thermal anomalies, hot springs, or steam
vents, and the site is considered inactive. The craggy surface of the
dome and the steep beach cliffs have become a popular nesting area for
a huge population of puffins, murres, and gulls. The island lies within
the Aleutian Wildlife Refuge.

Mount Peulik

Waring (1917) reported a thermal-spring site near Mount Peulik
(1,600 m). The site is plotted on the south flank of Peulik Volcano
in Miller's 1973 compilation of Alaskan hot springs. A series of

springs draining into "Hot Springs Creek," a stream that drains the south flank of Peulik (Ugashik C-2 1:63,360 Quadrangle, 1951) were investigated by DGGS. The springs were found to be cold, highly mineralized waters that drain from the base of a large recent volcanic cone that is set in the middle of the Peulik caldera. The cone may have been associated with a major eruption reported to have occurred in 1814 (Coats, 1950). The springs were undoubtedly warm at one time. Fossil hydrothermal mounds and sinter cones occur at lower elevations on the south flank of the mountain, but there are no associated thermal springs nearby.

Ukinrek maars

Two explosion craters, located about 2 km south of Becherof Lake, were formed in the spring of 1977 during a series of phreatomagmatic eruptions described by Kienle and others (1978). Waters at the floor of the west maar had cooled considerably from $81^{\circ}C$ in 1977 to $11^{\circ}C$ in 1980. The crater lake in the east maar appeared cold; the lake waters were not sampled because of the treacherous crater embankment.

Sites Not Visited, Thermal Activity Probable or Certain

Atka North

Located 4 km north of the Korovin thermal area on northeast Atka Island, this site was reported to B. Marsh (pers. comm.) and tentatively identified on aerial photos but a field confirmation was not made.

Seguam

This site, located 100 km northeast of Atka Island is a remote island with an active volcano. On the basis of earlier Russian accounts, Waring (1917) reported thermal-spring and mudpot activity. Coats (1950) lists a major eruption on the island in 1902 and minor activity in 1927. Seguam is included within the Aleutian National Wildlife Refuge.

Chuginadak

Chuginadak is located in the Islands of Four Mountains southwest of Umnak Island. Waring (1917), on the basis of earlier Russian accounts, listed hot-spring activity at the base of the volcano on Chuginadak. The island is within the Aleutian National Wildlife Refuge.

Kagamil

Also located in the Islands of Four Mountains is Kagamil. Hot gases were reported by Waring (1917). During an archeological expedition in 1936 Hrdlicka (1945) observed steam jets, warm caves, and steaming beach areas on the south side of the island. The island lies within the Aleutian National Wildlife Refuge.

Okmok

Okmok is an active, large shield volcano located on the northeast side of Umnak Island. Thermal springs and fumarolic activity within the caldera are described by Byers and Brannock (1949). New lavas erupted since 1946 have covered much of the caldera floor. A large, highly pressurized steam vent with vapor plumes rising several hundred meters into the air is located in the west part of the caldera (C. Nye, pers. comm.).

Unimak

The largest of the Aleutian Islands, Unimak is located directly southwest of the Alaska Peninsula. Most of the island is included in the Izembek Wildlife Refuge. Several large stratovolcanoes occur on the island, including the highly active and picturesque Shishaldin Volcano. Waring (1917) reported hot springs in a marshy area at the northern base of Pogromni Volcano. Another small warm spring on Unimak was reported by a resident of False Pass village to be located at an elevation of about 600 m, about 2 km west of the village.

Pavlof

An active volcano located on the Alaska Peninsula directly west of Pavlof Bay. Pavlof has erupted numerous times in the past decade. Fumarolic activity was observed near the summit during an overflight by DGGS in August 1980. The volcano subsequently erupted in November 1980.

Surprise Lake

This site is a warm crater lake within Aniakchak caldera which is included in the Aniakchak National Monument. A study of the caldera and thermal-spring waters was made by T. Miller and I. Barnes of the U.S. Geological Survey (unpub. data).

Gas Rocks

This hot spring is reported by Barnes and McCoy (1979) as located on the south shore of Becherof Lake at the base of Gas Rocks. The thermal spring is thought to have formed in conjunction with the recent eruptive activity at Ukinrek Maars, 2 km to the south. The thermal waters were reported to issue at 53°C and are highly concentrated in sodium and chloride. The spring could not be located during a brief reconnaissance in 1980.

Sites Not Visited, Existence of Thermal Activity Questioned

Atka west

This site is listed by Waring (1917) and in the compilations of Miller (1973) and Markle (1980). Waring based his report on vague earlier Russian accounts. Local inhabitants knew of no thermal-spring area west of their village, and the site is presumed to be one of those that occur on northeast Atka.

Akun

On the basis of earlier accounts of Grewingk (1850) and Dall (1870), Waring (1917) listed two thermal-spring sites in this area, one occurring on the northwest side of the island, the other on the southeast side. The only thermal-spring site on or around Akun known to Akutan villagers is the site discussed on p. 106 of this report. Mild solfatara activity near the summit of Mount Gilbert, a volcano on the northern part of the island, is described by Maddren (1919), but this activity apparently ceased by 1945 (Byers and Barth, 1953). The thermal springs listed as occurring on Rootak Island south of Akun Island in Marble's 1980 compilation probably do not exist.

Amagat Island

On the basis of Grewingk's (1850) account of hot springs on a little island at the entrance of Morzhovoi Bay, Waring (1917) placed the site on Amagat Island. The site is probably actually the one located on Egg Island.

Frosty Peak

Miller (1973) lists a thermal-spring site as occurring near Frosty Peak and lists Waring (1917) as a reference. No reference to this site could be found in Waring (1917) by DGGS and local inhabitants knew of no thermal springs occurring in the general location given in Miller (1973). The existence of these springs is considered doubtful.

Balboa Bay, Stepovak Bay, and Port Heiden

Vague accounts pertaining to the existence of thermal springs in these three general areas were given by Waring (1917) who was in turn referenced by Miller (1973) and Markle (1980). Local inhabitants could not confirm the existence of springs in any of these three areas; no thermal springs were sighted during an aerial reconnaissance of these localities by DGGS in 1980.

SUMMARY

Three conditions have provided a favorable setting for the development of hydrothermal convective systems in the Aleutian arc: (a) active volcanic systems, (b) the likelihood of shallow, magmatically heated rocks and (c) deep, penetrating fracture systems created by major tectonic stresses. Over 30 thermal-spring areas have been reported to exist in the region of the Aleutian arc extending from Atka Island to Becherof Lake, the area of study of this report. The locations of these sites are shown in figure 1. During July and August of 1980 DGGS performed field investigations on 20 of these reported sites, many of which had not been previously described in the literature. A summary of 17 of these sites is provided in tables 46-49.

Thermal activity of the three other sites visited by DGGS either had diminished substantially or no longer existed (Ukinrek, Bogoslof, and Peulik). At least seven additional sites occur in the study area at which thermal-spring activity is probable or certain but were not visited by DGGS because of their remoteness or because of time constraints. The existence of several other reported thermal-spring sites could not be verified; these sites are considered questionable.

Subsurface reservoir temperatures in excess of 150°C are estimated for 10 of the thermal-spring sites investigated (tables 47 and 48). These sites all occur in or near (<15 km) regions of Recent volcanism. Five of the sites are characterized by fumaroles and steaming ground, which indicates the presence of at least a shallow vapor-dominated zone (table 47). Makushin Valley and Glacier Valley thermal areas both occur on the flanks of the active Makushin Volcano, located on Unalaska Island, and may be connected to a common source of heat. The Geyser Bight fumarole areas on Umnak Island are probably associated with a boiling subsurface hot-water system that feeds the extensive thermal-springs area that occurs at lower elevations in the valley north of the fumaroles. Gas geothermometry suggests that the reservoir feeding the Kliuchef thermal field located on the flanks of Kliuchef Volcano of northeast Atka Island may be as high as 239°C. The Korovin thermal field lies near the floor of a valley 6 km southeast of Korovin Volcano and 5 km northwest of the Kliuchef thermal field. The alignment of the Korovin and Kliuchef sites is similar to those dikes that are exposed on the island and to the direction of plate convergence in this sector of the Aleutian arc.

The Geyser Bight thermal-springs area constitutes the hottest and most extensive hot-water hydrothermal-convective system known in Alaska. The thermal springs, most of which are at or near boiling, are dispersed over a 4-km^2 area on central Umnak Island. Deep reservoir temperatures are conservatively estimated at 210°C and may be as high as 264°C. Although spring temperatures in 1980 were similar to those measured in

Table 47. Identified hydrothermal convective systems having vapor-dominated zones---
Aleutian arc, Atka Island to Becherof Lake

Site	Surface manifestation	Estimated reservoir temperatures (°C)	Comments
Kliuchef, Atka Island	Numerous fumaroles, steam vents, vigorously boiling springs, low-chloride acid springs (pH 3-4) and intense hydrothermal alteration. Thermal field covers area of 50,000 m² at 650 m elevation on west flank of Kliuchef volcano.	239 (?)	The thermal field is located about 12 km north of village of Atka. The system may be a shallow vapor-dominated system capping a deeper hot-water system. Reservoir temperature estimate was made by using gas geothermometry. Two additional thermal fields lie on the south flank of the volcano at elevations of 1,000 and 1,300 m. Host rocks are late Quaternary shallow-dipping basalt and andesitic lava flows.
Korovin, Atka Island	Steam vents, mudpots, acid-sulface and neutral springs, some boiling vigorously, and acid-sulfate water lake, all low in chloride. Two sites about 0.5 km apart, each 50,000 m² at 225 m elevation in stream valley about 6 km SW of Korovin Volcano.	> 150 (?)	The thermal fields occur within and around craterlike depressions. The systems may be pockets of vapor-dominated convection overlying a deeper hot-water system. Cold-water streams run adjacent to the thermal fields. Another thermal field lying 4 km north of the Korovin sites has been tentatively identified from aerial photographs. Host rocks are flat-lying Quaternary basalt and andesitic flows.
Glacier Valley, Northern Un-Alaska Island	Numerous fumaroles, steam vents, and vigorously boiling low-chloride springs. Intense hydrothermal alteration. Thermal field covers area 1/2 km² at 650 elevation on SW flank of Makushin Volcano. Numerous neutral low-chloride hot springs and seeps at lower elevation.	> 150 (?)	This thermal field may be connected to the same thermal source driving the Makushin Valley thermal field. The volcano has a small caldera, 4 km in diameter, suggesting a shallow magma chamber. Country rock is an intensely fractured granodiorite and gabbro overlain by basaltic flows.
Makushin Valley, northern Un-Alaska Island	Fumaroles, steam vents, mudpots, and boiling acid-sulfate, low-chloride springs. Intense hydrothermal alteration. Thermal field covers area 1/2 km² at 825 m elevation on E flank of Makushin Volcano. Neutral low-chloride hot springs and seeps at lower elevation.	> 150 (?)	The thermal field is located at the head of Makushin Valley 23 km west of Unalaska village and about 2 km north of the Glacier Valley site. Country rock is intensely fractured granodiorite and gabbro overlain by basaltic flow. Both the Glacier Valley and Makushin Valley systems may be shallow vapor-dominated systems overlying a deeper hot-water system.
Geyser Bight, Umnak Island	Two small areas consisting of fumaroles, mudpots, and steam vents at 325 m elevation at head of Geyser Bight valley. Areas are 10,000 m² and about 1/2 km apart. Thermal fields probably connected to deeper hot-water system.	> 150 (?)	The proximity of these thermal fields the series B Geyser Bight hot springs (<1 km west) suggests they represent a shallow vapor-dominated system with steam supplied from a subsurface boiling water table.

Site	No. of springs	Est. total flow (lpm)	Spring temperature (°C)	Estimated reservoir temperature (°C)	Comments
Geyser Bight, Umnak Island	Numerous	1,000	60-100	210	Five separate hot-spring areas and two fumarole fields occur along a 4-km stretch of Geyser Creek drainage. Springs lowest in elevation lie 3 1/2 km south of Geyser Bight. Hottest surface spring temperatures and subsurface temperature estimates occur at sites C, H, and J; all three have small geysers. The fumarole fields may be connected to the deeper hot-water system. Springs mostly occur along valley sides and emerge from shallow pools in valley alluvium. Most springs are depositing silica in outflow channels. Spring J has an extensive silica apron covering over 500 m² . Geyser Bight valley lies between the highly active Okmok caldera system 40 km to the southwest. Country rock consists of late Tertiary and Quaternary volcanic rocks overlying middle Tertiary plutonic rocks.
Akutan H. Spr. Akutan Island	Numerous	600	84	180	The hot springs lie along or near Hot Springs Creek in a 3 km long zone extending south from Hot Springs Cove. Springs emerge from pools in valley alluvium or from fissures in hydrothermally cemented scream-bank sediments. The springs are located 4 km northwest of Akutan Harbor and 18 km northeast of the active Akutan volcano. Country rock is a massive Quaternary debris flow intruded by basaltic dikes.
Emmons Lake H. Spr., AK Peninsula	12	600	65	178	Two clusters of hot springs lie along the northwest shore of Emmons Lake. The lake occupies a trough that is thought to be related to caldera collapse. The area east of the lake is volcanically active with several lava flows emplaced in Holocene times. Quaternary volcanics compose the surrounding country and host rock. Site is located 24 km north of the village of Belkofski.
Hot Springs Cove, Umnak Isl.	6	180	93.5	171	The major set of springs are located in the southwest corner of the hot-springs valley 1 1/2 km south of Hot Springs Cove. These springs emerge from pools in the valley alluvium or from fissures in the country bedrock. Additional springs occur at the beach and are exposed only at low tides. Country rock consists of late Tertiary and Quaternary volcanics.
Mother Goose H. Spr., AK Peninsula	Numerous	4,000	66	>150 (?)	Numerous springs and seeps occur along and above the southwest side of Volcano Creek, which drains the north flank of the volcano Mt. Chiginagak into Mother Goose Lake 16 km to the west. The combined flow is very large. Silica geothermometer suggests subsurface temperatures as high as 194°C. The extremely high Mg content of the waters does not allow an unambiguous application of the cation geothermometer. Sulfate geothermometry performed by USGS indicates a relatively cold reservoir (80°C). Country rock consists of Cretaceous and Jurassic sandstones, siltstones, conglomerates, and limestones overlain by Tertiary and Quaternary volcanic flows from Mt. Chiginagak.

Table 49. Identified hot-water hydrothermal convection systems 90°C<T<150°C---
Aleutian arc, Atka Island to Becherof Lake

Site	No. of springs	Est. total flow (lpm)	Spring temperature (°C)	Estimated reservoir temperature (°C)	Comments
Partov Cove H. Spr., Umnak Isl.	Several seeps	200	84	132	These springs are located 1 km from the Pacific Ocean and 4 km east of the Hot Springs Cove hot springs. The two spring systems may be related to the same subsurface reservoir. The Pacific-side springs emerge as seeps along the northern bank of a creek that drains into the Pacific Ocean.
Cold Bay H. Spr., AK Peninsula	17	700	54	130	Several clusters of hot springs are located 7 km east of Cold Bay and 17 km east of the village of Cold Bay. Over 17 springs emerge from pools or as seeps along the shallow northern slope of a small knoll that lies in a broad valley north of Mount Dutton. Valley sediments consist of glacier drift and alluvium. Underlying bedrock is thought to be Tertiary and Quaternary volcanic rocks.
False Pass H. Spr., AK Peninsula	2	225	62	103	The springs are located in a broad glacier valley 1 km east of Hot Springs Bay and 16 km northeast of the village of False Pass. The springs emerge from shallow pools in valley alluvium at the base of the southern valley wall. The area is unmapped; reconnaissance geology indicates host rock consists of late Tertiary and Quaternary volcanic rocks.
Akun Strait H. Spr. near Akun Isl.	1 major, several minor	40	43	97	The springs are located on the eastern beach of a small island adjacent and west of Akun Island, directly across from an abandoned village. The springs discharge along a basaltic dike at about half-tide level. Mixing of cold ocean water near the surface is probable and reservoir temperatures are probably higher than estimated.
Port Moller H. Spr., AK Peninsula	1 major, 1 minor	250	71	71	The springs are located on the southwest side of Port Moller Bay, 16 km south of the village of Port Moller. The springs discharge into a pool lying at the head of a shallow gully west of an isolated north-south-trending low bedrock ridge. Local bedrock is Lower Cretaceous sandstone. Numerous middens surround the springs; C-14 dates obtained from the middens indicate the springs have been used for over 1,000 years.

Table 50. Identified hot-water hydrothermal convection systems T≥90°C---
Aleutian arc, Atka Island to Bechorof Lake.

Site	No. of springs	Est. total flow (l/s)	Spring temperature (°C)	Estimated reservoir temperature (°C)	Comments
Egg Island H. Spr., AK Peninsula	1	:0	51	79	The springs are located on the south beach of Egg Island, which lies adjacent to the southwest coastline at the mouth of Portzhovi Bay. The springs emerge at half-tide level along a basaltic dike. Mixing of cold ocean water is probable and subsurface temperatures may be underestimated.
Kenmore H. Spr., AK Peninsula	2	:0	43	76	The springs are located on the Pacific side near the southwest end of the Alaska Peninsula 8 km south across a low pass from False Pass hot springs. The springs emerge at half-tide level from among beach boulders adjacent to a basaltic dike. Mixing of colder ocean water is probable and subsurface temperatures may be underestimated.
Summer Bay H. Spr., Unalaska Isl.	1	~50	35	60 (?)	A single spring is located 6 km northeast of Unalaska Village and 1 km inland from Summer Bay. Recent drilling encountered a warm-water aquifer with a temperature of 50°C at a depth of 40 ft. Carion geothermometer gave anomalously low values. Silica trend indicates deep reservoir temperatures may be as high as 160°C.

1947, the combined flow from the hot springs, estimated at 1,000 lpm in 1980, appears to have decreased appreciably since the 1947 observations. A decrease in discharge of thermal springs at Hot Springs Cove, northeast of Geyser Bight, was also noted. A geothermal reservoir temperature of 180°C is estimated for Akutan hot springs, a 1-km long zone of thermal springs with an estimated flow rate 600 lpm located 10 km northeast of the active Akutan Volcano. The proximity of this resource to Akutan Harbor (4 km) and Akutan village make the site a promising candidate for future development. Emmons Lake hot-springs site, located in a remote region of the southwest Alaska Peninsula, is estimated to have a reservoir temperature of 178°C. Discharge from the 60°C thermal springs was measured at 600 lpm. Mother Goose hot springs, located at the base of Mt. Chiginagak, an active volcano on the Alaska Peninsula, are distinguished by their enormous rate of discharge (~4,000 lpm) and the mixed character of their thermal-water chemistry. Deep-reservoir temperatures at Mother Goose are tentatively estimated at >150°C.

Five thermal-spring sites were identified to have reservoir temperatures in the range of 90° to 150°C. Partov hot springs may be related to the thermal springs of Hot Springs Cove. The sites lie about 5 km apart on central Umnak Island. The Cold Bay, False Pass, and Port Moller sites are all relatively remote (>20 km) from areas of Recent volcanism. Akun Strait hot springs are located in an intertidal zone; Port Moller hot springs are a few meters above high-tide level. The False Pass, Akun, and Port Moller sites all appear to be associated with local fracture systems.

Two of the three sites identified as having reservoir temperatures greater than 90°C (Egg Island and Kenmore) occur in intertidal zones and are associated with dikes and fracture systems. The Summer Bay thermal spring occurs 2 km inland and is fed from a mixed warm-water aquifer. Comparison of chemistries of water samples obtained from two shallow drill holes and the spring suggests that the parent thermal water mixing with colder surface waters within the acquifer may originate from a reservoir having a temperature as high as 160°C.

The thermal-springs sites in the study region tend to fall into three general terrain associations: a) those that occur on the flanks or at the base of Recent volcanoes; b) those systems that occur near Recent volcanoes and on or near lineations that suggest fracture or fault control for the thermal-spring occurrence; and c) those systems that are remote from any Recent volcano, typically occur at or near the coast, and appear to be related to local fractures or dikes. These associations are reflected in the wide variation in water chemistry of the Aleutian arc thermal springs that were sampled (App. C). Figure 40 presents the major-ion chemistry plotted on a Piper Diagram. Springs directly associated with fumarole and steam fields on or near Recent volcanoes are characterized by extremely low chloride (<50 ppm) and often low pH. Some of the near-neutral, low-chloride springs are comparatively rich

SAMPLE CODE

1 Summer Bay
2 Makushin - Glacier Valley 1
3 Makushin - Glacier Valley 3
4 Makushin Valley 1
5 Makushin Valley 2
6 Partov Cove
7 Hot Springs Cove E1
8 Hot Springs Cove E5
9 Geysers Bight GB
10 Geysers Bight J
11 Geysers Bight K
12 Geysers Bight L
13 Akutan A2
14 Akutan D2
15 Akun
16 False Pass
17 Kenmore
18 Egg Island
19 Cold Bay
20 Emmons Lake
21 Port Moller
22 Mother Goose
23 Ukinrek Maars
24 Korovin Bay A
25 Korovin Bay B
* Sea Water
+ Average River Water

Figure 40. Piper diagram illustrating major-ion chemistry of eastern Aleutian--western Alaska Peninsula thermal springs.
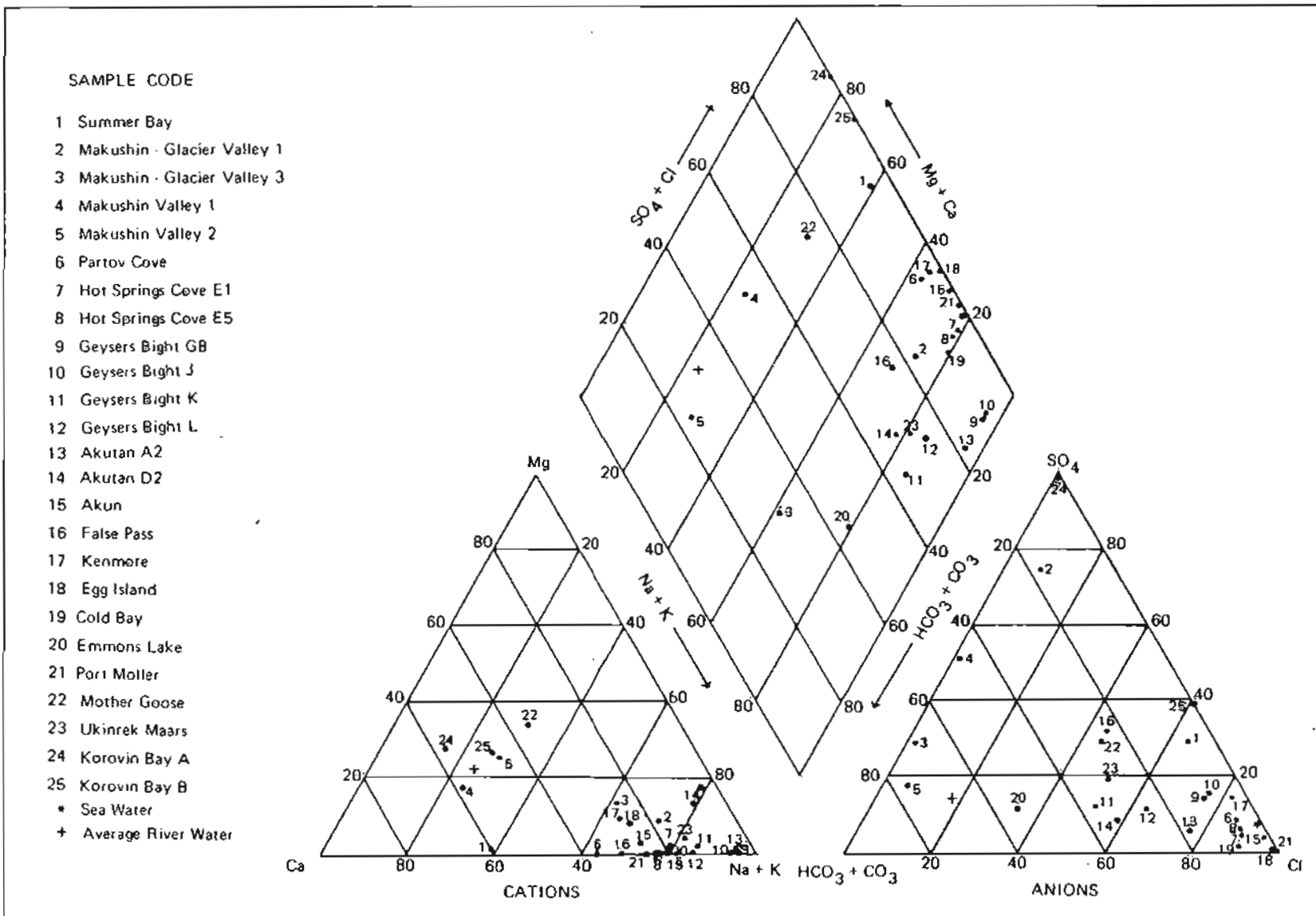
in bicarbonate and sulfate and have high levels of magnesium and calcium relative to sodium and potassium. Such waters appear to originate from the heating of surface waters circulating in shallow reservoirs by condensing steam and volcanic gases rich in H_2S and CO_2.

Thermal waters from high-temperature systems associated with inferred deep-fracture systems such as Geyser Bight and Akutan hot springs are typified by mild to moderate concentrations of alkali-chlorides, low Na:K ratios, and high levels of silica. Geyser Bight and Hot Spring Cove are also characterized by high levels of boron compared to other Aleutian arc hot springs. The constituents of these thermal waters are probably derived largely from the interaction of hot-water with wall rocks during long-term residence in deep-seated geothermal reservoirs. Depths to such reservoirs are largely unknown, but on the basis of occurrences elsewhere in the world, they probably lie 1 to 3 km deep. Some constituents may also come from even deeper primary higher temperature soidum-chloride brines, which are thought to develop over cooling bodies of magma.

Thermal springs that are associated with relatively low subsurface temperatures and occur at or near the coast are commonly a moderately concentrated sodium-chloride water usually with measurable quantities of bromide. The constituents in these waters probably originated in part from the circulation of seawater in deep-fracture systems, with magnesium and sulfate being selectively removed in high-temperature water-rock reactions.

Carbon dioxide is the dominant gas present in all but one of the nine gas samples obtained from hot springs and fumaroles located in the region of study. Methane predominates at Port Moller hot springs. Notably high proportions of hydrogen (5.9 percent) and hydrogen sulfide (1.6 percent) were detected in samples obtained from the Kliuchef thermal field. Enrichments of ^3He in gases obtained from Makushin Valley fumaroles are typical of island-arc settings. The excess ^3He is thought to be of mantle origin.

Many of the hydrothermal systems in the study region appear to be intimately associated with the magmatic activity that pervades most of the Aleutian arc. Deep reservoirs probably reside in most cases in magmatically heated, porous, and permeable older rock formations that underlie the Quaternary volcanics. Widespread lava flows and hydrothermal cementation can act as effective caps on such hydrothermal reservoirs. Fracture and fault systems generated by the convergence of two major tectonic plates probably help provide avenues for the deep circulation of surface waters into these magmatically heated reservoir rocks and perhaps also contribute to the release of deeper magmatic fluids. These fluids eventually emerge as hot springs and fumaroles. Thermal springs remote from centers of Recent volcanism probably derive their heat solely from the regional geothermal gradient by circulation along deep fracture systems.

Three locations have been identified in this study where the potential for the development and utilization of geothermal energy ranges from highly promising to outstanding: Akutan Island, northern Unalaska Island, and northeast Atka Island. All three have high-temperature (150°C) geothermal resources that are located near existing population centers that have excellent, well-protected, deep-water harbors. Two of these centers, Akutan and Unalaska villages, presently serve as the major supply and processing ports for most of the Aleutian-Bering Sea fishing fleets. The third, Atka Village, is presently a subsistence community and is actively seeking an energy base for the development of a local fish processing industry. The estimated reservoir temperatures are probably sufficient for producing moderate amounts of electrical power (1-5 MW) in all three localities with Rankine-type binary systems or perhaps through flash-steam production. Cascaded uses are possible for direct space heating and industrial processing.

Although the Geyser Bight geothermal resource is the hottest and most extensive thus far identified in Alaska, the lack of protected deep-water harbors and potential users on Umnak Island make the development of this resource impractical at this time.

ACKNOWLEDGMENTS

REFERENCES CITED

Baker, R.O., Lebida, R.C., Pyle, W.D., and Britch, R.P., 1977, An investigation
    of selected Alaska geothermal spring sources as possible salmon hatchery
    sites: National Technical Information Service IDO/1624-1, 173 p.
Barnes, Ivan, 1964, Field measurement of alkalinity and pH: U.S. Geological
    Survey Water-Supply Paper 1535-H, 17 p.
Barnes, R.B., 1975, The determination of specific forms of aluminum in natural
    water: Chemical Geology, v. 15, p. 177-191.
Barnes, I., and McCoy, G.A., 1979, Possible role of mantle-derived CO_2 in
    causing two "phreatic" explosions in Alaska: Geology, v. 7, p. 434-435.
Barrett, J.K., and Pearl, R.H., 1978, An appraisal of Colorado's geothermal
    resources: Colorado Geological Survey Bulletin 39, 224 p.
Black, R.F., 1975, Late Quaternary geomorphic processes: Effects on the ancient
    Aleuts of Umnak Island in the Aleutians: Arctic, v. 28, no. 3,
    p. 159-169.
Brooks, C.A., Mariner, R.H., Mabey, D.R., Swanson, J.R., Guffanti, Marianne,
    and Muffler, L.J.P., 1979, Hydrothermal convection systems with reservoir
    temperatures 90°C, in Muffler, L.J.P., (ed.), Assessment of geothermal
    resources of the United States--1978: U.S. Geological Survey Circular 790,
    p. 18-85.
Burk, C.A., 1965, Geology of the Alaska Peninsula-Island Arc and continental
    margin, parts 1, 2, and 3: Geological Society of America Memoir 99,
    250 p., 3 maps.
Byers, F.M., Jr., 1959, Geology of Umnak and Bogoslof Islands, Aleutian Island,
    Alaska: U.S. Geological Survey Bulletin 1028-L, p. 107-367.
Byers, F.M., Jr., and Barth, T.F.W., 1953, Volcanic activity on Akun and
    Akutan Islands: Pacific Science Congress, 7th, New Zealand, 1949,
    Proceedings, v. 2, p. 382-397.
Byers, F.M., Jr., and Brannock, W.W., 1949, Volcanic activity on Umnak and
    Great Sitin Islands, 1946-1948: American Geophysical Union Transactions,
    v. 30, no. 5, p. 719-734.
Coats, R.R., 1950, Volcano activity in the Aleutian Arc: U.S. Geological Survey
    Bulletin 974-B, p. 1-47.
Craig, H., 1963, The isotopic geochemistry of water and carbon in geothermal
    areas, in Tongiorgi, E. (ed.), Nuclear geology in geothermal areas,
    Spoleto, 1963: Pisa, Italy, Consiglio Nationale Delle Ricerche,
    Laboratorio di Geologia Nucleare, p. 17-53.
Craig, H., Lupton, J.E., Welhan, J.A., and Poreda, R., 1978, Helium isotope
    ratios in Yellowstone and Lassen Park volcanic gases: Geophysical Research
    Letters, v. 5, no. 11, p. 897-900.
Dall, W.H., 1870, Alaska and its resources: Boston, Lee and Shepard, 627 p.
    (Reprinted in 1970 by Arno & New York Times Press, American Environmental
    Studies series.)
Dames and Moore, 1980, Geothermal drilling studies near Unalaska, Alaska:
    Unpublished final report submitted to State of Alaska Division of Energy
    and Power Development, Anchorage, 5 p.
D'Amore, Franco, and Panichi, Costanzo, 1980, Evaluation of deep temperatures
    of hydrothermal systems by a new gas geothermometer: Geochimica et
    Cosmochimica Acta, v. 44, p. 549-556.
Drewes, H., Fraser, G.D., Snyder, G.L., and Barnett, H.F., Jr., 1961, Geology
    of Unalaska Island and adjacent insular shelf, Aleutian Islands, Alaska:
    U.S. Geological Survey Open-file Report 1028-S, p. 583-676.

Ellis, A.J., and Mahon, W.A.J., 1964, Natural hydrothermal systems and
    experimental hot water/rock interactions: Geochimica et Cosmochimica Acta,
    v. 28, p. 1323-1357.
_____, 1977, Chemistry and geothermal systems: New York, Academic Press,
    392 p.
Fournier, R.O., 1973, Silica in thermal waters: Laboratory and field
    investigations. in Proceedings of symposium on hydrogeochemistry and
    biogeochemistry, Japan, 1979, v. 1, Hydrochemistry: Washington, D.C., J.W.
    Clark Co., p. 122-139.
_____, 1977, Chemical geothermometers and mixing models for geothermal
    systems: Geothermics, v. 5, p. 41-50.
_____, 1979, Geochemical and hydrologic considerations and the use of
    enthalpy-chloride diagrams in the prediction of underground conditions of
    hot-springs systems: Journal of Volcanology and Geothermal Research, v. 5,
    p. 1-16.
_____, 1980, Application of water geochemistry to geothermal exploration
    and reservoir engineering, in Rybach, L., and Muffler, L.P. (eds.),
    Geothermal systems: Principles and case histories: New York, John Wiley &
    Sons, Ltd., p. 109-143.
Fournier, R.O., and Potter, R.W., 1978, A magnesium correction for the Na-K-Ca
    chemical geothermometer: U.S. Geological Survey Open-file Report 78-486,
    24 p.
Fournier, R.O., and Rowe, J.J., 1966, Estimation of underground temperatures
    from the silica content of water from hot springs and wet-stream wells:
    American Journal of Science, v. 264, p. 685-697.
Fournier, R.O., and Truesdell, A.H., 1973, An empirical Na-K-Ca geothermometer
    for natural waters: Geochimica et Cosmochimica Acta, v. 37, p. 1255-1275.
_____, 1974, Geochemical indicators of subsurface temperature, Part 2:
    Estimation of temperature and fraction of hot water mixed with cold water:
    U.S. Geological Survey Journal of Research, v. 2, no. 3, p.263-270.
Grewingk, C., 1850, Beitrag zur Kenntniss der orographischen und geognostischen
    Beschaffenheir der Nordwest-Kuste Amerikas mit den anliegenden Inseln
    (Contribution to knowledge of the orographic (topographic) and geognostic
    (geologic) condition of the northwest cost of America with the adjacent
    islands): abstracted from Verhandlungen der Russich-Kaiserlichen
    Mineralogischen Gesellschalt zur St. Petersburg, Jahrgan 1848 ung 1849,
    p. 76-342.
Hrdlicka, Ales, 1945, The Aleutian and Commander Islands and their inhabitants:
    Philadelphia, Wister Institute of Anatomy and Biology, 630 p.
Keenan, J.H., Keyes, F.G., and Moore, J.G., 1969, Steam tables. Thermodynamic
    properties of water, including vapor, liquid, and solid phases: New York,
    John Wiley & Sons, Inc., 162 p.
Kennedy, G.C., and Waldron, H.H., 1955, Geology of Pavlof Volcano and vicinity,
    Alaska: U.S. Geological Survey Bulletin 1028-A, p. 1-18.
Kienle, J., Kyle, P.R., Self, S., Motyka, R.J., and Loreng, V., 1980, Ukinrek
    Maars, Alaska, I. April 1977 eruption sequence, petrology and tectonic
    setting: Journal of Volcanology and Geothermal Research, v. 7, p. 11-37.
Kienle, J., Motyka, R.J., Lalla, D.J., Estes, S.A., and Hust, J.P., 1980,
    Formation of two maars behind the Aleutian volcanic arc, Alaska Peninsula,
    April 1977: Alaska Earthquake Analysis Center, Seismological Report 4, UAG
    R-257.
Lupton, J.E., and Craig, H., 1975, Excess ^{3}He in oceanic basalts: Evidence
    for terrestrial primordial helium: Earth and Planetary Science Letters,
    v. 26, p. 133-139.

Maddren, A.G., 1919, Sulphur on Unalaska and Akun Islands and near Stepovak
    Bay, Alaska: U.S. Geological Survey Bulletin 692-E, p. 283-298.
Mahon, W.A.J., Klyen, L.E., and Rhode, M., 1980, Neutral sodium/bicarbonate/
    sulphate hot waters in geothermal systems: Journal of Japan Geothermal
    Energy Association, v. 17, p. 11-24.
Mazor, E., and Wasserberg, G.J., 1965, Helium, neon, argon, krypton, and xenon
    in gas emanations from Yellowstone and Lassen volcanic National Parks:
    Geochimica et Cosmochimica Acta, v. 29, p. 443-454.
Mariner, R.H., and Willey, L.M., 1976, Geochemistry of thermal waters in Long
    Valley, Mono County, California: Journal of Geophysical Research, v. 81,
    no. 5, p. 792-800.
Mariner, R.H., Brook, C.A., Swanson, J.R., and Mabey, D.R., 1978, Selected data
    for hydrothermal convection systems in the United States with estimated
    temperatures 90°C: U.S. Geological Survey Open-file Report 78-858,
    475 p.
Markle, D.R., 1979, Geothermal energy in Alaska: Site data base and development
    status: Report prepared for U.S. Department of Energy under contract
    DE-AC03-79SF1049, 2 vol, 545 p.
McKenzie, W.F., and Truesdell, A.H., 1977, Geothermal reservoir temperatures
    estimated from the oxygen isotope compositions of dissolved sulfate and
    water from hot springs and shallow drillholes: Geothermics, v. 5,
    p. 51-61.
Miller, T.P. (compiler), 1973, Distribution and chemical analyses of thermal
    springs in Alaska: U.S. Geological Survey Open-file Map 570.
Morgan, L., (ed.), 1980, The Aleutians: Alaska Geographic, v. 7, no. 3, 224 p.
Motyka, R.J., Moorman, M.A., and Reeder, J.W., 1980, Assessment of thermal
    springs sites in southern Southeastern Alaska---Preliminary results and
    evaluation: Alaska Division of Geological and Geophysical Surveys Open-
    file Report 127, 72 p.
Muffler, L.J.P., (ed.), 1979, Assessment of geothermal resources of the United
    States---1978: U.S. Geological Survey Circular 790, 163 p.
Muffler, L.J.P., White, D.E., and Truesdell, A.H., 1971, Hydrothermal explosion
    craters in Yellowstone National Park: Geological Society of America
    Bulletin, v. 82, p. 723-740.
Nakamura, K., Jacob, K.H., and Davies, J.N., 1977, Volcanoes as possible
    indicators of tectonic stress orientation - Aleutians and Alaska: Pure and
    Applied Geophysics, v. 115, p. 87-112.
Nathenson, Manuel, 1978, Methodology of determining the uncertainty in the
    accessible geothermal resource base of identified hydrothermal convection
    systems: U.S. Geological Survey Open-file Report 78-1003, 50 p.
Nehring, N.L., Truesdell, A.H., and Janik, C.J., 1980, Procedure for collecting
    and analyzing gas samples from geothermal and volcanic systems: U.S.
    Geological Survey Open-file Report (in press).
Okada, H., and Okada, A., 1980, Prehistory of the Alaska Peninsula as seen from
    the hot springs site, Port Moller, in Kotani, Y., and Workman, W.B.
    (eds.), Alaska Native culture and history: Senri Ethnological Studies, no.
    4, National Museum of Ethnology, Osaka, Japan, p. 103-112.
Oki, Y., and Hirano, T., 1970, The geothermal system of the Hakone Volcano, in
    U.N. symposium on the development and utilization of geothermal resources,
    Pisa, 1970, v. 2, pt. 2: Geothermics Special Issue 2, p. 1157-1166.
Orion Research, Inc., 1977, Instruction manuals for Orion ionalyzer specific
    ion electrodes, Cambridge, Massachusetts, 35 p.
Presser, T.S., and Barnes, Ivan, 1974, Special tecniques for determining
    chemical properties of geothermal waters: U.S. Geological Survey Water-
    Resources Investigation 22-74, 11 p.

Rand, M.C., Greenberg, A.E., and Taras, M.J. (eds.), 1975, Standard methods for the examination of water and waste water, fourteenth edition: Washington, D.C., American Public Health Association, 1193 p.

Ryzhenko, B.N., 1967, Determination of hydrolysis of sodium silicate and calculation of dissociation constants of orthosilicic acid at elevated temperatures: Geochemistry International v. 4, 99-107 (translated from Gokhimiya, no. 2, 161-169).

SEAN (Scientific Event Alert Network Bulletin), 1980: National Technical Information Service, U.S. Department of Commerce publication no. PR 81-9157.

Seward, T.M., 1974, Determination of the first ionization constant of silicic acid from quartz solubility in borate buffer solutions to 350°C: Geochimica et Cosmochimica Acta, v. 38, p. 1651-1664.

Skougstad, M.W., Fishman, M.J., Friedman, M.J., Erdmann, D.E., and Duncan, S.S. (eds.), 1979, Methods for determination of inorganic substances in water and fluvial sediments: U.S. Geological Survey Techniques of Water-Resources investigations, book 5, chapter A1, 626 p.

Truesdell, A.H., and Fournier, R.O., 1977, Procedure for estimating the temperature of a hot-water component in a mixed water by using a plot of dissolved silica versus enthalpy: Journal of Research, U.S. Geological Survey, v. 5, no. 1, p. 49-52.

Turner, D.L., Forbes, R.B., Albanese, M.D., Macbeth, J., Lockhart, A.B., and Seed, S.M., 1980, Geothermal resources of Alaska: Report to U.S. Department of Energy, Division of Geothermal Energy, contract DE-AS07-78ID01720, UAG R-279, 19 p., 2 pl.

Waldron, H.H., 1961, Geologic reconnaissance of Frosty Peak Volcano and vicinity, Alaska: U.S. Geological Survey Bulletin 1028-T, p. 677-708.

Waring, G.A., 1917, Mineral springs of Alaska: U.S. Geological Survey Water-Supply Paper 418, 114 p.

_____ (revised by R.R. Blankenship and Ray Bentall), 1965, Thermal springs of the United States and other countries of the world - a summary: U.S. Geological Survey Professional Paper 492, 383 p.

White, D.E., 1957, Thermal waters of volcanic origin: Geological Society of America Bulletin, v. 68, p. 1637-1658.

_____, 1968, Hydrology, activity and heat flow of the Steamboat Springs thermal system, Washoe County, Nevada: U.S. Geological Survey Professional Paper 458-C, 109 p.

White, D.E., Muffler, L.J.P., and Truesdell, A.H., 1971, Vapor-dominated hydrothermal systems compared to hot-water systems: Economic Geology, v. 66, p. 75.

White, D.E., and Williams, D.L. (eds.), 1975, Assessment of geothermal resources of the United States-1975: U.S. Geological Survey Circular 726, 155 p.

APPENDIX A

ABBREVIATIONS, UNIT SYMBOLS, AND CONVERSION FACTORS

1. Abbreviations

DGGS	– Alaska Division of Geological and Geophysical Surveys
ICAP	– Inductively coupled argon plasma
nd	– not determined
USGS	– U.S. Geological Survey

2. Unit symbols

^{o}C	– degrees Celsius
cm	– centimeter
J	– joule
kg	– kilogram
km	– kilometer
l	– liter
lpm	– liter per minute
m	– meter
mg	– milligram
ug	– microgram
ug/l	– microgram per liter
mm	– millimeter
m.y.	– million years
ppm	– parts per million
umhos	– micro mhos

3. Conversion factors

^{o}C	– 5/9 ^{o}Fahrenheit – 32
$^{o}C/km$	– 5/9 ^{o}F –32/0.621 mile
cm	– 0.394 inches
gm	– 0.035 ounce
joule	– 0.239 calorie (cal)
	– 9.480 x 10^{o-4} British thermal unit (Btu)
$10^{18}j$ – 10^{15} Btu	– 1 quad
kg	– 2.205 pounds
km	– 0.621 mile
l	– 0.264 gallon
lpm	– 0.264 gallons per minute
m	– 3.281 feet
mm	– 0.039 inch

APPENDIX B

PRECISION OF WATER ANALYSES
(from Skougstad and others, 1979)

Constituent	Analyses	Mean (mg/l)	Relative deviation percent
SiO_2	12	5.87	9
	19	36.5	3
Al	4	0.0750	23
	3	0.433	9
Fe	17	0.100	31
Ca	17	12.6	7
	23	110	8
Mg	23	1.98	9
	20	22.0	5
	17	35.6	17
Na	26	3.44	9
	19	43.7	4
	23	78.8	4
K	15	0.8	14
	32	5.2	11
Li	10	0.054	9
	18	0.484	5
Cl	10	1.56	26
	9	194	4
F	13	0.62	16
	6	1.1	26
	14	3.8	11
B	9	0.072	78
	5	0.522	14
SO_4	16	21.0	6
	5	104	5
	16	141	6
Sr	17	82	34
	8	1,400	9

APPENDIX C

WATER CHEMISTRY, ALEUTIAN ARC HOT SPRINGS. UNITS ARE MG/L UNLESS OTHERWISE NOTED.

	Kliuchef		Korovin		Geyser Bight							Hot Springs Cove		Partov	Glacier Valley	
	A	B	A	B	G6	G8	H1	H6	J	K	L	E3	E5	Cove	B1	B2
SiO_2	12.5	10	140	67	178	270	170	190	272	148	160	120	90	113	94	125
Ca	6.4	3.6	60.0	26.8	22.9	19.3	33.2	36.2	19.1	25.1	39.7	164	134	233	11.7	32.1
Mg	2.6	1.3	19.0	9.2	1.2	0.15	0.26	0.07	0.01	2.8	1.4	1.1	1.2	2.7	4.0	10.6
Na	1.87	3.82	15.5	15.5	248	487	355	442	447	179	280	664	531	456	52	87.2
K	0.75	0.47	10.0	4.1	17.1	30.9	16.3	19.9	31.7	13.9	20.1	34.2	24.5	19.0	4.8	5.7
Li	<.01	<.01	<.01	<.01	1.78	3.9	2.8	3.4	3.5	1.18	1.78	2.62	2.26	3.10	<.01	<.01
HCO_3	—	—	--	--	n.d.	146	n.d.	n.d.	113	266	262	142	133	138	37	288
SO_4	39.5	24.9	300	8.6	96.5	170	131	154	168	63.6	90.3	91.4	83.2	163	129	95
Cl	<5	5	<5	10	339	630	492	591	591	225	370	1255	1010	1050	10	5
F	<.01	0.01	0.20	<.01	0.90	2.3	1.27	1.55	2.4	0.90	1.6	0.86	0.72	1.0	0.14	0.28
Br	n.d.	n.d.	n.d.	n.d.	1.90	2.20	1.68	1.92	2.13	1.22	1.07	3.98	3.29	2.35	n.d.	n.d.
I	n.d.	n.d.	n.d.	n.d.	0.7	1.1	1.1	1.2	1.0	0.5	0.7	0.74	0.60	0.67	n.d.	n.d.
B	<0.5	0.5	2.0	<0.5	15	60	51.5	58.3	50	18.8	30	31.3	23.8	27.3	<0.5	<0.5
pH	3.28	3.28	4.16	5.96	7.54	8.00	7.30	7.32	7.62	7.83	6.85	6.47	6.36	6.57	6.60	6.50
TDS	65.06	49.77	554.6	138.95	922.3	1823.0	1254.8	1499.8	1701.0	946.2	1259.0	2513	2040	2219.9	342.81	649.41
Temp. °C	94.2	82.2	99.3	48	97.3	100.1	100.3	9.9	82	67	85.5	93.5	71.8	84	96.8	82.4
Flow, lpm	n.d.	465	n.d.	n.d.	20	75	300	30	n.d.	n.d.	200	62	101	200	n.d.	n.d.
$TSiO_2$°C(QZ)	—	—	157	—	167	185	159	165	186	160	165	148	132	144	134	143
TNa/K°C	—	--	--	—	187	182	158	157	189	196	190	166	159	152	—	—
TNa-K-Ca°C	—	—	—	--	166	175	149	151	180	166	166	152	1451	134	—	—
T 18 (SO_4—H_2O)°	—	—	—	--	264[a]	—	--	—	--	--	--	--	—	—	—	—

	Makushin Valley		Summer Bay			Akutan Island		Akun	False		Egg	Cold	Emmons	Port	Mother
	B	C	Spring	Well 1	Well 2	A2	D2	Straits	Pass	Kenmore	Island	Bay	Lake	Moller	Goose
SiO_2	140	88	18	35	23	145	91	50	63	41	47	125	148	63	245
Ca	64.3	23.1	202	460	372	11.3	11.0	475	20.4	275	869	162	30	228	227
Mg	12.2	8.0	1.0	6.34	10.3	2.5	11.8	45.5	0.01	66.0	6.2	5.7	0.97	0.16	131
Na	28	13.9	150	332	276	323	128	1660	50.6	783	2030	751	139	292	198
K	5.0	3.4	3.0	6.49	5.45	24.8	9.3	34.9	2.6	13.2	18.3	16.4	9.8	12.3	47.4
Li	<.01	<.01	0.3	0.16	0.12	1.28	0.34	0.55	0.08	0.20	0.85	0.95	0.6	0.34	0.22
HCO_3	191	116	73	n.d.	n.d.	172	128	82	45	102	67	248	292	71	560
SO_4	155.3	21.4	245	528	423	42.7	26.4	222	46.9	359	26.5	14.0	51.5	16.5	491
Cl	5	5	404	923	741	424	136	3440	53	1570	4505	1370	102	1615	528
F	0.12	0.11	0.22	0.44	0.40	1.1	0.88	0.67	0.30	0.25	0.37	0.67	1.7	2.7	0.41
Br	—	—	1.25	3.02	2.65	1.31	--	11.25	--	5.19	14.79	4.11	--	5.34	—
I	—	—	—	0.19	--	0.42	--	0.86	--	0.09	2.94	1.0	—	0.85	0.21
B	<0.5	<0.5	0.5	0.5	0.5	11.4	3.4	5.7	1.5	3.0	32.5	25	4.6	13	0.8
pH	5.48	5.32	6.98	n.d.	n.d.	6.98	6.82	7.47	8.44	7.39	7.66	6.70	6.24	8.24	6.35
TDS	606.9	279.04	1099.1	2297.2	1858.1	1161	546.24	6037.3	261	3220	7625	2726.5	780.8	2824.6	2430.4
Temp. °C	87.4	67.0	35.0	50	44	84.0	58.8	47.8	62.2	43.3	50.6	53.6	65.0	71.0	66.0
Flow, lpm	--	--	64	180	30	118	<20	15	225	20	—	100	560	251.5	2567
$TSiO_2$°C(QZ)	149	127	60	86	72	159	132	102	113	93	99	150	160	113	194
TNa/K°C	—	—	109	108	109	195	191	112	166	101	72	114	189	97	292
TNa-K-Ca°C	—	—	92	95	95	183	164	118	129	104	70	116	156	102	20[b]
T 18 (SO_4—H_2O)°	—	—	—	--	--	186[a]	--	--	--	--	—	--	184[a]	—	86[a]

[a] M. Nehring, USGS, Menlo Park Analyst. [b] Mg- Corrected. n.d. = not determined.